UNIVERSITY OF COPENHAGEN

PhD Thesis

Mads Søgaard

Scattering Amplitudes via Algebraic Geometry Methods

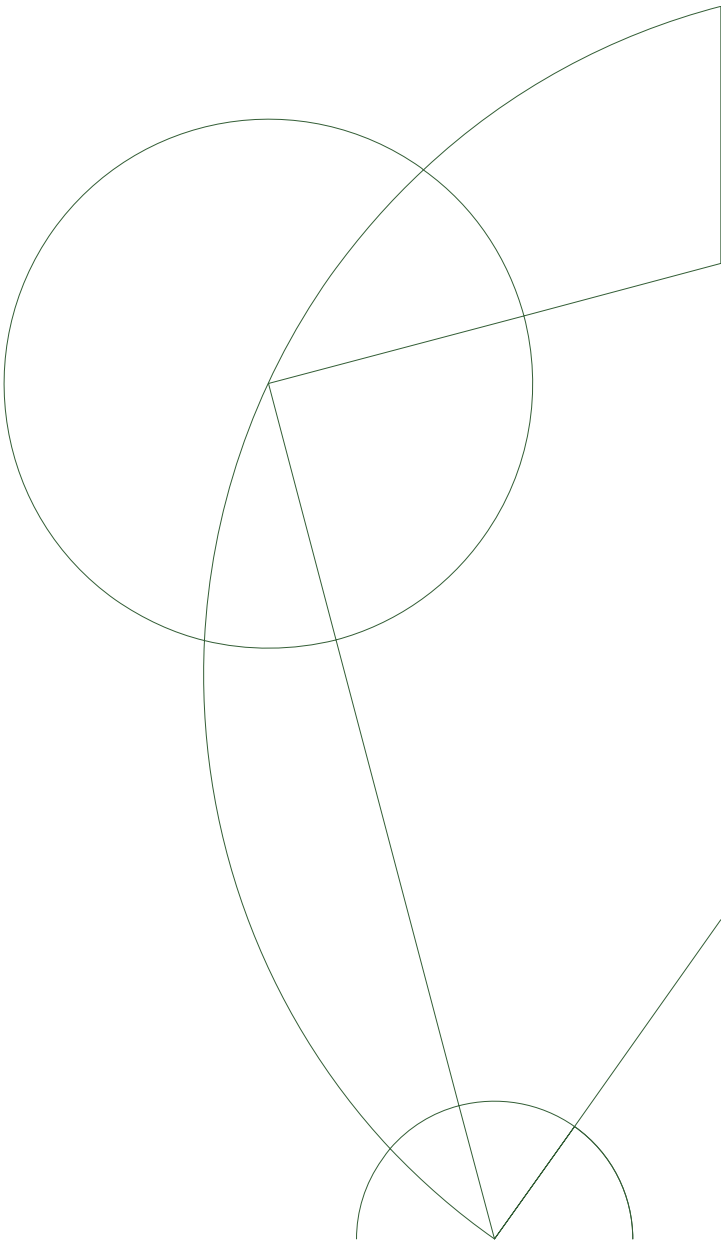

Academic advisors:
Emil Bjerrum-Bohr
Poul Henrik Damgaard

Submitted March 19, 2015

Scattering Amplitudes via Algebraic Geometry Methods

by

Mads Søgaard

Submitted for the degree of Doctor of Philosophy in Physics
at the Niels Bohr Institute, Faculty of Science,
University of Copenhagen

March 2015

Abstract

This thesis describes recent progress in the understanding of the mathematical structure of scattering amplitudes in quantum field theory. The primary purpose is to develop an enhanced analytic framework for computing multiloop scattering amplitudes in generic gauge theories including QCD without Feynman diagrams. The study of multiloop scattering amplitudes is crucial for the new era of precision phenomenology at the Large Hadron Collider (LHC) at CERN. Loop-level scattering amplitudes can be reduced to a basis of linearly independent integrals whose coefficients are extracted from generalized unitarity cuts. We take advantage of principles from algebraic geometry in order to extend the notion of maximal cuts to a large class of two- and three-loop integrals. This allows us to derive unique and surprisingly compact formulae for the coefficients of the basis integrals. Our results are expressed in terms of certain linear combinations of multivariate residues and elliptic integrals computed from products of tree-level amplitudes. Several explicit examples are provided.

Resume (in Danish)

Naturens fundamentale love og vekselvirkninger udforskes ved partikelkollisioner ved meget høje energier og hastigheder nær lysets. Verdens kraftigste partikelaccelerator er CERN Large Hadron Collider (LHC), hvor man i 2012 opdagede den berømte Higgspartikel. Den enorme mængde af data som indsamles ved eksperimenterne på CERN tillader nu fysikere at stille skarpt på de store uløste gåder.

Udfaldet af partikelkollisionerne kan forudsiges teoretisk ved hjælp af såkaldte spredningsamplituder, der beregnes i kvantefeltteorier så som QCD. Præcise teoretiske forudsigelser er afgørende for LHC-programmet, idet en fuldstændig forståelse af baggrundsprocesserne i Standardmodellen er en forudsætning for at opdage ny fysik. Desværre har det i løbet af de seneste årtier vist sig at være ekstremt svært at beregne de nødvendige spredningsamplituder, på trods af at resultaterne oftest er overraskende simple og besidder uforudsete symmetrier.

Denne afhandling beskriver de seneste års fremskridt i vores forståelse af spredningsamplituder i kvantefeltteori med fokus på deres matematiske strukturer og beregningsmæssige komplikationer. Det primære formål er at udvikle en forbedret analytisk metode til at beregne kvantekorrektioner (også kaldet loop-korrektioner) til spredningsamplituder i vilkårlige kvantefeltteorier uden brug af traditionelle teknikker herunder Feynman-diagrammer. Spredningsamplituder kan på loop-niveau reduceres til en basis af lineært uafhængige Feynman-integraler. Basisintegralerne er universelle og opgaven er derfor blot at ekstrahere deres koefficienter via såkaldte cuts.

Vi demonstrerer hvordan principper fra algebraisk geometri kan udnyttes til at udvide anvendelsen af disse cuts til en større klasse af integraler, som er essentielle for 2- og 3-loop spredningsamplituder i QCD. Resultaterne omfatter unikke og meget kompakte formler for integralkoefficienterne. Metoden er baseret på residuer i højere dimensioner samt elliptiske integraler. Der indgår adskillige eksplicitte eksempler og beregninger.

List of Publications

The bulk of this thesis comprises work described in a series of papers.

I M. Sogaard and Y. Zhang, *Elliptic Functions and Maximal Unitarity*, to appear in Phys.Rev.D. [arXiv:1412.5577].

II M. Sogaard and Y. Zhang, *Massive Nonplanar Two-Loop Maximal Unitarity*, JHEP **12** (2014) 006 [arXiv:1406.5044].

III M. Sogaard and Y. Zhang, *Unitarity Cuts of Integrals with Doubled Propagators*, JHEP **07** (2014) 112 [arXiv:1403.2463].

IV M. Sogaard and Y. Zhang, *Multivariate Residues and Maximal Unitarity*, JHEP **12** (2013) 008 [arXiv:1310.6006].

V M. Sogaard, *Global Residues and Two-Loop Hepta-Cuts*, JHEP **09** (2013) 116 [arXiv:1306:1496].

Contents

1 Introduction

The main objective of high energy physics is the identification and understanding of the fundamental constituents and principles of Nature. What is regarded as fundamental is merely a question of energy scale; as new experiments were performed and improved throughout history, fundamental principles have changed drastically and constituents believed to be fundamental turned out to be composite.

In the beginning of the 20th century, an accumulation of theoretical and experimental observations strongly suggested that Nature behaves peculiarly at and below the atomic level. The idea of physical determinism was challenged by completely unexpected phenomena, which seemed to be inherit features of Nature itself. This led to the invention of quantum mechanics, which has governed our view of Nature at its most fundamental level ever since.

Today, particle physicists continue to unravel the fundamental laws of Nature by accelerating protons at almost the speed of light and smashing them together to study how elementary particles scatter off each other. This is the only viable method of exploration as the objects of interest are extremely small and intangible, moving either at the speed of light or decaying almost instantaneously after being produced. The world's largest and most powerful particle collider is the CERN Large Hadron Collider (LHC) which is able to peer subatomic physics at unbelievable scales. The enormous amount of data delivered by the LHC allow physicists to finally test theoretical predictions and address unresolved questions of particle physics.

1.1 The Standard Model

The Standard Model (SM) of particle physics is an extremely (and so far the most) successful theory: it consistently classifies all observed particles and describes the electromagnetic and the weak and strong nuclear interactions. In particular, the discoveries of for instance the top quark at Fermilab (1995) and more recently a Higgs-boson-like particle [109, 110] with a mass around 125 GeV at CERN (2012) have lent substantial credence to the SM whose current form was settled around 40 years ago.

The guiding principles that govern the structure of the SM are merely the presence of continuous local gauge symmetry and renormalizability. The set of allowed operators in the SM Lagrangian is highly constrained, guaranteeing that the theory will have predictive power once the fundamental fields and their internal symmetries are specified.

The SM dictates that all matter consists of three generations of charged quarks and charged and neutral leptons. Quarks and leptons are called fermions due to their statistical properties. The dynamics of the SM is controlled by three sectors: the electroweak sector, the Higgs sector and the Quantum Chromodynamics (QCD) sector. The interactions are mediated by gauge bosons that are elementary particles of the theory. The electroweak sector has four gauge bosons: the photon γ and the $W^{\pm}$ and Z bosons. The $W^{\pm}$ bosons carry electric charge whereas the photon and the Z boson are electrically neutral. While the photon remains massless, the $W^{\pm}$ and Z bosons acquire masses through spontaneous symmetry breaking $SU(2) \times U(1) \longrightarrow U(1)$ via the Higgs mechanism at energies below the electroweak scale at approximately 250 GeV. The strong interactions between the quarks are mediated through exchange of eight massless fundamental particles — the gluons g — governed by QCD. In short, the particle content of the SM forms the periodic table of the 20th century.

Although it remains unchallenged by any particle physics data, the SM is not a complete description of Nature. The SM provides no explanation for phenomena of general relativity, neutrino oscillations nor the peculiar predictions of the existence of unobserved dark matter and dark energy. Accordingly, an appropriate extension introducing new particles is certainly necessary. Perhaps the most attractive scenario is provided by incorporation of supersymmetry. Supersymmetry is a very beautiful, yet speculative, symmetry between fermions and bosons. The idea is that for every boson of the theory there is a supersymmetric partner which is a fermion and vice versa. Theories with supersymmetry contain natural dark matter candidates as well as numerous other particles. Moreover, supersymmetry is believed to be an important ingredient in constructing a finite theory of quantum gravity. Generically, introducing a broader variety of elementary particles yields a more complicated theory. On the other hand, if the additional particles are constrained by supersymmetry, the intermediate steps produce significant cancellations and the end results simplify dramatically.

Scientific breakthrough in the form of discoveries of beyond the SM physics depends on our ability to take advantage of the overwhelming amount of data recorded by the experiments at the LHC. In order words, it is crucial to gain a quantitative understanding of all relevant scattering processes in the SM. We distinguish between background processes and signal processes. The vast majority of events at the LHC is accounted for by precisely the QCD background. In a sense extracting signals of new physics requires subtracting the background from the experimental data.

1.2 Scattering Amplitudes in a Nutshell

The physical quantity that describes the outcome of particle collisions in collider experiments is the (differential) scattering cross section. The cross section measures the quantum mechanical probability for a given process to occur. This quantum mechanical probability always arises as the absolute value squared of a quantum mechanical amplitude, which is referred to as a scattering amplitude.

Scattering amplitudes represent fundamental objects of quantum field theory, being the furthest a theorist can push calculations without making assumptions of other physical processes or details of the experimental setup. The origin of this statement can be understood in terms of indistinguishability and quantum interferences. A scattering amplitude typically receives contributions from several processes that look the same to the detector in an experiment. Before calculating the cross section, all contributions must be added together. The total probability is not simply the sum of the individual

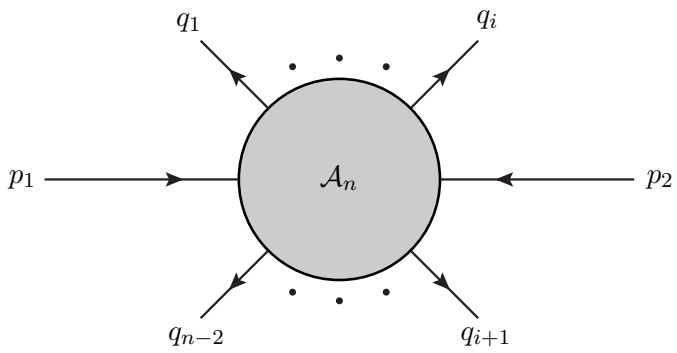

Figure 1.1: An illustration of a typical scattering event: two incoming particles with momenta p_1 and p_2 collide and produce $(n-2)$ outgoing particles with momenta $q_1, \ldots, q_{n-2}$.

probabilities; it also includes cross terms due to quantum mechanical interferences.

In order to gain insight into the basic theory of scattering amplitudes, let us imagine that we collide, for instance, two particles of definite momentum and produce $(n-2)$ new particles. The situation in mind is sketched in fig. 1.1. The incoming particles interact in a single point. Before the actual collision both particles are far away from each other. At the time of detection, the outgoing particles are again well separated. The probability distribution associated with a specific scattering process is determined by evolving the initial state from infinite past to infinite future and computing the overlap with the desired final state. The evolution operator is the unitary S-matrix, customarily decomposed into a trivial piece and an interaction part,

$$S = \mathbf{1} + iT \; . \tag{1.1}$$

The scattering amplitude $\mathcal{A}_n$ itself is conventionally defined by sandwiching the T-matrix between incoming and outcoming states,

$$\langle q_1 q_2 \cdots q_{n-2} | iT | p_1 p_2 \rangle \equiv (2\pi)^4 \delta^{(4)}\left(p_1 + p_2 - \sum_{i=1}^{n-2} q_i\right) i\mathcal{A}_n \; , \tag{1.2}$$

where an overall four-momentum conserving delta function was extracted explicitly.

Scattering amplitudes are traditionally calculated perturbatively within a mathematical framework called Quantum Field Theory (QFT). Interacting QFTs cannot be solved in exact form, so instead we calculate a leading approximation and obtain smaller corrections order by order. The leading approximation is given by tree-level diagrams, while corrections pictorially form loops. We simply draw all possible Feynman diagrams that contribute to the process in consideration and translate them to a definite mathematical expression using the Feynman rules. The latter may be derived directly from the Lagrangian and are in principle sufficient to compute any scattering amplitude. We refer to text books [119, 120] for a more comprehensive treatment of the subject.

Let us here consider the example of scattering five gluons. The leading terms are tracked by 25 diagrams. If we follow the Feynman prescription, the associated calculation yields a result which takes up more than 25 pages. In practice, such amplitude calculations are rapidly obscured by the obvious proliferation of color and spacetime indices. Moreover, at higher multiplicity, the number of diagrams is huge. For these reasons, even tree-level calculations may be severely cumbersome. Indeed, for tree-level

gluon scattering we have

$g + g \longrightarrow g + g$	4 diagrams
$g + g \longrightarrow g + g + g$	25 diagrams
$g + g \longrightarrow g + g + g + g$	220 diagrams

and $g + g \to 8g$ receives contributions from more than one million diagrams. Using supercomputers, leading order calculations to high multiplicities are trivial. However, if we go to the next-to-leading order (NLO) or next-to-next-to-leading order (NNLO) contributions, the calculation completely explodes. In fact, the full five-gluon amplitude in QCD is not known beyond NLO.

1.2.1 Unexpected Hidden Structures and Simplicity

Although the intermediate steps are impossible to carry out without modern supercomputers, the final results are typically extremely simple and compact. The four-gluon amplitude is nonvanishing in the Maximally-Helicity-Violating (MHV) configuration only. This amplitude has precisely two negative helicity gluons and two positive helicity gluons and can in fact be written

$$A_4^{\text{tree}}(1^-, 2^-, 3^+, 4^+) = \frac{\langle 12\rangle^4}{\langle 12\rangle\langle 23\rangle\langle 34\rangle\langle 41\rangle} \,. \tag{1.3}$$

This form utilizes the spinor-helicity formalism for massless particles, see for instance pedagogical reviews by Dixon [106, 108] and by Elvang and Huang [107]. In the 1980s, Stephen Parke and Tomasz Taylor were able to generalize the formula to scattering of n gluons and conjecture that the simplicity of the four-point MHV amplitude extends to all multiplicities, for example,

$$A_n^{\text{tree}}(1^-, 2^-, 3^+, \ldots, n^+) = \frac{\langle 12\rangle^4}{\langle 12\rangle\langle 23\rangle\cdots\langle n1\rangle} \tag{1.4}$$

and similarly,

$$A_n^{\text{tree}}(1^+, 2^+, 3^+, \ldots, n^+) = 0 \,, \tag{1.5}$$
$$A_n^{\text{tree}}(1^-, 2^+, 3^+, \ldots, n^+) = 0 \,. \tag{1.6}$$

This is truly astonishing from the viewpoint of Feynman diagrams. Nair further observed that all amplitudes in the MHV sector are given by a natural and very simple generalization of the Parke-Taylor formula,

$$A_n^{\text{tree}}(\lambda, \tilde{\lambda}, \eta) = i(2\pi)^4 \frac{\delta^{(4)}\left(\sum_{i=1}^n \lambda_i^\alpha \tilde{\lambda}_i^{\dot{\alpha}}\right) \delta^{(8)}\left(\sum_{i=1}^n \lambda_i^\alpha \eta_i^A\right)}{\langle 12\rangle\langle 23\rangle\cdots\langle n1\rangle} \,, \tag{1.7}$$

where the Grassmann variables η conveniently keep track of the particle content of the supermultiplet.

In order to regain control, make hidden symmetries and structures manifest and not least improve the calculational techniques to facilitate precise predictions for collider experiments, a complete reformulation of quantum field theory scattering amplitudes is certainly necessary.

1.3 An Overview of On-Shell Methods

The last two or three decades have seen numerous brilliant attempts to surmount the computational bottleneck which have led to a tremendous progress in our understanding of quantum field theory scattering amplitudes. The upshot is to exploit analyticity and unitarity of the scattering matrix. Analyticity allows for amplitudes to be reconstructed from their singularity structure, whereas by unitarity, residues at the poles factorize onto products of simple amplitudes.

The most successful advances are perhaps the original unitarity method for loop amplitudes proposed by Bern, Dixon, Dunbar and Kosower [3, 4] and the Britto-Cachazo-Feng-Witten (BCFW) on-shell recursion relations [1, 2] for tree-level amplitudes. These works revealed striking and otherwise completely unexpected structures and simplicity by virtue of retaining only physical on-shell information with no reference to the Lagrangian or Feynman diagrams. The most important implications are that all trees may now be constructed recursively and further fused into loops.

The BCFW relations construct tree-level amplitudes recursively by factorizing them onto products of amplitudes involving fewer particles. The process bootstraps all amplitudes from just three-particle amplitudes, whose form we are able to fully fix from general principles of quantum field theory. In other words, the BCFW recursion (more or less) trivializes the computation of all relevant tree-level amplitudes. Needless to say, this was a huge achievement. A similar construction lies behind the Cachazo-Svrcek-Witten (CSW) rules [42] and the MHV vertex expansion [43].

The philosophy of the unitarity method (see also later papers, e.g. refs. [5–24]) is to reconstruct scattering amplitudes from unitarity cuts that place propagators in a given channel on their mass-shell and break it into a product of trees. Examining all unitarity cuts eventually fixes the amplitude unambiguously. The unitarity method has granted otherwise unfeasible computations of scattering processes in QCD to be carried out. Despite its success, the unitarity method has a disadvantage. Many individual integrals contribute to the same unitarity cut and are therefore hard to separate without carrying out intermediate algebraic steps. In that view, the generalized unitarity method of Britto, Cachazo and Feng [7] and Forde [18] is more efficient as it allows several propagators to be cut simultaneously. This implies that only a small subset of integrals are extracted at the same time, leading to compact formulae for their coefficients. As a simple example we can consider the box contribution to the one-loop amplitude. Thanks to generalized unitarity, the box term can be reconstructed entirely from the four three-point tree-level amplitudes sitting at its corners. The box is easy to distinguish from the triangle and the bubble contributions. However, triple cuts are contaminated by boxes which share the three propagators. Knowing the answer for the box from the quadruple cut which cuts all four lines, allows us to in a sense subtract that result and isolate the triangle.

It is fair to say that the unitarity method has revolutionized the way amplitudes are computed, especially at one loop. More importantly, it has facilitated enhanced theoretical predictions of numerous scattering processes of elementary particles relevant for experiments at modern particle colliders. Many of the on-shell techniques are now systematized in software libraries [26–34]. Further developments related to the unitarity method can be found in refs. [35–41].

Another notable advance was the uncovery of Bern-Carrasco-Johansson (BCJ) relations and also the double-copy construction [93–95] which works at both tree- and loop-level. The BCJ relations, proven by Bjerrum-Bohr, Damgaard and Vanhove [96] in a string theory inspired approach, involve tree-level amplitudes that are not related

by recursion. They significantly reduce the number of independent amplitudes to be computed and are thus directly applicable to processes in LHC physics.

The new frontier in amplitude physics in QCD at the LHC consists of NNLO corrections at the two-loop level. Precise theoretical predictions at NNLO are decisive to the success of the LHC program. Developing a consistent and computationally favorable framework for two-loop amplitudes has turned out to be a surprisingly hard problem. Pursuing calculations at the level of a planar two-loop integral basis, the maximal unitarity method proposed by Kosower and Larsen [55], later clarified in ref. [56] by Caron-Huot and Larsen, emerged as a natural continuation of the direct extraction procedures at one loop [7, 18, 19]. The main object of computation is the coefficient in front of each master integral. The hope is that for each basis integral there exists a unique prescription that expresses its coefficient in terms of tree-level data. In previous papers by Johansson, Kosower, Larsen [55, 57, 58] and Caron-Huot and Larsen [56] it has been shown how to extract the coefficients of both planar double-box master integrals with up to four massive external legs using multidimensional contours encircling the global poles of the loop integrand. Zhang and the present author extended the analysis to the nonplanar sector with external masses [59, 61, 62] and even to massless planar triple-box integrals [60]. Very recently it was explained how to treat planar double-box contributions with internal masses in any gauge theory by also taking topological cycles into account [63]. The advantage of maximal unitarity is that one may circumvent the explicit reduction from the integrand basis onto master integrals. However, the increase of complexity compared to one loop still requires a sophisticated approach. The aim of this research direction is to understand the hidden structures to extend the unitarity method in a way that trivializes the computation of two-loop amplitudes for processes that are phenomenologically important to the LHC.

Multiloop amplitudes can also be calculated by integrand-level reduction as demonstrated at several occasions during the last couple of years. The generalization of the Ossola–Papadopoulos–Pittau (OPP) approach at one-loop [15] has been worked out by Badger, Frellesvig, and Zhang [68], and also by Mastrolia and Ossola in ref. [69]. We recommend that the reader also consults refs. [70–78]. In particular, Badger, Frellesvig and Zhang gave the first analytic results for the planar part of the all-plus two-loop five gluon amplitude in QCD in ref. [72] and also obtained partial results at three loops in any gauge theory [70]. We also mention that maximal unitarity cuts without complete localization onto global poles have been studied and used in multiloop problems in supersymmetric gauge and gravity theories [45–52]. Ref. [81]. applied the unitarity method two-loop diagrams to determine their integral bases. Arkani-Hamed and collaborators have developed an integrand-level recursion [87, 88] specialized to the planar contributions in maximally supersymmetric theory, valid to all loop orders. See also refs. [82–86] for related studies. The leading singularity method of refs. [44, 45] previously addressed hepta-cuts and octa-cuts of four-, five- and six-point two-loop amplitudes in $\mathcal{N} = 4$ super Yang-Mills theory. An analysis of the global poles and associated residues of the two-loop six-point $\mathcal{N} = 4$ integrand appeared in ref. [67]. Finally, fascinating iterative structures have been observed [89–92].

1.4 Outline of this Thesis

The body of this thesis features four chapters. The first chapter mainly focuses on reviewing background material on efficient methods for calculating one-loop scattering amplitudes by exploiting unitarity, whereas the remaining three chapters are based on

recent developments described in papers I-V. For the benefit of the reader, we very briefly recap the content of chapters 3-5.

Chapter 3 presents the extension of the generalized unitarity method of Britto, Cachazo and Feng [7] and Forde [18] to two-loop amplitude contributions in generic gauge theories with arbitrary number of fermions and scalars in the adjoint representation of the gauge group. The new framework known as maximal unitarity was recently proposed by Kosower and Larsen [55] (see ref. [56–58] for subsequent developments). Several new extensions are presented, including nonplanar corrections with and without massive external states. In particular, we see that the previously observed simplicity at the tree- and one-loop level continues to leak out at two loops.

A new feature of multiloop amplitudes is the appearance of degenerate multivariate residues in generalized unitarity cuts. Therefore, chapter 4 presents a technique to calculate such residues using methods from computational algebraic geometry. We extend the maximal unitarity formalism to amplitude contributions whose maximal cuts define multivariate algebraic varieties. As an example we demonstrate how to obtain the planar triple-box contribution to three-loop four-gluon scattering with remarkable simple results. The formalism is also used to define generalized cuts of Feynman integrals with higher powers of propagators, which otherwise were meaningless.

The purpose of chapter 5 is to generalize the maximal unitarity formalism to a novel class of Feynman integrals which are presumably not expressible solely in terms of generalized polylogarithms. These integrals have maximal cuts that give rise to algebraic varieties with irrational irreducible components. Our primary example is the four-point planar double-box integral with internal masses. We show how to extract the master integral coefficients uniquely in terms of multivariate residues along with Weierstrass' elliptic functions. Furthermore, we show how to generate the leading-topology part of otherwise infeasible integration-by-parts identities analytically from exact meromorphic differential forms.

Unitarity Methods 2

Every great and deep difficulty bears in itself its own solution.
It forces us to change our thinking in order to find it.
— Niels Bohr (1885–1962)

Scattering amplitudes at loop level are notoriously more complicated objects to calculate than at tree-level. For that reason, loop-level scattering amplitudes are extremely important for our understanding of the underlying structure of quantum field theories such as $\mathcal{N} = 4$ super Yang-Mills and QCD. It is our hope that a deeper control of loop-level corrections will lead to new crucial insights and pave the way for advances in phenomenological aspects of particle physics.

In connection with amplitudes at loop level, we will refer to three basic objects, namely loop integrands, loop integrals and integrated expressions.

(i) The loop integrand is a rational function of internal and external kinematical variables. It consists of a numerator factor and a number of inverse propagators in the denominator.

(ii) The loop integral is a formal object; it is the combination of the loop integrand and the loop-momentum integration measure. The integration region is not specified and divergences are not addressed.

(iii) The integrated expression associated with a loop integral or a loop amplitude is obtained by performing each of the loop-momentum integrations over real Minkowski space $\mathbb{R}^{3,1}$. Regularization is typically required to avoid divergences. The result is expressed in terms of multiple polylogarithms[1] and more generally also elliptic functions.

This chapter starts with a discussion of the implications of unitarity and calculations of discontinuities of amplitudes across branch cuts, primarily based on the text book by Peskin & Schroeder [120], with minor modifications along the way. A radical approach to the computation of loop-level amplitudes is provided by the unitarity method, which is mentioned very briefly. The chapter ends with an introduction to generalized unitarity at one-loop in generic gauge theories with derivations of formulae for the box and triangle contributions.

[1]Multiple polylogarithms form a general class of iterated integrals of which ordinary logarithms, polylogarithms and harmonic polylogarithms are all special cases.

2.1 Implications of Unitarity

Unitarity of the S-matrix, $S^\dagger = S^{-1}$, is a consequence of conservation of probability and implies that the T-matrix introduced in eq. (1.1) must satisfy the condition

$$2\,\mathrm{Im}\,T = -i(T - T^\dagger) = T^\dagger T\ . \tag{2.1}$$

This equation immediately implies what is commonly known as the optical theorem which states that the imaginary part of any forward scattering amplitude is proportional to the total scattering cross section of the process. Further insight on the implications of unitarity may be gained by expanding T perturbatively in the coupling constant,

$$T = \sum_{n=4}^{\infty} g^{n-2}\big(T_n^{(0)} + g^2 T_n^{(1)} + g^4 T_n^{(2)} + \cdots\big)\ , \tag{2.2}$$

and inserting this expression into eq. (2.1). The superscripts refer to the order in perturbation theory, e.g. $T_n^{(0)}$ is a tree-level contribution. The first nontrivial relation is extracted at $\mathcal{O}(g^4)$,

$$-i\big(T_4^{(1)} - T_4^{(1)\dagger}\big) = T_4^{(0)\dagger} T_4^{(0)}\ . \tag{2.3}$$

In order words, the imaginary part of a one-loop amplitude is determined by a product of tree-level amplitudes. Similarly, one can argue that the imaginary parts of two-loop amplitudes are related to products of tree-level and one-loop amplitudes.

2.1.1 Cutkosky Rules and Unitarity Cuts

The qualitative statements about the cross-order relations discussed above may be concretized if we study the S-matrix as an analytic function of the kinematical variables upon which it depends. In general, a one-loop amplitude acquires a branch cut singularity in the presence of a nonzero imaginary part. This follows from the Schwarz reflection principle, see e.g. Peskin & Schroeder [120]. The discontinuity can be calculated by virtue of the Cutkosky rules.

(Cutkosky Rules). The s-channel discontinuity of the Feynman expression

$$\mathcal{M}_n^{(1)}(s) = \int \frac{d^D q}{(2\pi)^D} \frac{N(q)}{((k/2-q)^2 - m^2 + i\epsilon)((k/2+q)^2 - m^2 + i\epsilon)} \tag{2.4}$$

is computed by applying the simultaneous replacements

$$\frac{1}{(k/2 \pm q)^2 - m^2 + i\epsilon} \longrightarrow -2\pi i \delta^{(+)}((k/2 \pm q)^2 - m^2)\ , \tag{2.5}$$

where

$$\delta^{(+)}(\cdots) \equiv \theta(k^0)\delta(\cdots)\ . \tag{2.6}$$

The proof of the Cutkosky rules involves closing the integration contour into the complex plane, carefully keeping track of the intricate pole structure implied by the Feynman $i\epsilon$-prescription. For now we refer to the proof in ref. [120] which only requires minor augmentations in order to conform with the more general case considered here. The discontinuity only receives contributions from momenta that simultaneously put the

two propagators in the specific channel on their mass shell. On the support of the two delta functions, the numerator factorizes onto the product of two on-shell tree-level amplitudes. More specifically, the discontinuity can be written

$$\begin{aligned}\mathrm{Disc}_s\, \mathcal{M}_n^{(1)}(s+i\epsilon) = \\ (-2\pi i)^2 \int \frac{d^D q}{(2\pi)^D} \delta^{(+)}(k/2-q)^2 - m^2)\delta^{(+)}(k/2+q)^2 - m^2) \\ \times \tilde{A}_L^{\text{tree}}(k_1,\ldots,k_j,k/2+q,k/2-q)\tilde{A}_R^{\text{tree}}(k_{j+1},\ldots,k_n,-(k/2-q),-(k/2+q))\,,\end{aligned} \tag{2.7}$$

where the tildes remind us that the trees are not on-shell before the delta functions are integrated out. We will refer to the simultaneous replacements (2.5) as two-particle unitarity cuts.

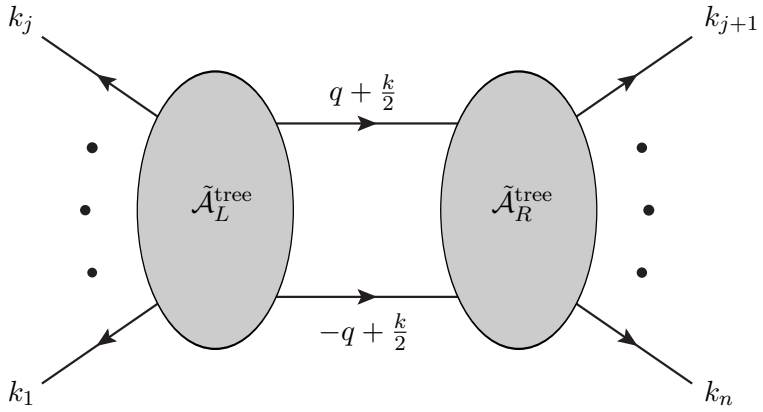

Figure 2.1: A generic s-channel Feynman diagram contributing to the n-point one-loop amplitude. The gray blobs are essentially off-shell trees.

2.1.2 Kramers-Kronig Relations

We have seen that tree-level data suffices to compute the imaginary part of one-loop amplitudes. For sufficiently well-behaved gauge theories (such as supersymmetric theories) the real part can be obtained as a dispersion integral and the amplitude can be determined completely. This was essentially the philosophy of the analytic S-matrix program pursued back in the 1960s.

One-loop amplitudes of supersymmetric theories are holomorphic functions of s in the upper half of the complex s-plane. Under these circumstances, the imaginary and real parts of the amplitude are no longer independent, and must satisfy the Kramers-Kronig relations,

$$\mathrm{Re}\,\mathcal{M}_n^{(1)}(s) = +\frac{1}{\pi}\,\mathrm{PV}\int_{-\infty}^{+\infty} ds' \frac{\mathrm{Im}\,\mathcal{M}^{(1)}(s')}{s'-s}\,, \tag{2.8}$$

$$\mathrm{Im}\,\mathcal{M}_n^{(1)}(s) = -\frac{1}{\pi}\,\mathrm{PV}\int_{-\infty}^{+\infty} ds' \frac{\mathrm{Re}\,\mathcal{M}^{(1)}(s')}{s'-s}\,. \tag{2.9}$$

The Kramers-Kronig relations are trivial to derive by closing the integration contour and invoking Cauchy's residue theorem.

2.1.3 The Unitarity Method

The analytic S-matrix program of the 1960s experienced a breakdown caused by the difficulty of carrying out the required dispersion integrals in order to also reconstruct the real part of the amplitudes. The origin of the problem was the presence of additional singularities. In the early 1990s, Bern, Dixon, Dunbar and Kosower (BDDK) realized that the structure of the appearing one-loop integrals is much simpler than it ought to be. In particular, BDDK expressed the amplitude as a linear combination of a small set of integrals — an ansatz — and computed the discontinuities in all possible channels on both sides of the equation,

$$\mathcal{A}_n^{L-\text{loop}} = \sum_{j \in \text{Ansatz}} c_j I_j \implies \text{Disc}\, \mathcal{A}_n^{L-\text{loop}} = \sum_{j \in \text{Ansatz}} c_j \,\text{Disc}\, I_j \,. \tag{2.10}$$

A pictorial representation of the cut ansatz can be found in fig. 2.2. The principle is simply to enlarge the ansatz until all unitarity cuts can be satisfied. Following this procedure, BDDK were able to relate the integral coefficients to products of tree-level amplitudes through the Cutkosky rules and unambiguously determine a widespread of amplitudes in supersymmetric and nonsupersymmetric theories. This led to the resurrection of unitarity and the unitarity method has undoubtedly proven to be one of the most important developments in the field of scattering amplitudes.

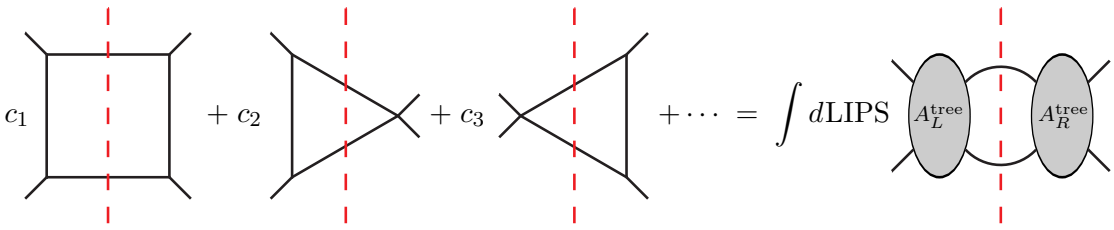

Figure 2.2: The unitarity cut (indicated by the dashed red line) of the four-point one-loop amplitude (right) and the corresponding ansatz (left). The $\cdots$ denote additional terms that may have support on this cut, such as the bubble integral. There is an implicit sum over internal states and helicity configurations between the subamplitudes.

2.2 Reduction Techniques

The existence of a simple basis of linearly independent one-loop Feynman integrals has underpinned important developments in the area of one-loop amplitudes in gauge theories including QCD. Here we review the content of the one-loop integral basis and also comment on the integrand basis. We will take the external momenta to be strictly four-dimensional throughout this thesis. All internal momenta are massless, whereas external lines may be massive (for example representing sums of massless momenta in the original kinematics).

Any one-loop integral can be constructed by attaching external legs to the one-loop vacuum diagram as illustrated in fig. 2.3. In particular, the topology of a one-loop integral is completely characterized by the number of external legs. We shall denote the one-loop scalar integral as follows,

$$I_n(K_1, \ldots, K_n)[1] \equiv \int \frac{d^D\ell}{(2\pi)^D} \frac{1}{\ell^2(\ell - K_1)^2(\ell - K_{12})^2 \cdots (\ell - K_{1\cdots(n-1)})^2} \,, \tag{2.11}$$

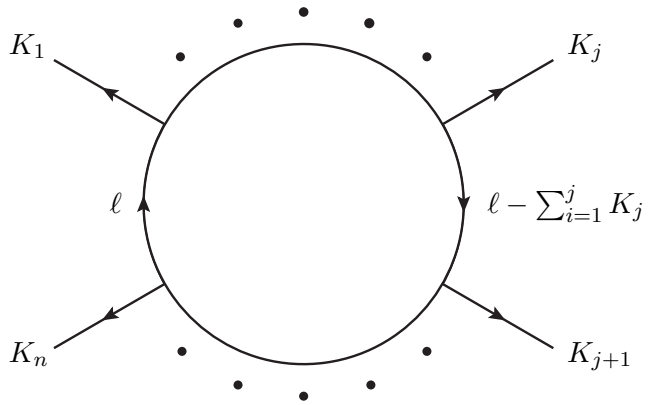

Figure 2.3: The general one-loop integral with n cyclically ordered external legs with momenta $K_1, \ldots, K_n$. Internal particles are assumed to be massless.

where $K_{i\cdots j} = K_i + \cdots K_j$. All external momenta are assumed to be outgoing by convention. A generic n-point gauge theory amplitude gives rise to integrals with up to n powers of the loop momentum in the numerator. We will refer to a one-loop integral that has a generic numerator $\Phi(\ell)$ with nontrivial loop-momentum dependence as a tensor integral and use the notation $I_n[\Phi(\ell)]$.

2.2.1 Integral Basis

Instead of evaluating tensor integrals directly, one uses integral reduction equations to relate the desired integral to a linear combination of simpler integrals. It is a well-established fact that any one-loop integral can be reduced to a minimal basis of scalar integrals with at most four propagators in strictly four dimensions. The basis integrals have topologies of boxes, triangles, bubbles and tadpoles. In particular, we can bring the whole one-loop amplitude into the form

$$\mathcal{A}_n^{(1)} = \sum_{\text{boxes}} c_{\square} I_{\square} + \sum_{\text{triangles}} c_{\triangle} I_{\triangle} + \sum_{\text{bubbles}} c_{\circ} I_{\circ} + \sum_{\text{tadpoles}} c_{-\circ} I_{-\circ} + \text{rational terms} \quad (2.12)$$

where the sums include all possible ways of distributing the n cyclically ordered external legs at the vertices of the integrals. Note that the integral coefficients are independent of the dimensional regulator; additional rational terms appear as compensation. The integrals themselves are computed in dimensional regularization once and for all. The expansion coefficients then become the main object of calculation. The basis decomposition is depicted in fig. 2.4.

The independent configurations of the box integral are four-mass, three-mass, two-mass easy, two-mass hard, one-mass and zero-mass,

$$\{I_4^{4m}, I_4^{3m}, I_4^{2me}, I_4^{2mh}, I_4^{m}, I_4^{0m}\} \,. \quad (2.13)$$

The two-mass easy integral has massive momenta at diagonally opposite corners, while the two-mass hard integral has adjacent massive momenta. There are three independent triangle master integrals, namely the three-mass, two-mass and one-mass configurations,

$$\{I_3^{3m}, I_3^{2m}, I_3^{m}\} \,. \quad (2.14)$$

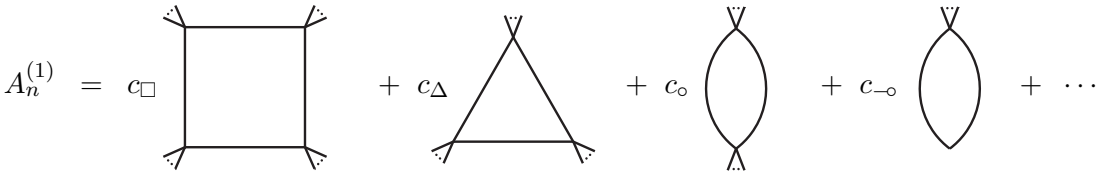

Figure 2.4: A graphical representation of a generic one-loop amplitude in terms of master integrals: boxes, triangles, bubbles and tadpoles (only present in the general case of massive propagators). The trailing dots indicate that there is an implicit sum over all inequivalent distributions of the (cyclically ordered) external legs.

For scalar bubble and tadpoles integrals, all external momenta are necessarily massive, so we only have the master integrals $I_2[1]$ and $I_1[1]$. All one-loop basis integrals can be found in fig. 2.5.

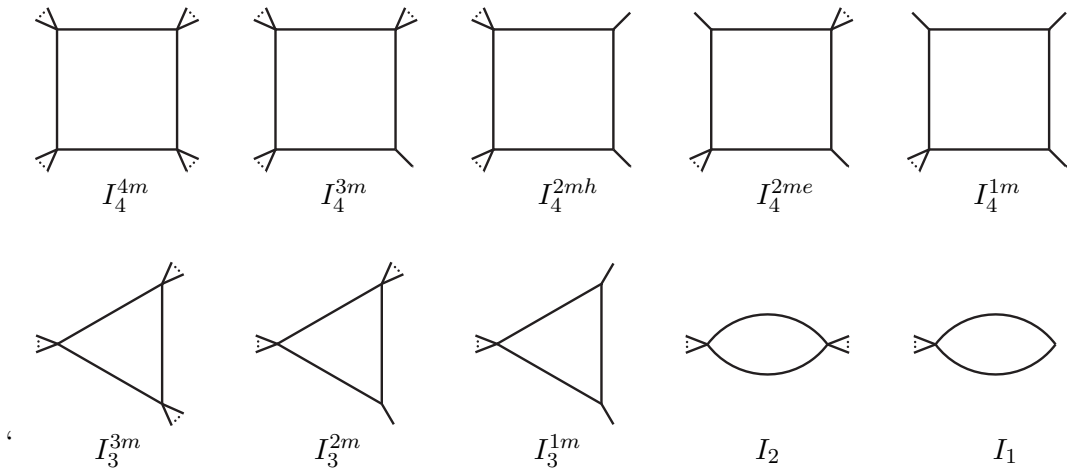

Figure 2.5: Master integrals at the one-loop level: the four-mass, three-mass, two-mass-hard, two-mass-easy, one-mass boxes, the one-, two- and three-mass triangles along with the bubble and tadpole. The four-point zero-mass configuration of the box was omitted here.

2.2.2 Integrand Basis

Although the scalar basis decomposition (2.12) is very general and holds for an arbitrary one-loop scattering amplitude, it has an implicit assumption which is crucial to shed light on. The integral reduction onto masters relies on integrals being evaluated in real Minkowski space, or equivalently, in Euclidean space by Wick rotation. More generally, we will think of complexifying the internal degrees of freedom and deform the integration into $\mathbb{C}^4$. In fact, this is precisely the philosophy which underlies the operation of taking generalized unitarity cuts as will become clear through the remainder of this thesis.

Let us consider the box term of eq. (2.12). The momenta of the four corners are subject to the condition $\sum_i^4 K_i = 0$. We are able to span the four-dimensional momentum space by supplementing three of the momenta, say, K_1, K_2 and K_4 by an orthogonal

direction which we call ω. Thus, $\omega \cdot K_i = 0$ with $\omega^2 \geq 0$. Any four-dimensional vector can be expanded as a linear combination of these momenta. Moreover, all dot products between the loop momentum and external vectors are trivially expressed in terms of inverse propagators. On the contrary, the remaining dot product $(\ell \cdot \omega)$ is an irreducible scalar product (ISP). As such, we arrive at the parametrization

$$N_{\square}(\ell) = \sum_{\alpha \in \text{Basis}} c_\alpha (\ell \cdot \omega)^\alpha \, . \tag{2.15}$$

The terms in the sum are constrained by a Gram determinant relation which implies that $(\ell \cdot \omega)^2$ is a reducible scalar product (RSP). The integrand basis for the box term is therefore given by

$$N_{\square}(\ell) = 1 + c_1 (\ell \cdot \omega) \, . \tag{2.16}$$

It can be shown that $(\ell \cdot \omega) \propto \varepsilon(\ell, K_1, K_2, K_4)$. The linear term in the box integrand is called spurious or parity-odd because it vanishes identically upon integration over the real slice. Indeed, restricting the integration contour to $\mathbb{R}^D$ implies

$$\int_{\mathbb{R}^D} \frac{d^D \ell}{(2\pi)^D} \frac{\varepsilon(\ell, K_1, K_2, K_4)}{\ell^2 (\ell - K_1)^2 (\ell - K_{12})^2 (\ell + K_4)^2} = 0 \, . \tag{2.17}$$

The integrand-level reduction (2.16) is known as the OPP approach to one-loop amplitudes [15].

A similar analysis applies to the triangle topology [15]. Here we follow ref. [68]. The triangle only has two independent external momenta, so we need two auxiliary vectors ω_1 and ω_2 in order to span the four-dimensional momentum space. There are two ISPs, namely $(\ell \cdot \omega_1)$ and $(\ell \cdot \omega_2)$. Accordingly, we parametrize the triangle integrand as follows,

$$N_{\Delta}(\ell) = \sum_{\{\alpha,\beta\} \in \text{Basis}} c_{\alpha\beta} (\ell \cdot \omega_1)^\alpha c_{\alpha\beta} (\ell \cdot \omega_2)^\beta \, . \tag{2.18}$$

Renormalizability requires that $\alpha + \beta \leq 3$. Applying Gram determinants leads to the integrand basis

$$\begin{aligned} N_{\Delta}(\ell) = {} & c_{00} + c_{10}(\ell \cdot \omega_1) + c_{01}(\ell \cdot \omega_2) + c_{11}(\ell \cdot \omega_1)(\ell \cdot \omega_2) \\ & + c_{12}(\ell \cdot \omega_1)(\ell \cdot \omega_2)^2 + c_{21}(\ell \cdot \omega_1)^2 (\ell \cdot \omega_2) + c_{20;02}((\ell \cdot \omega_1)^2 - (\ell \cdot \omega_2)^2) \, . \end{aligned} \tag{2.19}$$

In this way all terms proportional to $(\ell \cdot \omega_i)$ integrate to zero on $\mathbb{R}^D$.

2.3 Basics of Multivariate Residues

Generalized unitarity cuts of Feynman integrals are naturally formulated in terms of multidimensional contour integrals that compute multivariate residues rather than using the delta function prescription. The explanation is that multifold unitarity cuts are not supported on the real slice for generic external momenta. Consequently, cutting the propagators on-shell yields a trivial equation. The obvious generalization of integrating out a Dirac delta function on the real line, i.e.

$$\int_{-\infty}^{+\infty} dq \delta(q - q_0) f(q) = f(q_0) \, , \tag{2.20}$$

is immediately realized by defining

$$\delta(q-q_0) \equiv \frac{1}{2\pi i}\frac{1}{q-q_0} \tag{2.21}$$

and replacing the contour $\mathbb{R} \to C(q_0)$. The contur integral

$$\frac{1}{2\pi i}\oint_{C(q_0)} \frac{f(q)}{q-q_0} \tag{2.22}$$

simply computes the residue by Cauchy's residue theorem. In this section we will motivate the higher-dimensional analog.

Let the meromorphic function $F : \mathbb{C}^2 \to \mathbb{C}$ be given by

$$F(z_1,z_2) = \frac{h(z_1,z_2)}{(az_1+bz_2+c)(ez_1+fz_2+g)}\ , \tag{2.23}$$

and assume regularity of $h : \mathbb{C}^2 \to \mathbb{C}$. We denote $f_1(z_1,z_2) = az_1+bz_2+c$ and $f_2(z_1,z_2) = ez_1+fz_2+g$ and examine the simultaneous zeros of the denominator factors. These points are referred to as *global poles* $\mathcal{G}_1$ and $\mathcal{G}_2$ of the integrand,

$$\mathcal{G}_1 \cup \mathcal{G}_2 = \{\, z \in \mathbb{C}^2 \mid f_1(z) = 0\,,\ f_2(z) = 0\,\}\ . \tag{2.24}$$

We would like to make sense of the residues of F at the global poles. A natural definition is achieved as follows. Consider the contour integral of F taken over a small torus $T^2(\xi) \simeq (S^1)^2$ encircling the point $\xi \in \{\mathcal{G}_1,\mathcal{G}_2\}$. We can specify the discussion at the origin by changing variables $w_1 = f_1(z_1,z_2)$ and $w_2 = f_2(z_1,z_2)$. The transformation of the contour integral,

$$\oint_{T^2(\xi)} \frac{h(z_1,z_2)dz_1dz_2}{(az_1+bz_2+c)(ez_1+fz_2+g)} = \oint_{T^2(0)} \frac{dw_1dw_2}{w_1w_2}\frac{h(z_1(w),z_2(w))}{\det\left(\frac{\partial(w_1,w_2)}{\partial(z_1,z_2)}\right)}\ , \tag{2.25}$$

suggests that we define the residue of F at $\xi \in \{\mathcal{G}_1,\mathcal{G}_2\}$ by

$$\mathrm{Res}_{\xi\in\{\mathcal{G}_1,\mathcal{G}_2\}}F(z_1,z_2) = \left.\frac{h(z_1(\omega),z_2(\omega))}{\det\frac{\partial(w_1,w_2)}{\partial(z_1,z_2)}}\right|_{z=\xi}\ . \tag{2.26}$$

The generalization to functions $F : \mathbb{C}^n \to \mathbb{C}$ of n complex variables $z = (z_1,\ldots,z_n)$ and $m \geq n$ denominator factors,

$$F(z_1,\ldots,z_z) = \frac{h(z_1,\ldots,z_n)}{p_1(z_1,\ldots,z_n)\cdots p_m(z_1,\ldots,z_n)}\ , \tag{2.27}$$

is straightforward. Indeed, we impose $p_{i_1}(z) = \cdots = p_{i_n}(z) = 0$ to determine a set of global poles $\{\mathcal{G}_i\}$. The residue of F evaluated at $\xi \in \{\mathcal{G}_i\}$ takes the form

$$\mathrm{Res}_{\xi\in\{\mathcal{G}_i\}}F(z) = \left.\frac{h(z(w))}{\prod_{i\neq(i_1,\ldots,i_n)}p_i(z(w)))\det\frac{\partial(p_{i_1},\ldots,p_{i_n})}{\partial(z_1,\ldots,z_n)}}\right|_{z=\xi} \tag{2.28}$$

provided that the Jacobian is nonvanishing; in this case, the residue is termed nondegenerate. The general case is treated in chap. 4.

2.4 Quadruple Cuts and Box Coefficients

Let us focus our attention on extracting the coefficient in front of the one-loop scalar box integral in eq. (2.12), working to leading order in the dimensional regulator. This problem was first addressed by means of quadruple cuts by Britto, Cachazo and Feng (BCF) in ref. [7] and the derivation was later clarified in ref. [55]. The virtue of the quadruple cut is that it only selects box integrals.

The box integral shown in fig. 2.7 is

$$I_{\Box} = \int \frac{d^D\ell}{(2\pi)^D} \frac{1}{\ell^2(\ell-k_1)^2(\ell-K_{12})^2(\ell+k_4)^2} = \int \frac{d^D\ell}{(2\pi)^D} \frac{1}{\prod_{i=1}^4 p_i^2(\ell)} \,, \tag{2.29}$$

where $k_1, \ldots, k_4$ are the massless external momenta attached to the four corners. For each such a quartet of momenta, the solution set for the quadruple cut equations that simultaneously put all propagators on-shell consists of a complex conjugate pair[2],

$$\begin{aligned} \mathcal{G} = \big\{ \ell \in \mathbb{C}^4 \mid \ell^2 = 0 \,,\ (\ell-k_1)^2 = 0 \,, \\ (\ell-k_1-k_2)^2 = 0 \,,\ (\ell+k_4)^2 = 0 \big\} = \mathcal{G}_1 \cup \mathcal{G}_2 \,. \end{aligned} \tag{2.30}$$

The kinematical structure of the quadruple cut solutions can be understood from the two allowed configurations of nonconsecutive chiral and antichiral three-vertices. This part is explained in fig. 2.6 and the two branches of the quadruple cut are illustrated in fig. 2.7.

Figure 2.6: Momentum conservation in the massless three-particle vertex implies that either (i) the chiral spinors are proportional, denoted by a black blob, allowing only a $\overline{\text{MHV}}$ vertex to be attached or (ii) the antichiral spinors are proportional, denoted by a white blob, allowing only a MHV vertex to be attached. Be aware that the notation of chiral and antichiral vertices is not uniform in the literature.

We can easily evaluate the quadruple cut of the box integral and localize the integrand to a point specified by either of the two solutions. However, the presence of two solutions raises an immediate question: what is the relative normalization? The naive prescription is just to take an average of the two quadruple cut residues. It only works because this example is so simple. In general, calculating the quadruple cut on both sides of eq. (2.12) along an arbitrary linear combination of tori encircling $\mathcal{G}_1$ and $\mathcal{G}_2$ produces inconsistent results. The remedy is to impose the constraint

$$I_{\Box}[N_{\Box}(\ell)] = I_{\Box}[1] \implies I_{\Box}[N_{\Box}(\ell)]\big|_{4-\text{cut}} = I_{\Box}[1]\big|_{4-\text{cut}} \,, \tag{2.31}$$

[2]Technically speaking, identification by complex conjugation presumes reality of the external momenta.

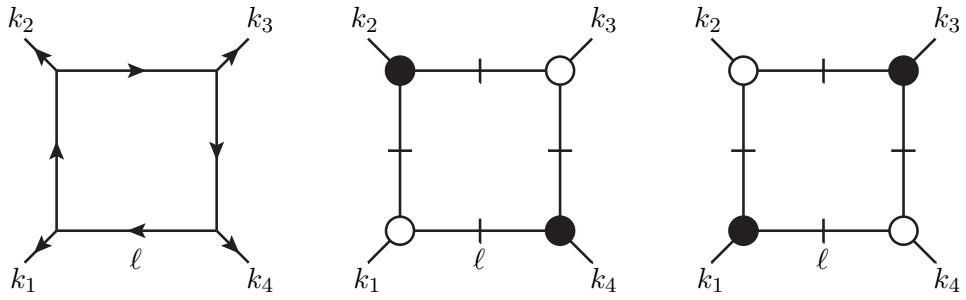

Figure 2.7: The one-loop box integral (left) along with diagrams corresponding to the two quadruple cut solutions $\mathcal{G}_1$ and $\mathcal{G}_2$.

or equivalently,

$$0 = \int_{\mathbb{R}^D} \frac{d^D\ell}{(2\pi)^D} \frac{\varepsilon(\ell, k_1, k_2, k_4)}{\prod_{i=1}^4 p_i^2(\ell)} \implies \sum_{\xi\in\{\mathcal{G}_1,\mathcal{G}_2\}} \Omega_a \int_{T^4(\xi)} \frac{d^4\ell}{(2\pi)^4} \frac{\varepsilon(\ell, k_1, k_2, k_4)}{\prod_{i=1}^4 p_i^2(\ell)} = 0\,. \quad (2.32)$$

Note that deforming the integration contour away from real Minkowski space renders the integral infrared finite, so the dimensional regulator may be neglected. It is elementary that eq. (2.32) is respected if we compute the quadruple cut with a relative normalization of integration contours that is a simple average of the infinitesimal four-tori encircling each global pole [55]. In fact, this is the unique prescription. For a generic numerator function $\Phi(\ell)$ we will therefore simply define the augmented quadruple cut

$$\int_{\mathbb{R}^D} \frac{d^D\ell}{(2\pi)^D} \frac{\Phi(\ell)}{\prod_{i=1}^4 p_i^2(\ell)}\bigg|_{4-\text{cut}} \equiv \frac{1}{2} \sum_{\xi\in\{\mathcal{G}_1,\mathcal{G}_2\}} \oint_{T^4(\xi)} \frac{d^4\ell}{(2\pi)^4} \frac{\Phi(\ell)}{\prod_{i=1}^4 p_i^2(\ell)}\,. \quad (2.33)$$

Freezing the internal lines at the values specified by the on-shell solutions factorizes the one-loop amplitude onto a product of four tree amplitudes which are summed over all possible assignments of internal particles and helicities. Applying the quadruple cut to the master integral reduction equation yields the schematic relation

$$\frac{c_\square}{2} \sum_{\xi\in\{\mathcal{G}_1,\mathcal{G}_2\}} \oint_{T^4(\xi)} \frac{d^4\ell}{(2\pi)^4} \prod_{i=1}^4 \frac{1}{p_i^2(\ell)} = \frac{1}{2} \sum_{\xi\in\{\mathcal{G}_1,\mathcal{G}_2\}} \sum_{\substack{\text{helicities}\\ \text{particles}}} \oint_{T^4(\xi)} \frac{d^4\ell}{(2\pi)^4} \prod_{i=1}^4 \frac{1}{p_i^2(\ell)} A_i^{\text{tree}}(p_i(\ell), p_{i+1}(\ell), k_i)\,. \quad (2.34)$$

In order to isolate $c_\square$ from eq. (2.34) and derive the desired closed-form BCF formula for the box integral coefficient we have to consider the Jacobians

$$J_{\text{BCF}}(\xi) = \left(\det_{i,\mu} \frac{\partial p_i^2}{\partial \ell^\mu}\right)\bigg|_{\xi\in\{\mathcal{G}_1,\mathcal{G}_2\}} \quad (2.35)$$

associated with change of variables from ℓ^μ to $p_i^2(\ell)$ on each side of the quadruple cut equation. The specific form of the Jacobian is not important for our purposes as it gives the same result for $\mathcal{G}_1$ and $\mathcal{G}_2$. Hence we just cancel the Jacobian on both sides

of eq. (2.34). The box coefficient is therefore given by the product of the four tree-level amplitudes evaluated at complex momenta arising by cutting all internal lines on-shell,

$$\boxed{c_{\square} = \frac{1}{2} \sum_{a=1,2} \sum_{\substack{\text{helicities} \\ \text{particles}}} \prod_{i=1}^{4} A_i^{\text{tree}}(p_i(\xi), p_{i+1}(\xi), k_i)\big|_{\mathcal{G}_a} .} \tag{2.36}$$

This derivation is easily repeated for any other configuration of massless and massive external momenta, with the same result.

The BCF quadruple cut formula is beautiful and strikingly simple. It uniquely expresses any one-loop gauge theory scalar box integral coefficient in terms of just a product of four tree amplitudes evaluated at complex momenta arising by simultaneously promoting all internal lines to on-shell values.

2.4.1 Example: $--++$ Helicities

We demonstrate the BCF formula for massless scattering of four gluons with external helicities $--++$. Consider the quadruple cut box in fig. 2.8. It suffices to work out the details appropriate to branch $\mathcal{G}_1$. By chirality considerations follows that

$$p_1^{\mu} = \frac{1}{2}\langle p_1|\gamma^{\mu}|p_1] \propto \langle 4|\gamma^{\mu}|1] , \quad p_2^{\mu} = \frac{1}{2}\langle p_2|\gamma^{\mu}|p_2] \propto \langle 2|\gamma^{\mu}|1] . \tag{2.37}$$

The constants of proportionality are easily fixed by imposing momentum conservation $p_2 = p_1 - k_1$, with the result

$$p_1^{\mu} = -\frac{1}{2}\frac{\langle 12\rangle}{\langle 24\rangle}\langle 4|\gamma^{\mu}|1] , \quad p_2^{\mu} = -\frac{1}{2}\frac{\langle 14\rangle}{\langle 24\rangle}\langle 2|\gamma^{\mu}|1] . \tag{2.38}$$

The remaining two internal lines can be treated similarly and solution $\mathcal{G}_2$ can be obtained by spinor conjugation, so we will spare the reader for the explicit expressions.

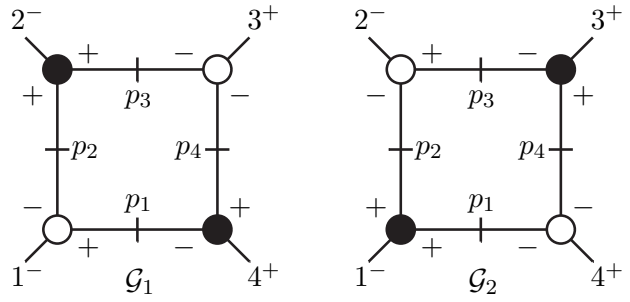

Figure 2.8: The depicted quadruple cut forbids scalars and fermions to propagate in the loop on either of the two branches $\mathcal{G}_1$ and $\mathcal{G}_2$. This can easily be seen from the internal helicity labels.

The valid assignments of helicities at the internal lines in fig. 2.8 allows only gluons to circulate in the loop. This in turn implies that our example applies to any massless gauge theory, including QCD and $\mathcal{N} = 4, 2, 1$ super Yang-Mills theory.

A short exercise in spinor manipulations shows that

$$\sum_{\substack{\text{helicities} \\ \text{particles}}} \prod_{i=1}^{4} A_{(i)}^{\text{tree}}\Big|_{\mathcal{G}_{1,2}} = i s_{12} s_{14} A_{--++}^{\text{tree}} , \tag{2.39}$$

where the overall tree-level amplitude is given by the Parke-Taylor formula (1.4),

$$A^{\text{tree}}_{--++} = \frac{i\langle 12\rangle^4}{\langle 12\rangle\langle 23\rangle\langle 34\rangle\langle 41\rangle} \,. \tag{2.40}$$

Feeding this expression through the BCF formula (2.36) immediately produces the desired box coefficient; the result is simply

$$c_\Box = \frac{1}{2}\sum_{a=1,2}\sum_{\substack{\text{helicities}\\ \text{particles}}}\prod_{i=1}^{4} A^{\text{tree}}_{(i)}\Big|_{\mathcal{G}_a} = is_{12}s_{14}A^{\text{tree}}_{--++} \,. \tag{2.41}$$

2.5 Triple Cuts and Triangle Coefficients

We will also present a compact formula for the coefficient of the scalar triangle integral with possibly massive corners K_1, K_2 and K_3, valid in any gauge theory. A direct extraction procedure for the triple-box coefficient was first reported by Forde [18]. The present derivation follows ref. [118].

The triangle in question is depicted in fig. 2.9 and the scalar integral expression is given by

$$I_\Delta(K_1,K_2,K_3) = \int \frac{d^D\ell}{(2\pi)^D}\frac{1}{\ell^2(\ell-K_1)^2(\ell-K_1-K_2)^2} = \int \frac{d^D\ell}{(2\pi)^D}\prod_{i=1}^{3}\frac{1}{p_i^2(\ell)} \,. \tag{2.42}$$

To solve the problem, we apply to eq. (2.12) a triple cut which projects out a unique

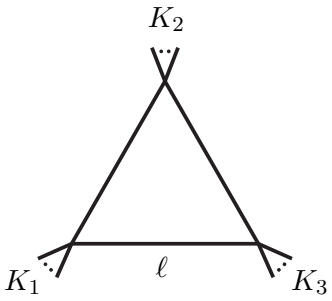

Figure 2.9: The one-loop triangle diagram with external momenta K_1, K_2 and K_3.

triangle integral with coefficient c_Δ along with multiple boxes, each of which has an additional propagator. We construct a pair of massless flattened vectors $K_1^{\flat,\mu}$ and $K_2^{\flat,\mu}$ in order to obtain a convenient parametrization of the loop momentum,

$$\ell^\mu = \alpha_1 K_1^{\flat,\mu} + \alpha_2 K_2^{\flat,\mu} + \alpha_3\langle K_1^\flat|\gamma^\mu|K_2^\flat] + \alpha_4\langle K_2^\flat|\gamma^\mu|K_1^\flat] \,. \tag{2.43}$$

For more information about the flattening procedure, refer to sec. 3.2.5. The inverse propagators of the triangle integral take the following form in terms of the parametrization (2.43),

$$p_1^2(\alpha) = \gamma(\alpha_1\alpha_2 - 4\alpha_3\alpha_4) \,, \tag{2.44}$$

$$p_2^2(\alpha) = \gamma((\alpha_1-1)(\alpha_2 - S_1/\gamma) - 4\alpha_3\alpha_4) \,, \tag{2.45}$$

$$p_3^2(\alpha) = \gamma((\alpha_1 - S_2/\gamma - 1)(\alpha_2 - S_1/\gamma - 1) - 4\alpha_3\alpha_4) \,. \tag{2.46}$$

Evidently, the joint solution of $p_1^2 = p_2^2 = p_3^2 = 0$ is

$$\alpha_1 = \frac{\gamma(S_2+\gamma)}{\gamma^2 - S_1S_2}\,, \quad \alpha_2 = \frac{S_1S_2(S_1+\gamma)}{\gamma(S_1S_2-\gamma^2)}\,, \quad \alpha_3\alpha_4 = -\frac{S_1S_2(S_1+\gamma)(S_2+\gamma)}{4(\gamma^2-S_1S_2)^2}\,. \tag{2.47}$$

The third on-shell equation in eq. (2.47) gives rise to two distinct classes of kinematical solutions depending on whether $S_1S_2 = 0$ or not. Let us start by considering the case $S_1S_2 = 0$, assuming $S_1 = 0$ and $S_2 \neq 0$. In those circumstances, there are two kinematically inequivalent solutions $\mathcal{S}_1$ and $\mathcal{S}_2$,

$$\mathcal{S}_1 : \begin{cases} \alpha_1 = 1 + S_2/\gamma\,, & \alpha_2 = 0\,, \\ \alpha_3 = z\,, & \alpha_4 = 0\,, \end{cases} \qquad \mathcal{S}_2 : \begin{cases} \alpha_1 = 1 + S_2/\gamma\,, & \alpha_2 = 0\,, \\ \alpha_3 = 0\,, & \alpha_4 = z\,, \end{cases} \tag{2.48}$$

parametrized by a single complex variable $z \in \mathbb{C}$. It suffices to average over the two configurations in order to project out parity-odd terms which integrate to zero on the real slice, as was the case for the quadruple cut above. The augmented triple cut takes the form,

$$\begin{aligned} \frac{1}{2}\sum_{\xi\in\{\mathcal{S}_1,\mathcal{S}_2\}} \oint_{T^3(\xi)} \frac{d^4\alpha}{(2\pi)^4} \left(\det_{\mu,i} \frac{\partial \ell^\mu}{\partial \alpha_i}\right) \prod_{i=1}^3 \frac{1}{p_i^2(\alpha)} \left(c_\Delta + \sum_{\text{boxes}} c_\square I_\square\big|_{3-\text{cut}}\right) = \\ \frac{1}{2}\sum_{\xi\in\{\mathcal{S}_1,\mathcal{S}_2\}} \sum_{\substack{\text{helicities} \\ \text{particles}}} \oint_{T^3(\xi)} \frac{d^4\alpha}{(2\pi)^4} \left(\det_{\mu,i} \frac{\partial \ell^\mu}{\partial \alpha_i}\right) \prod_{i=1}^3 \frac{1}{p_i^2(\alpha)} A_i^{\text{tree}}(p_i(\alpha), p_{i+1}(\alpha), K_i)\,, \end{aligned} \tag{2.49}$$

where the sum in the parenthesis on the left hand side includes all cut boxes sharing the three internal momenta of the triangle in question.

The three-dimensional residues associated with the two branches of the triangle cut evaluate with the same result,

$$\left(\det_{i,j} \frac{\partial p_i^2}{\partial \alpha_j}\right)\Big|_{\mathcal{S}_{1,2}} = 4\gamma(\gamma^2 - S_1S_2)z\,, \tag{2.50}$$

and our expression for the triple-cut triangle integral therefore becomes,

$$I_\Delta\big|_{3-\text{cut}} = \frac{i\gamma}{8(\gamma^2 - S_1S_2)} \sum_{\xi\in\{\mathcal{S}_1,\mathcal{S}_2\}} \oint_{T^3(\xi)} \frac{dz}{z}\,. \tag{2.51}$$

The pole at $z = 0$ which arises in the Jacobian is known as a composite leading singularity. The triple-cut box integrals can be computed in a similar fashion. The specific expressions are not important for our purpose though. Indeed, it suffices to realize that the additional propagator from a box integral merely has a simple pole at a finite value of z,

$$I_\square\big|_{3-\text{cut}} \propto \sum_{\xi\in\{\mathcal{S}_1,\mathcal{S}_2\}} \oint_{T^3(\xi)} \frac{dz}{z(z - z_{\square,\xi})}\,, \tag{2.52}$$

The crucial observation is that the triple cut box integrals have vanishing residues at $z = \infty$, which is easy to argue from power counting. This implies that we can easily construct triangle projectors by encircling this pole. Accordingly, from eq. (2.49),

$$\boxed{S_1S_2 = 0 : \quad c_\Delta = \frac{1}{2}\sum_{a=1,2} \sum_{\substack{\text{helicities} \\ \text{particles}}} \oint_{C(\infty)} \frac{dz}{z} \prod_{i=1}^3 A_i^{\text{tree}}(z)\Big|_{\mathcal{S}_a}\,.} \tag{2.53}$$

This is essentially the result obtained by Forde [18].

In the nondegenerate case $S_1 S_2 \neq 0$, there is just a single simultaneous zero of p_1^2, p_2^2 and p_3^2. By direct calculation, we find that this triple cut corresponds to setting the parameters to the following values,

$$\mathcal{S}: \begin{cases} \alpha_1 = \dfrac{\gamma(S_2+\gamma)}{\gamma^2 - S_1 S_2}\,, & \alpha_2 = \dfrac{S_1 S_2 (S_1+\gamma)}{\gamma(\gamma^2 - S_1 S_2)}\,, \\ \alpha_3 = z\,, & \alpha_4 = -\dfrac{S_1 S_2 (S_1+\gamma)(S_2+\gamma)}{4(\gamma^2 - S_1 S_2) z}\,. \end{cases} \tag{2.54}$$

The above derivation of the triangle coefficient extends seamlessly to the new problem at hand, except that we no longer have multiple branches to average over. In that view, we immediately find

$$\boxed{S_1 S_2 \neq 0: \quad c_\Delta = \sum_{\substack{\text{helicities} \\ \text{particles}}} \oint_{C(\infty)} \frac{dz}{z} \prod_{i=1}^{3} A_i^{\text{tree}}(z)\Big|_{\mathcal{S}}\,.} \tag{2.55}$$

This remarkably simple formula for the triangle coefficient completes our discussion of procedures for direct extraction of integral coefficients from amplitudes at the one-loop level.

Maximal Unitarity 3

One of the most remarkable discoveries in elementary particle physics has been that of the existence of the complex plane.
— Julian Schwinger (1918–1994)

This chapter begins with an overview of the developments within the maximal unitarity method [55, 56] — a proposed multiloop generalization of the direct extraction procedures of Britto, Cachazo and Feng [7] and Forde [18] for one-loop master integral coefficients. Maximal unitarity was originally demonstrated for the massless planar double-box topology in strictly four dimensions [55]. Properly accounting for the underlying structure of maximal cuts led to the uniqueness conjecture for all two-loop master integral projectors [56]. Subsequent studies extended the formalism to planar double-box integrals with up to four massive external legs [57, 58].

One of the open question was how to augment the formalism to tackle the nonplanar sector at two loops. The second part of this chapter presents a thorough analysis of this particular problem. In particular, we show how to extract the coefficients of nonplanar double-box integrals with up to four massive external legs and explain the fascinating properties of the maximal cuts. The main references are papers II and V.

3.1 The Planar Sector

Although the planar sector is relatively simple for $2 \to 2$ scattering of massless particles [100], a complete two-loop integral basis has not yet been written down. General steps towards obtaining such a basis were taken by Gluza, Kajda and Kosower in ref. [53] and by Schabinger in ref. [54].

3.1.1 Notation for Planar Integrals

We start by introducing some of the principal objects in our study, namely planar two-loop integrals. Let us recall the notation for one-loop integrals around eq. (2.11),

$$I_n[1] = \int \frac{d^D\ell}{(2\pi)^D} \frac{1}{\ell^2(\ell - K_1)^2(\ell - K_{12})^2 \cdots (\ell - K_{1\cdots(n-1)})^2} \,, \tag{3.1}$$

Basically we distinguish between two kinds of two-loop integrals: those that factor into a product of one-loop integrals when certain internal lines are cut; and those that are

genuinely two-loop and remain connected upon cutting any of the internal lines. Phrased slightly differently, integrals that are genuinely two-loop are constructed by attaching external legs to one or two of the outer internal lines and possibly also to one or both of the vertices of the nonfactorizable two-loop vacuum diagram. This class of integrals may be further organized into three types [53], labeled by distribution of the external legs on the vacuum diagram. The three types of integrals are illustrated in fig. 3.1 and the corresponding expressions are

$$P_{n_1,n_2}[\Phi(\ell_1,\ell_2)] = \int \frac{d^D\ell_1}{(2\pi)^D}\int \frac{d^D\ell_2}{(2\pi)^D}\, \frac{\Phi(\ell_1,\ell_2)}{\ell_1^2(\ell_1-K_1)^2\cdots(\ell_1-K_{1\cdots n_1})^2(\ell_1+\ell_2+K_{n_1+n_2+2})^2} \times \frac{1}{\ell_2^2(\ell_2-K_{n_1+n_2+1})^2\cdots(\ell_2-K_{(n_1+2)\cdots(n_1+n_2+1)})^2}\,, \tag{3.2}$$

$$P^*_{n_1,n_2}[\Phi(\ell_1,\ell_2)] = \int \frac{d^D\ell_1}{(2\pi)^D}\int \frac{d^D\ell_2}{(2\pi)^D}\, \frac{\Phi(\ell_1,\ell_2)}{\ell_1^2(\ell_1-K_1)^2\cdots(\ell_1-K_{1\cdots n_1})^2(\ell_1+\ell_2)^2} \times \frac{1}{\ell_2^2(\ell_2-K_{n_1+n_2+1})^2\cdots(\ell_2-K_{(n_1+2)\cdots(n_1+n_2+1)})^2}\,, \tag{3.3}$$

$$P^{**}_{n_1,n_2}[\Phi(\ell_1,\ell_2)] = \int \frac{d^D\ell_1}{(2\pi)^D}\int \frac{d^D\ell_2}{(2\pi)^D}\, \frac{\Phi(\ell_1,\ell_2)}{\ell_1^2(\ell_1-K_1)^2\cdots(\ell_1-K_{1\cdots n_1})^2(\ell_1+\ell_2)^2} \times \frac{1}{\ell_2^2(\ell_2-K_{n_1+n_2})^2\cdots(\ell_2-K_{(n_1+1)\cdots(n_1+n_2)})^2}\,. \tag{3.4}$$

In these definitions, $\Phi(\ell_1,\ell_2)$ is a generic numerator polynomial that depends on dot products between the two loop momenta ℓ_1 and ℓ_2 and external vectors.

3.1.2 Maximal Cuts of Double-Box Integrals

Our aim is to determine the coefficients appearing in front of double-box master integrals in the two-loop amplitude. Let us start by considering purely massless scattering.

We may span the four-dimensional momentum space by three external momenta, say k_1, k_2, k_3, supplemented with a spurious direction ω that is perpendicular to the subspace spanned by the momenta. All contractions between loop momenta and external vectors are expressible in terms of eight fundamental scalar products, $\ell_i \cdot e_j$, where $e = (k_1, k_2, k_4, \omega)$. Odd powers of $\ell_1 \cdot \omega$ and $\ell_2 \cdot \omega$ vanish identically after integration, whereas even powers are reducible in four dimensions. It is trivial to show that $\ell_1 \cdot k_1$, $\ell_1 \cdot k_2$ and $\ell_2 \cdot k_4$ can be written in terms of the double-box inverse propagators and external invariants. Furthermore, $\ell_2 \cdot k_2$ can be expressed linearly in terms of $\ell_1 \cdot k_4$ and $\ell_2 \cdot k_1$. We may for example select the latter two as irreducible scalar products (ISP) and parametrize the most general double-box numerator polynomial as follows [68],

$$N(\ell_1,\ell_2) = c_{000} + c_{100}(\ell_1\cdot k_4) + c_{010}(\ell_2\cdot k_1) + c_{001}(\ell_1\cdot\omega) + \cdots\,. \tag{3.5}$$

The terms are restricted by renormalizability requirements and the completion of the integrand reduction is achieved by multivariate polynomial division with respect to a Gröbner basis constructed from the double-box inverse propagators. This part is

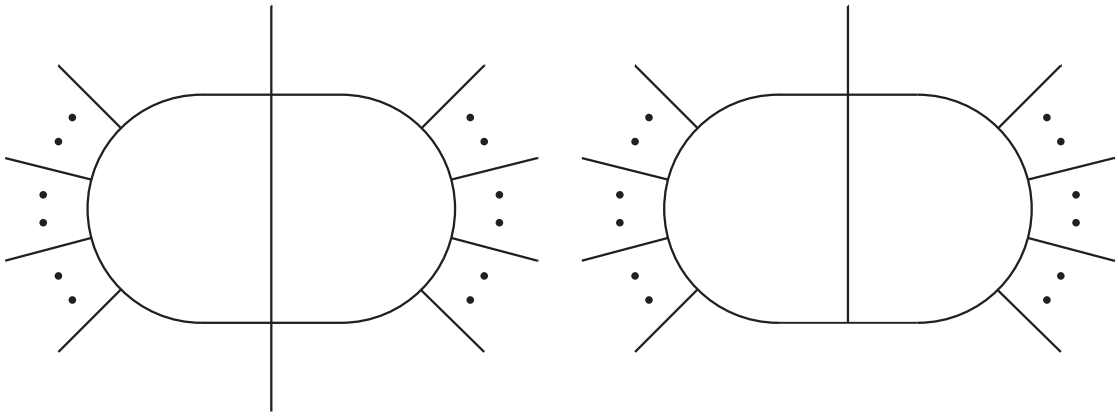

P_{n_1,n_2} $P^*_{n_1,n_2}$

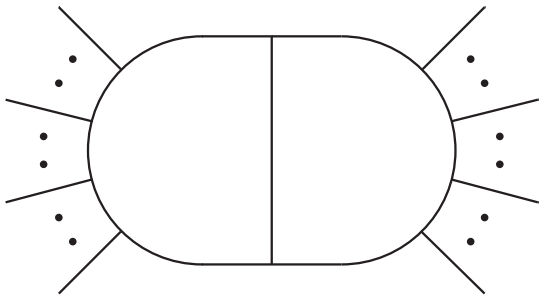

$P^{**}_{n_1,n_2}$

Figure 3.1: The three types of genuine two-loop integrals in the planar sector, labeled by the number of legs attached to each side of the vacuum diagram: (a) P_{n_1,n_2}, (b) $P^*_{n_1,n_2}$, (c) $P^{**}_{n_1,n_2}$. We indicate the absence of external line attached to a vertex by a superscripted star.

automatically carried out by the Mathematica package BasisDet [71]. The final double-box integrand consists of 16 parity-even and 16 parity-odd terms.

The double-box integrals that appear in gauge theories are thus

$$P^{**}_{2,2}[m,n] \equiv P^{**}_{2,2}[(\ell_1 \cdot k_4)^m (\ell_2 \cdot k_1)^n] \,. \tag{3.6}$$

Many of these integrals are in fact still reducible and can be written as linear combinations of integrals with lower-rank tensors and fewer than seven propagators. The reduction is carried out due to integration-by-parts (IBP) relations that follow from inserting a total derivative into the loop integrand and discarding the boundary in D dimensions. For the purely massless double-box, the 16 integrals of the form eq. (3.6) can be reduced onto two master integrals. A common choice of masters involves the scalar integral and a rank-1 tensor,

$$P^{**}_{2,2}[m,n] = c_1 P^{**}_{2,2}[0,0] + c_1 P^{**}_{2,2}[1,0] + \cdots \,. \tag{3.7}$$

In other words, the double-box contribution to the two-loop amplitude is

$$A^{(2)}_4 = c_1 P^{**}_{2,2}[0,0] + c_1 P^{**}_{2,2}[1,0] + \cdots \,. \tag{3.8}$$

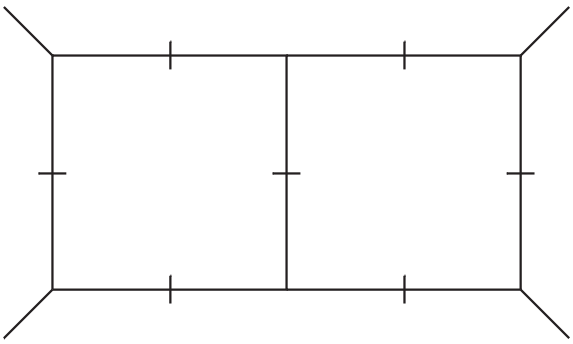

Figure 3.2: The maximally cut four-point planar double-box diagram.

We can extract both of the double-box integrals from eq. (3.8) by applying a double-box hepta-cut on both sides; no other integrals share this particular cut. The double-box hepta-cut places all seven propagators on their mass-shell and the diagram falls apart into a product of six on-shell three-point amplitudes. This situation is sketched in fig. 3.2. The unitarity cut equations form a polynomial equation system and these equations define an algebraic set, i.e. the solution set of the cut equations in the space spanned by the eight loop-momentum variables. The two loop momenta have a total of eight degrees of freedom, so after we have applied the hepta-cut we will be left with one free parameter. In other words, the hepta-cut equations define an algebraic curve. The solution set is

$$\begin{aligned}\mathcal{S} \equiv \big\{ (\ell_1, \ell_2) \in (\mathbb{C}^4)^{\otimes 2} \mid \ell_1^2 = 0\,,\ (\ell_1 - k_1)^2 = 0\,,\ (\ell_1 - K_{12})^2 = 0\,,\\ \ell_2^2 = 0\,,\ (\ell_2 - k_3)^2 = 0\,,\ (\ell_2 - K_{34})^2 = 0\,,\ (\ell_1 + \ell_2)^2 = 0 \big\}\,.\end{aligned} \tag{3.9}$$

It is hard in practice to examine this algebraic curve and hence the singularity structure of the double-box loop integrand directly from the defining system of polynomial equations. Instead, it is customary to study the solutions locally by means of a judiciously chosen loop-momentum parametrization [55],

$$\ell_1^\mu = \alpha_1 k_1^\mu + \alpha_2 k_2^\mu + \frac{s_{12}\alpha_3}{2\langle 14\rangle[42]}\langle 1^-|\gamma^\mu|2^-\rangle + \frac{s_{12}\alpha_4}{2\langle 24\rangle[41]}\langle 2^-|\gamma^\mu|1^-\rangle\,, \tag{3.10}$$

$$\ell_2^\mu = \beta_1 k_3^\mu + \beta_2 k_4^\mu + \frac{s_{12}\beta_3}{2\langle 31\rangle[14]}\langle 3^-|\gamma^\mu|4^-\rangle + \frac{s_{12}\beta_4}{2\langle 41\rangle[13]}\langle 4^-|\gamma^\mu|3^-\rangle\,, \tag{3.11}$$

which to a large extent linearizes the double-box hepta-cut equations. Although the equations are straightforward, we will not attempt to solve them here. We will merely quote the result for the six solutions in fig. 3.3 [55]. It follows that the six solutions are in one-to-one correspondence with the generically valid distributions of chiral and antichiral three-vertices.

With the hepta-cut solutions at hand we can apply the hepta-cut to the double-box integral. The hepta-cut involves six nondegenerate seven-dimensional residues associated with the poles of the integrand where all propagators take on on-shell values simultaneously. The residues are obtained via eq. 2.28. Direct calculation yields the same simple result for all six hepta-cut solutions,

$$P^{**}_{2,2}[1]|_{\mathcal{S}_i} \propto \oint \frac{dz}{z(z+\chi)}\,, \tag{3.12}$$

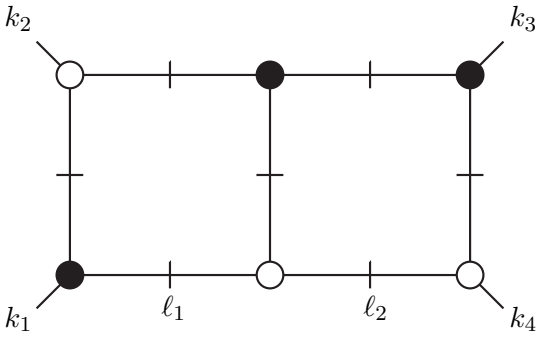

Solution $\mathcal{S}_1$, obtained by setting

$$\alpha_3 = -\chi\,, \qquad \beta_3 = z\,,$$
$$\alpha_4 = 0\,, \qquad \beta_4 = 0\,.$$

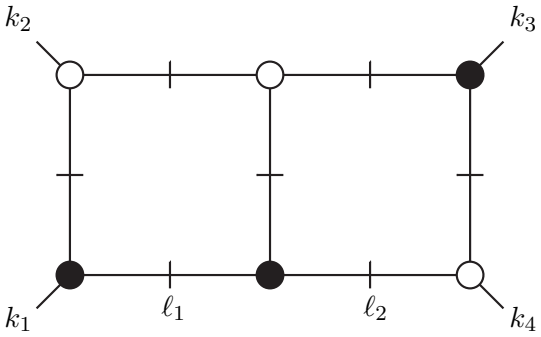

Solution $\mathcal{S}_2$, obtained by setting

$$\alpha_3 = z\,, \qquad \beta_3 = -\chi\,,$$
$$\alpha_4 = 0\,, \qquad \beta_4 = 0\,.$$

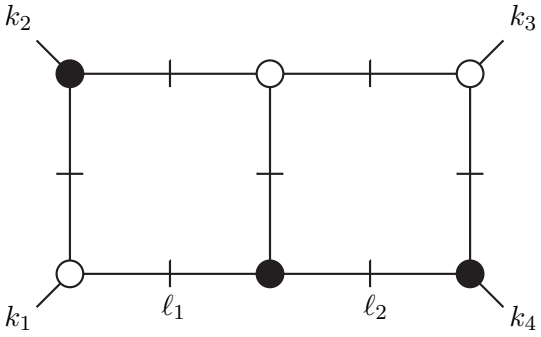

Solution $\mathcal{S}_3$, obtained by setting

$$\alpha_3 = 0\,, \qquad \beta_3 = 0\,,$$
$$\alpha_4 = -\chi\,, \qquad \beta_4 = z\,.$$

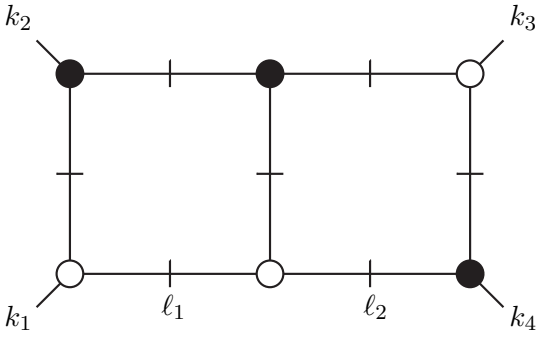

Solution $\mathcal{S}_4$, obtained by setting

$$\alpha_3 = 0\,, \qquad \beta_3 = 0\,,$$
$$\alpha_4 = z\,, \qquad \beta_4 = -\chi\,.$$

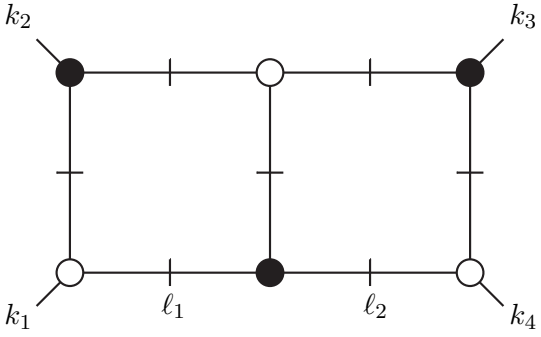

Solution $\mathcal{S}_5$, obtained by setting

$$\alpha_3 = 0\,, \qquad \beta_3 = -(\chi+1)\tfrac{z+\chi}{z+\chi+1}\,,$$
$$\alpha_4 = z\,, \qquad \beta_4 = 0\,.$$

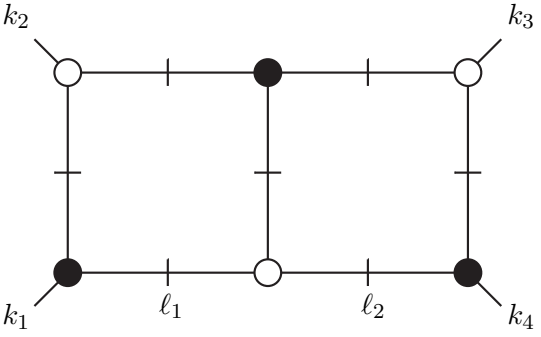

Solution $\mathcal{S}_6$, obtained by setting

$$\alpha_3 = z\,, \qquad \beta_3 = 0\,,$$
$$\alpha_4 = 0\,, \qquad \beta_4 = -(\chi+1)\tfrac{z+\chi}{z+\chi+1}\,.$$

Figure 3.3: The six solutions to the hepta-cut equations for purely massless double box. White and black blobs denote chiral and antichiral three-particle vertices. These figures are equivalent to those of ref. [55] identifying $\bullet = \oplus$ and $\circ = \ominus$.

where $\chi \equiv s_{14}/s_{12}$. The common constant of proportionality is not important for our purposes. We sum over all six solutions and write the hepta-cut in question as follows,

$$P^{**}_{2,2}[1]\big|_{7-\text{cut}} = \sum_{i=1}^{6} \oint \frac{dz}{z(z+\chi)} \,, \tag{3.13}$$

where the remaining one-dimensional contour is a priori unknown.

3.1.3 Uniqueness of Projectors

The left-over contour may be specified by general arguments. In particular, if the hepta-cut prescription is to make any sense at all, all relevant integral identities such as IBP relations must be respected. That is,

$$P^{**}_{2,2}[\Phi(\ell_1,\ell_2)] = 0 \Longrightarrow \text{cut}(P^{**}_{2,2}[\Phi(\ell_1,\ell_2)]) = 0 \,. \tag{3.14}$$

More specifically, we must demand that the reduction of the generic double-box integrand in eq. (3.5) onto the two master integrals remains valid no matter which contour we pick. But what is exactly the interpretation of the cut instruction in eq. (3.14)? Our best shot is to expand the most general contour as a linear combination of small circles around each of the z-poles,

$$\Gamma_i = \sum_{j\in\text{poles}} \omega_{i,j} C(z_j) \,, \tag{3.15}$$

where $\omega_{i,j}$ is the winding number around the pole z_j on branch $\mathcal{S}_i$. We then define the augmented hepta-cut as the completion of the contour according to this prescription,

$$\text{cut}(P^{**}_{2,2}[\Phi(\ell_1,\ell_2)]) = P^{**}_{2,2}[\Phi(\ell_1,\ell_2)]|_{\text{aug}} = \sum_{i=1}^{6} \oint_{\Gamma_i} \frac{dz}{z(z+\chi)} \,. \tag{3.16}$$

Naively, one would expect to find $6 \times 2 = 12$ Jacobians poles (those at $z = 0$ and $z = -\chi$). Moreover, solutions $\mathcal{S}_5$ and $\mathcal{S}_6$ give rise to additional poles at $z = -\chi - 1$ which may also be encircled. By inspection of the hepta-cut solutions in fig. 3.3,

$$\operatorname*{Res}_{z\in\mathcal{S}_i\cap\mathcal{S}_{i+1}} J(z)\Phi(\ell_1,\ell_2)\big|_{\mathcal{S}_i} = \pm \operatorname*{Res}_{z\in\mathcal{S}_i\cap\mathcal{S}_{i+1}} J(z)\Phi(\ell_1,\ell_2)\big|_{\mathcal{S}_i+1} \,, \tag{3.17}$$

where the relative sign depends on conventions. Accordingly, six of the residues are redundant. Remember, the hepta-cuts equations define an algebraic curve; more precisely, an elliptic curve that is topologically equivalent to a genus-0 Riemann sphere, i.e. a torus. In comparison, the only algebraic curve at one loop is a conic section from the triangle diagram. The elliptic curve in question is reducible and has six irreducible components, namely the six solutions [56]. The appropriate topological picture emerge by contracting the torus along lines passing through the object via its center. A sketch is provided in fig. 3.4

According to the above discussion, it suffices to encircle the following eight poles,

$$(\mathcal{G}_1,\ldots,\mathcal{G}_8) = (\mathcal{G}_{1\cap2},\, \mathcal{G}_{2\cap5},\, \mathcal{G}_{5\cap3}\,, \mathcal{G}_{3\cap4},\, \mathcal{G}_{4\cap6},\, \mathcal{G}_{6\cap1},\, \mathcal{G}_{5,\infty_R},\, \mathcal{G}_{6,\infty_R}) \,, \tag{3.18}$$

in order to produce a linearly independent basis of homology for $\mathcal{S}_1 \cup \cdots \cup \mathcal{S}_6$. The corresponding weights are denoted by,

$$\boldsymbol{\Omega} = (\omega_{1\cap2},\, \omega_{2\cap5},\, \omega_{5\cap3}\,, \omega_{3\cap4},\, \omega_{4\cap6},\, \omega_{6\cap1},\, \omega_{5,\infty_R},\, \omega_{6,\infty_R}) \,. \tag{3.19}$$

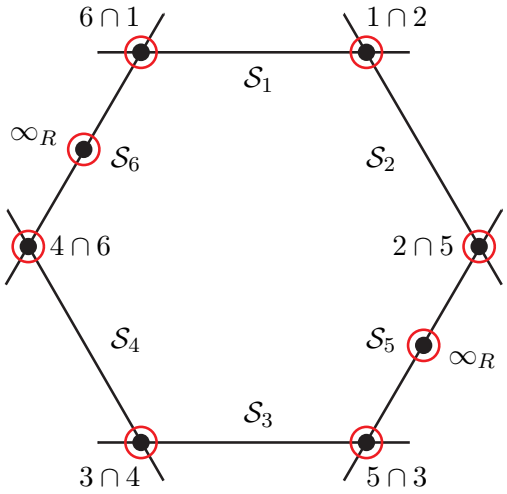

Figure 3.4: Global structure of the hepta-cut of the purely massless four-point double-box diagram. This figure in fact also applies to the one-mass, two-mass long and the two-mass diagonal diagrams [55]. The straight lines should be thought of as $\mathbb{CP}^1$. The poles at infinity are omitted as they can be eliminated by the global residue theorem.

Now, applying the augmented hepta-cut translates the consistency requirement into the overall statement

$$P^{**}_{2,2}[N(\ell_1,\ell_2)]\big|_{\text{aug}} = P^{**}_{2,2}[c_1 + c_2(\ell_1\cdot k_4)]\big|_{\text{aug}}\,. \tag{3.20}$$

Explicitly, for the parity-odd part of the integrand,

$$\begin{aligned} P^{**}_{2,2}[\epsilon(\ell_1,k_1,k_2,k_4)]\big|_{\text{aug}} &= P^{**}_{2,2}[\epsilon(\ell_2,k_1,k_2,k_4)]\big|_{\text{aug}} = 0\,,\\ P^{**}_{2,2}[\epsilon(\ell_1,\ell_2,k_1,k_2)]\big|_{\text{aug}} &= P^{**}_{2,2}[\epsilon(\ell_1,\ell_2,k_1,k_4)]\big|_{\text{aug}} = P^{**}_{2,2}[\epsilon(\ell_1,\ell_2,k_2,k_4)]\big|_{\text{aug}} = 0\,. \end{aligned} \tag{3.21}$$

Similarly, for the reduction of a few of the parity-even terms by IBP relations,

$$P^{**}_{2,2}[(\ell_1\cdot k_4)]\big|_{\text{aug}} = P^{**}_{2,2}[(\ell_2\cdot k_1)]\big|_{\text{aug}}\,, \tag{3.22}$$

$$P^{**}_{2,2}[(\ell_1\cdot k_4)(\ell_2\cdot k_1)]\big|_{\text{aug}} = \frac{1}{8}\chi s_{12}^2 P^{**}_{2,2}[1]\big|_{\text{aug}} - \frac{3}{4}s_{12}P^{**}_{2,2}[(\ell_1\cdot k_4)]\big|_{\text{aug}}\,. \tag{3.23}$$

The remaining IBP reduction equations can be found in e.g. ref. [59]. Surprisingly, only four of the parity-odd constraints and merely two of the sixteen parity-even IBP constraints are linearly independent when evaluated on the augmented hepta-cut. Hence, two weights are left undetermined. This pleasant freedom allows us to define the master contours,

$$\begin{aligned} \mathcal{M}_1\cdot(\text{Res}_{\{\mathcal{G}_i\}}P^{**}_{2,2}[1],\text{Res}_{\{\mathcal{G}_i\}}P^{**}_{2,2}[(\ell_1\cdot k_4)]) &= (1,0)\,,\\ \mathcal{M}_1\cdot(\text{Res}_{\{\mathcal{G}_i\}}P^{**}_{2,2}[1],\text{Res}_{\{\mathcal{G}_i\}}P^{**}_{2,2}[(\ell_1\cdot k_4)]) &= (0,1)\,. \end{aligned} \tag{3.24}$$

Here, $\mathcal{M}_1$ and $\mathcal{M}_2$ are simply particular choices of the winding numbers (3.19), such that only the contribution from one of the basis integrals is picked up and further normalized

to unity. From the augmented hepta-cut of the master equation,

$$\sum_{i=1}^{6} \oint_{\Gamma_i} \frac{dz}{z(z+\chi)} \sum_{\substack{\text{particles}\\ \text{helicities}}} \prod_{j=1}^{6} A_{(j)}^{\text{tree}}(z)\big|_{\mathcal{S}_i} = \\ c_1 \sum_{i=1}^{6} \oint_{\Gamma_i} \frac{dz}{z(z+\chi)} + c_2 \sum_{i=1}^{6} \oint_{\Gamma_i} \frac{dz}{z(z+\chi)} (\ell_1 \cdot k_4)\big|_{\mathcal{S}_i} \,, \tag{3.25}$$

we immediately project either c_1 or c_2 and arrive at the compact master formula [55],

$$\boxed{c_i = \oint_{\mathcal{M}_i} \frac{dz}{z(z+\chi)} \sum_{\substack{\text{particles}\\ \text{helicities}}} \prod_{j=1}^{6} A_{(j)}^{\text{tree}}(z) \,,} \tag{3.26}$$

which holds in any gauge theory. The master integral coefficients can be written explicitly in terms of the residues picked up by the contour integrals,

$$\begin{aligned} c_1 = &+ \frac{1}{4} \sum_{i=1,3} \operatorname*{Res}_{z=-\chi} \frac{1}{z+\chi} \sum_{\substack{\text{particles}\\ \text{helicities}}} \prod_{j=1}^{6} A_{(j)}^{\text{tree}}(z)\big|_{\mathcal{S}_i} \\ &+ \frac{1}{4} \sum_{i=5,6} \operatorname*{Res}_{z=-\chi} \frac{1}{z+\chi} \sum_{\substack{\text{particles}\\ \text{helicities}}} \prod_{j=1}^{6} A_{(j)}^{\text{tree}}(z)\big|_{\mathcal{S}_i} \\ &- \frac{\chi}{4(1+\chi)} \sum_{i=5,6} \operatorname*{Res}_{z=-\chi-1} \sum_{\substack{\text{particles}\\ \text{helicities}}} \prod_{j=1}^{6} A_{(j)}^{\text{tree}}(z)\big|_{\mathcal{S}_i} \,, \end{aligned} \tag{3.27}$$

$$\begin{aligned} c_2 = &- \frac{1}{2s_{12}\chi} \sum_{i=1,3} \operatorname*{Res}_{z=-\chi} \frac{1}{z+\chi} \sum_{\substack{\text{particles}\\ \text{helicities}}} \prod_{j=1}^{6} A_{(j)}^{\text{tree}}(z)\big|_{\mathcal{S}_i} \\ &+ \frac{1}{s_{12}\chi} \sum_{i=5,6} \operatorname*{Res}_{z=0} \frac{1}{z} \sum_{\substack{\text{particles}\\ \text{helicities}}} \prod_{j=1}^{6} A_{(j)}^{\text{tree}}(z)\big|_{\mathcal{S}_i} \\ &- \frac{1}{2s_{12}\chi} \sum_{i=5,6} \operatorname*{Res}_{z=-\chi} \frac{1}{z+\chi} \sum_{\substack{\text{particles}\\ \text{helicities}}} \prod_{j=1}^{6} A_{(j)}^{\text{tree}}(z)\big|_{\mathcal{S}_i} \\ &+ \frac{3}{2s_{12}(1+\chi)} \sum_{i=5,6} \operatorname*{Res}_{z=-\chi-1} \sum_{\substack{\text{particles}\\ \text{helicities}}} \prod_{j=1}^{6} A_{(j)}^{\text{tree}}(z)\big|_{\mathcal{S}_i} \,. \end{aligned} \tag{3.28}$$

3.1.4 External Masses and Topological Structure

Johansson, Kosower and Larsen extended the maximal unitarity method at two loops to double-box basis integrals with up to three external massive legs [57] and later on also to four external massive legs [58]. These papers lent additional nontrivial credence to the conjecture of uniqueness of master contours in ref. [56].

We will not attempt to reproduce the results of refs. [57, 58] here. Our focus is instead to provide a brief explanation of the global structure of the hepta-cut in presence

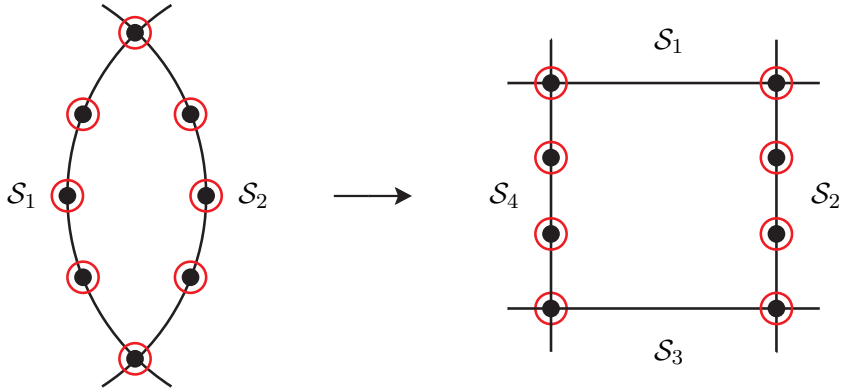

Figure 3.5: Global structure of the maximal cut of the planar double-box diagram with external legs configured according to class (a) (left) and (b) (right).

of external massive lines following refs. [56, 79]. Irrespective of the external kinematics, the hepta-cut equations define an elliptic curve. The simplest example with four external massless legs gave rise a degenerate curve associated with a sixtuply pinched torus. In considering the various kinematic configurations of the double box, three distinct classes appear: (a) when neither (k_1, k_2) nor (k_3, k_4) contains a massless momentum; (b) when exactly one of the pairs contains a massless momentum; (c) when both pairs contain a massless momentum [56]. The purely massless case is part of class (c) along with the one-mass, two-mass long side and two-mass diagonal diagrams. Class (b) covers the three-mass and two-mass short side double-boxes. Finally, the four-mass diagram belongs to class (a). The classification of diagrams is summarized in figs. 3.7, 3.8 and 3.9 for clarity.

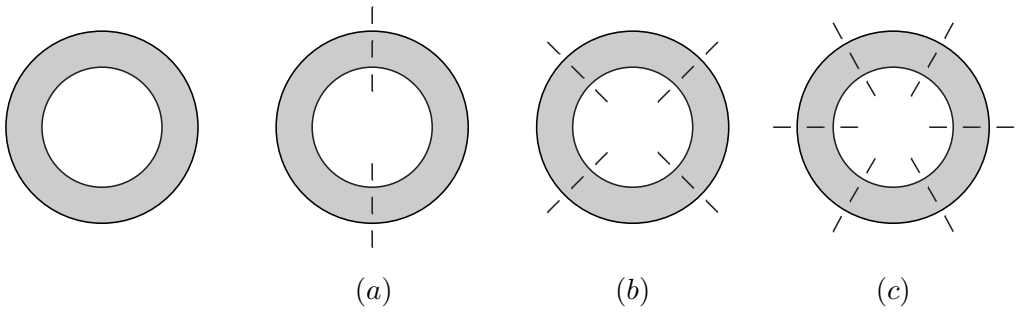

Figure 3.6: The pinched tori corresponding to class (a), (b) and (c) are obtained by contracting tubes along one, two and three lines passing through the object via its center respectively. This figure appeared in ref. [79].

The hepta-cut equations in class (b) yield four inequivalent solutions that intersect pairwise at four distinct points. The corresponding topological picture is that of a torus whose tubes have been contracted along two lines passing through the object via its center as illustrated in fig. 3.5. The hepta-cut equations in class (a) yield only two independent solutions that intersect at two points. In this case, the torus associated with the elliptic curve is only pinched twice along a single line. A perhaps more intuitive picture is given in fig. 3.6. It is important to note that the number of independent global poles is constant under the chiral branchings from $1 \to 2 \to 4 \to 6$ hepta-cut solutions.

Interestingly, the number of independent double-box basis integrals seems to be governed by the global structure of the hepta-cut. Indeed, according to the IBP relations generated by `FIRE` [103], class (a), (b) and (c) have four, three and two master integrals respectively. In the four-mass case, the two-amplitude can be written

$$A_4^{(1)} = c_1 P^{**}_{2,2}[1] + c_2 P^{**}_{2,2}[(\ell_1 \cdot k_4)] + c_3 P^{**}_{2,2}[(\ell_2 \cdot k_1)] + c_3 P^{**}_{2,2}[(\ell_1 \cdot k_4)(\ell_2 \cdot k_1)] \,. \quad (3.29)$$

There are four independent parity-odd constraints, but all IBP relations are automatically satisfied. The latter is rather surprising, all eight windings numbers are nevertheless uniquely determined on the four master contours [58]. The three masters in class (b) can be chosen as follows,

$$A_4^{(1)} = c_1 P^{**}_{2,2}[1] + c_2 P^{**}_{2,2}[(\ell_1 \cdot k_4)] c_3 P^{**}_{2,2}[(\ell_2 \cdot k_1)] + \cdots \,. \quad (3.30)$$

It happens that the IBP reduction equation

$$P^{**}_{2,2}[(\ell_1 \cdot k_4)(\ell_2 \cdot k_1)] = c_1' P^{**}_{2,2}[1] + c_2' P^{**}_{2,2}[(\ell_1 \cdot k_4)] + c_3' P^{**}_{2,2}[(\ell_2 \cdot k_1)] \,, \quad (3.31)$$

where trailing dots hide integrals with less than seven propagators, uniquely fixes all three master contours together with the four parity-odd constraints. Finally, the kinematics of class (c), where

$$A_4^{(1)} = c_1 P^{**}_{2,2}[1] + c_2 P^{**}_{2,2}[(\ell_1 \cdot k_4)] + \cdots \,, \quad (3.32)$$

gives rise to two linearly independent IBP constraints. One of them is inherited from the reduction (3.31) from $4 \to 3$ master integrals. The last constraint comes from the IBP identity relating the two rank-1 tensor integrals,

$$P^{**}_{2,2}[(\ell_2 \cdot k_1)] = c_1'' P^{**}_{2,2}[1] + c_2'' P^{**}_{2,2}[(\ell_1 \cdot k_4)] \,, \quad (3.33)$$

which is responsible for the reduction from $3 \to 2$ masters.

3.2 The Nonplanar Sector

The majority of the irreducible integrals in the nonplanar sectors at four external particles are nonplanar double boxes [101]. In a sequence of papers [59, 61, 62] Zhang and the author have extended the four-dimensional maximal unitarity formalism [55, 56] to cover such integrals. The principal results, which also may find application for higher-multiplicity scattering of massless particles, are unique projectors for all basis integral coefficients in all inequivalent configurations of massive and massless external momenta, valid to $\mathcal{O}(\epsilon^0)$ in the dimensional regulator. Remarkably, all salient features carry over directly from the planar sector.

3.2.1 Notation for Nonplanar Integrals

We will encounter two variants of the nonplanar double-box integral in this thesis. The two definitions differ by a cyclic permutation of the external legs and by the conventions

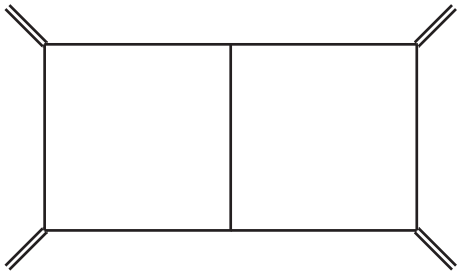

Figure 3.7: When considering only four external particles, class (a) only contains the four-mass double box. Note that we assume that all masses are distinct. The equal-mass case with, say, $m_1 = m_4$ and $m_2 = m_3$ was examined in ref. [58].

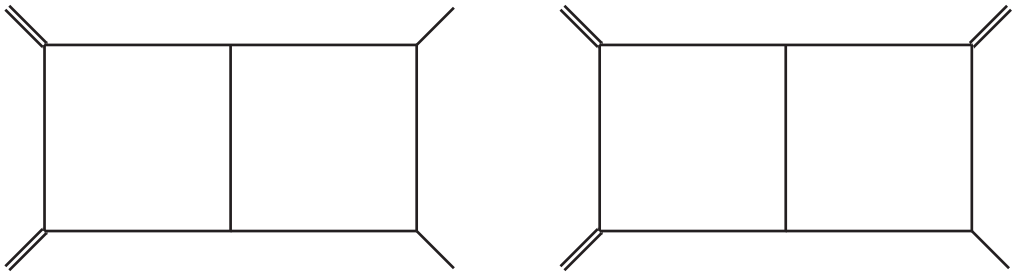

Figure 3.8: Class (b) contains the two-mass short and three-mass configurations of the double-box diagram.

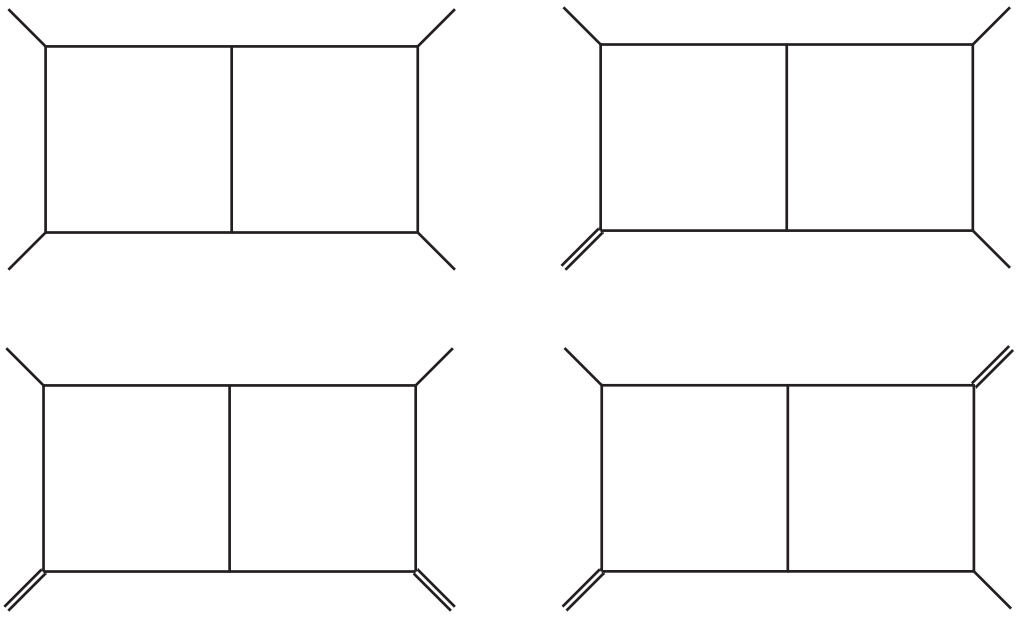

Figure 3.9: Class (c) contains the zero-mass, one-mass, two-mass long and two-mass diagonal configurations. We omit diagrams that are related by cyclic permutations of external legs.

for the momentum flow on the internal lines. The integral expressions are

$$X^{**}_{1,1,2}[\Phi(\ell_1,\ell_2)] \equiv \int \frac{d^D\ell_1}{(2\pi)^D}\int \frac{d^D\ell_2}{(2\pi)^D}\frac{\Phi(\ell_1,\ell_2)}{\ell_1^2(\ell_1+k_1)^2\ell_2^2(\ell_2+k_3)^2(\ell_2-k_4)^2(\ell_2-\ell_1+k_3)^2(\ell_2-\ell_1+K_{23})^2}\,, \tag{3.34}$$

$$X^{**}_{2,1,1}[\Phi(\ell_1,\ell_2)] \equiv \int \frac{d^D\ell_1}{(2\pi)^D}\int \frac{d^D\ell_2}{(2\pi)^D}\frac{\Phi(\ell_1,\ell_2)}{\ell_1^2(\ell_1-k_1)^2(\ell_1-K_{12})^2\ell_2^2(\ell_2-k_4)^2(\ell_1+\ell_2)^2(\ell_1+\ell_2+k_3)^2}\,. \tag{3.35}$$

The superscripted stars signify the absence of external lines attached to the two-loop vacuum diagram. The three subscripts indicate the number of external legs on the left-most, the middle and the right-most rungs respectively.

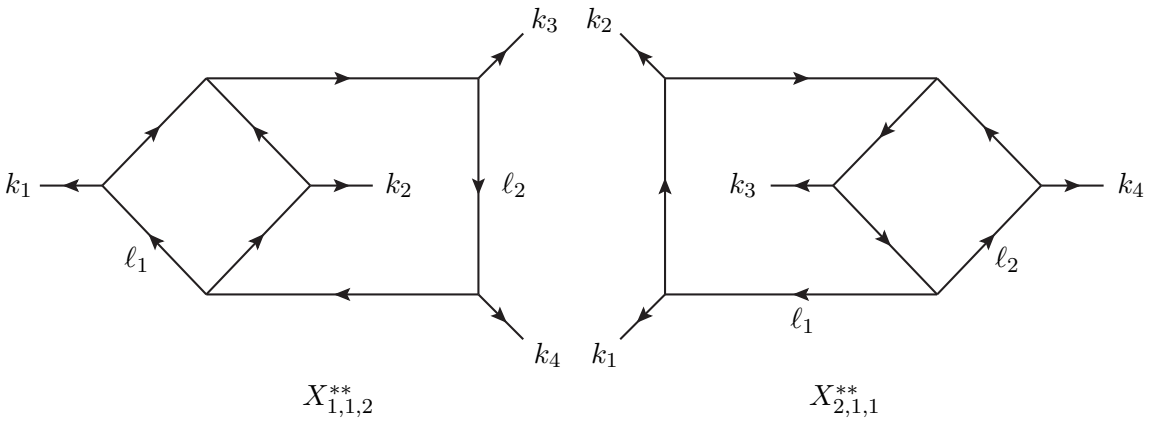

Figure 3.10: The nonplanar double-box integrals. Although the two figures merely differ by a cyclic permutation of the external legs, we will distinguish between them in the following. All external particles may be massive or massless.

3.2.2 Maximal Cuts of Nonplanar Double-Box Integrals

For simplicity we specialize purely massless scattering and postpone the more general analysis. The goal is to extract the nonplanar double-box master integral coefficients from the two-loop amplitude in arbitrary gauge theories.

Repeating the analysis of sec. 3.1.2 leads to the conclusion that the general nonplanar double-box numerator polynomial can be parametrized in terms of two parity-odd and two parity-even ISPs. We follow ref. [55] and choose the nonspurious ISPs to be $\ell_1 \cdot k_3$ and $\ell_2 \cdot k_2$. The numerator of the integrand can thus be written

$$N(\ell_1,\ell_2) = c_{000} + c_{100}(\ell_1\cdot k_3) + c_{010}(\ell_2\cdot k_2) + c_{001}(\ell_1\cdot\omega) + \cdots\,. \tag{3.36}$$

Constraining terms by the requirement of renormalizability along with performing the multivariate polynomial division of the numerator with respect to a Gröbner basis constructed form the nonplanar double-box inverse propagators completes the integrand-level reduction. The resulting integrand has 19 parity-even and 19 parity-odd terms as reported in ref. [68]. For more information on integrand-level reduction, consult e.g. ref. [71].

	α_1	α_2	α_3	α_4	β_1	β_2	β_3	β_4
$\mathcal{S}_1$	$\chi - z$	0	$\chi(z-\chi-1)$	0	0	0	z	0
$\mathcal{S}_2$	$\chi - z$	0	0	$\chi(z-\chi-1)$	0	0	0	z
$\mathcal{S}_3$	0	0	z	0	0	0	χ	0
$\mathcal{S}_4$	0	0	0	z	0	0	0	χ
$\mathcal{S}_5$	$\chi - z$	0	0	$(\chi+1)(z-\chi)$	0	0	z	0
$\mathcal{S}_6$	$\chi - z$	0	$(\chi+1)(z-\chi)$	0	0	0	0	z
$\mathcal{S}_7$	-1	0	0	z	0	0	$1+\chi$	0
$\mathcal{S}_8$	-1	0	z	0	0	0	0	$1+\chi$

Table 3.1: An overview of the hepta-cut solutions for the purely massless four-point nonplanar double box. The loop-momentum parameters $\alpha_1, \ldots, \alpha_4$ and $\beta_1, \ldots, \beta_4$ were defined in eq. (3.11).

We introduce the shorthand notation for the nominally-irreducible nonplanar double-box integrals,

$$X^{**}_{1,1,2}[m,n] \equiv X^{**}_{1,1,2}[(\ell_1 \cdot k_3)^m (\ell_2 \cdot k_2)^m] \,. \tag{3.37}$$

Invoking IBP technology, we find 17 linear relations among the integrals of the form (3.37). Hence, we are left with only two master integrals. In order to be able to compare results with ref. [68], we choose the following basis decomposition,

$$X^{**}_{1,1,2}[m,n] = c_1 X^{**}_{1,1,2}[1] + c_2 X^{**}_{1,1,2}[(\ell_1 \cdot k_3)] + \cdots \,. \tag{3.38}$$

In particular, the nonplanar double-box contribution to the two-loop amplitude can be written,

$$A^{(1)}_4 = c_1 X^{**}_{1,1,2}[1] + c_2 X^{**}_{1,1,2}[(\ell_1 \cdot k_3)] + \cdots \,, \tag{3.39}$$

where the $\cdots$ include integrals with other topologies (the planar double-box for example) or less than seven propagators.

The two nonplanar double-box integrals in eq. (3.39) are almost effortlessly extracted by means of a hepta-cut that places all seven propagators on-shell. No other integrals contribute to the cut in question, so the remaining problem is merely to disentangle the two nonplanar double-boxes from each other. The hepta-cut equations still define an algebraic curve. We will denote the set of hepta-cut solutions as follows,

$$\begin{aligned}\mathcal{S} \equiv \big\{ (\ell_1, \ell_2) \in (\mathbb{C}^4)^{\otimes 2} \mid \ell_1^2 = 0\,,\ (\ell_1 + k_1)^2 = 0\,,\ (\ell_2)^2 = 0\,,\ (\ell_2 + k_3)^2 = 0\,,\\ (\ell_2 - k_4)^2 = 0\,,\ (\ell_2 - \ell_1 + k_3)^2 = 0\,,\ (\ell_2 - \ell_1 + K_{23})^2 = 0 \big\}\,.\end{aligned} \tag{3.40}$$

The solutions may be expressed with regard to the loop-momentum parametrization in eq. (3.11). Keeping track of all possible branchings we find the four pairs of complex conjugate solutions shown in table 3.1. This is naturally expected in view of the, for generic external momenta, valid distributions of internal helicities in the six three-vertices. For a more detailed derivation of the hepta-cut solutions, see ref. [59].

The hepta-cut of the nonplanar double-box consists of eight nondegenerate seven-dimensional residues. Using eq. (2.28) we end up with the results [59]

$$X^{**}_{1,1,2}[1]\big|_{\mathcal{S}_{3,4}} = -\frac{1}{16s_{12}^3}\oint \frac{dz}{z(z+\chi)}\,, \tag{3.41}$$

$$X^{**}_{1,1,2}[1]\big|_{\mathcal{S}_{7,8}} = -\frac{1}{16s_{12}^3}\oint \frac{dz}{z(z-\chi-1)}\,, \tag{3.42}$$

$$X^{**}_{1,1,2}[1]\big|_{\mathcal{S}_{1,2,5,6}} = -\frac{1}{16s_{12}^3}\oint \frac{dz}{z(z-\chi)(z-\chi-1)}\,. \tag{3.43}$$

Further details on how to evaluate the residues in practice can be found in ref. [59]. Note that unlike the planar case, the analytic structure of the integrand vary from branch to branch. Summing over all eight contributions produces what we will refer to as the hepta-cut of the nonplanar double box,

$$X^{**}_{1,1,2}[1]\big|_{7-\text{cut}} = \frac{1}{16s_{12}^3}\Big[\sum_{i=1,2,5,6}\oint \frac{dz}{z(z-\chi)(z-\chi-1)} + \sum_{i=3,4}\oint \frac{dz}{z(z+\chi)} + + \sum_{i=7,8}\oint \frac{dz}{z(z-\chi-1)}\Big]\,. \tag{3.44}$$

3.2.3 Uniqueness of Projectors

It remains to examine whether the left-over contour can be uniquely determined by general arguments as for the planar double box. The basic principle is still that any integral identity must be respected, i.e.

$$X^{**}_{1,1,2}[\Phi(\ell_1,\ell_2)] = 0 \Longrightarrow X^{**}_{1,1,2}[\Phi(\ell_1,\ell_2)]) = 0\,. \tag{3.45}$$

For the problem at hand, the requirements is that the reduction of the generic nonplanar double-box integrand in eq. (3.36) onto the two basis integrals continues to hold on arbitrary contours away form the real slice. Accordingly, the most general contour is an expansion of small circles around each of the z-poles,

$$\Gamma_i = \sum_{j\in\text{poles}} \omega_{i,j} C(z_j)\,, \tag{3.46}$$

$\omega_{i,j}$ being the winding numbers. Completing the contour along these lines yields the augmented hepta-cut of the nonplanar double box.

Inspecting the singularity structure suggests a total of $4\times 3 + 2\times 2 + 2\times 2 = 18$ Jacobian poles. None of the hepta-cut solutions give rise to additional poles for finite values of z as all of them are holomorphically parametrized. However, many of the residues coincide:

$$\begin{aligned}
\operatorname*{Res}_{z=0} J_1(z)\Phi(\ell_1\ell_2)\big|_{\mathcal{S}_1} &= \pm \operatorname*{Res}_{z=0} J_6(z)\Phi(\ell_1\ell_2)\big|_{\mathcal{S}_6}\\
\operatorname*{Res}_{z=0} J_2(z)\Phi(\ell_1\ell_2)\big|_{\mathcal{S}_2} &= \pm \operatorname*{Res}_{z=0} J_5(z)\Phi(\ell_1\ell_2)\big|_{\mathcal{S}_5}\\
\operatorname*{Res}_{z=\chi} J_1(z)\Phi(\ell_1\ell_2)\big|_{\mathcal{S}_1} &= \pm \operatorname*{Res}_{z=-\chi} J_3(z)\Phi(\ell_1\ell_2)\big|_{\mathcal{S}_3}\\
\operatorname*{Res}_{z=\chi} J_2(z)\Phi(\ell_1\ell_2)\big|_{\mathcal{S}_2} &= \pm \operatorname*{Res}_{z=-\chi} J_4(z)\Phi(\ell_1\ell_2)\big|_{\mathcal{S}_4}
\end{aligned}$$

$$\begin{aligned}
\operatorname*{Res}_{z=\chi+1} J_1(z)\Phi(\ell_1\ell_2)\big|_{\mathcal{S}_1} &= \pm \operatorname*{Res}_{z=0} J_7(z)\Phi(\ell_1\ell_2)\big|_{\mathcal{S}_7} \\
\operatorname*{Res}_{z=\chi+1} J_2(z)\Phi(\ell_1\ell_2)\big|_{\mathcal{S}_2} &= \pm \operatorname*{Res}_{z=0} J_8(z)\Phi(\ell_1\ell_2)\big|_{\mathcal{S}_8} \\
\operatorname*{Res}_{z=\chi+1} J_5(z)\Phi(\ell_1\ell_2)\big|_{\mathcal{S}_5} &= \pm \operatorname*{Res}_{z=\chi+1} J_7(z)\Phi(\ell_1\ell_2)\big|_{\mathcal{S}_7} \\
\operatorname*{Res}_{z=\chi+1} J_6(z)\Phi(\ell_1\ell_2)\big|_{\mathcal{S}_6} &= \pm \operatorname*{Res}_{z=\chi+1} J_8(z)\Phi(\ell_1\ell_2)\big|_{\mathcal{S}_8} \\
\operatorname*{Res}_{z=\chi} J_5(z)\Phi(\ell_1\ell_2)\big|_{\mathcal{S}_5} &= \pm \operatorname*{Res}_{z=0} J_3(z)\Phi(\ell_1\ell_2)\big|_{\mathcal{S}_3} \\
\operatorname*{Res}_{z=\chi} J_6(z)\Phi(\ell_1\ell_2)\big|_{\mathcal{S}_6} &= \pm \operatorname*{Res}_{z=0} J_4(z)\Phi(\ell_1\ell_2)\big|_{\mathcal{S}_4} \,. \qquad (3.47)
\end{aligned}$$

Phrased slightly differently, the hepta-cut branches intersect each other at 10 distinct points. Hence we can immediately discard half of the residues, leaving only 10 independent weights to be determined. Interestingly, the picture alluded here is that of a genus-3 (hyperelliptic) curve. The hepta-cut equations are in one-to-one correspondence with the eight irreducible components. Moreover, the topological picture is obtained by contracting tubes along horizontal and vertical lines passing through the genus-3 surface via its center. For a depiction, see fig. 3.11.

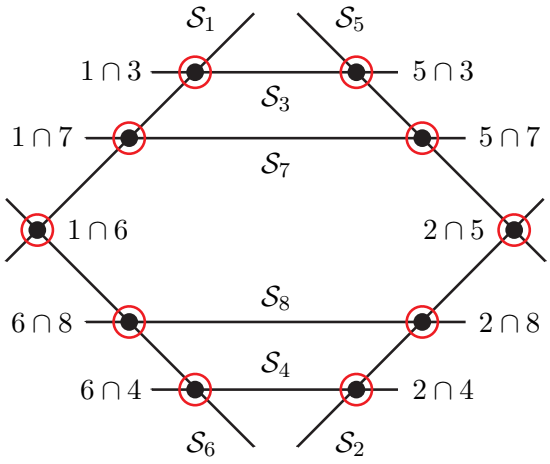

Figure 3.11: The maximal cut of the purely massless four-point nonplanar double-box diagram defines a nodal genus-3 algebraic curve. The irreducible components are drawn as straight lines, but should be interpreted as Riemann spheres.

All z-poles at finite values are located on branches $\mathcal{S}_1$, $\mathcal{S}_2$, $\mathcal{S}_5$ or $\mathcal{S}_6$, so the remaining four branches turn out to be redundant. It thus suffices to encircle ten global poles specified by the ordered list of winding numbers,

$$\Omega = (\omega_{1\cap 6},\, \omega_{1\cap 3},\, \omega_{1\cap 7}\,, \omega_{2\cap 5},\, \omega_{2\cap 4},\, \omega_{2\cap 8},\, \omega_{5\cap 3},\, \omega_{5\cap 7},\, \omega_{6\cap 4},\, \omega_{6\cap 8})\,, \qquad (3.48)$$

in order to produce a minimal basis of homology for $\mathcal{S}_1 \cup \cdots \cup \mathcal{S}_8$.

It remains to investigate the details of the constraints imposed on the contours. More precisely, we would like to know the implications of enforcing the condition

$$X^{**}_{1,1,2}[N(\ell_1,\ell_2)]\big|_{\text{aug}} = X^{**}_{1,2,2}[c_1 + c_2(\ell_1 \cdot k_3)]\big|_{\text{aug}}\,, \qquad (3.49)$$

where $N(\ell_1,\ell_2)$ is the general nonplanar double-box numerator function with 19 parity-odd and 19 parity-even monomials. All parity-odd constraints are respected as long as

we require that

$$\begin{aligned}
X^{**}_{1,1,2}[\epsilon(\ell_1,k_2,k_3,k_4)]\big|_{\rm aug} &= 0\ ,\\
X^{**}_{1,1,2}[\epsilon(\ell_2,k_2,k_3,k_4)]\big|_{\rm aug} &= 0\ ,\\
X^{**}_{1,1,2}[\epsilon(\ell_1,\ell_2,k_2,k_3)]\big|_{\rm aug} &= 0\ ,\\
X^{**}_{1,1,2}[\epsilon(\ell_1,\ell_2,k_2,k_4)]\big|_{\rm aug} &= 0\ ,\\
X^{**}_{1,1,2}[\epsilon(\ell_1,\ell_2,k_3,k_4)]\big|_{\rm aug} &= 0\ ,
\end{aligned} \tag{3.50}$$

Unlike the planar case, all five Levi-Civita constraints give rise to linearly independent [59] expressions. This was also expected since we now have five pairs of parity conjugate global poles. The complexity of the parity-even integral relations is modest. Typical examples are

$$\begin{aligned}
X^{**}_{1,1,2}[(\ell_1\cdot k_3)^2] &= -\frac{1}{16}(1+\chi)\chi s_{12}^2 X^{**}_{1,1,2}[1] + \frac{3}{8}(1+2\chi)s_{12}X^{**}_{1,1,2}[(\ell_1\cdot k_3)] + \cdots\ ,\\
X^{**}_{1,1,2}[(\ell_1\cdot k_3)(\ell_2\cdot k_2)] &= +\frac{1}{16}(1+\chi)\chi s_{12}^2 X^{**}_{1,1,2}[1] - \frac{3}{8}(1+2\chi)s_{12}X^{**}_{1,1,2}[(\ell_1\cdot k_3)] + \cdots\ .
\end{aligned} \tag{3.51}$$

The rest of the nonplanar double-box IBP relations along with the their cut expressions can be found in ref. [59]. Surprisingly, out of the 17 genuine IBP relations only three of them are linearly independent when evaluated on the augmented hepta-cut. The five parity-odd and three parity-even contour constraints uniquely determine the two master contours

$$\begin{aligned}
\mathcal{M}_1\cdot(\text{Res}_{\{\mathcal{G}_i\}}X^{**}_{1,1,2}[1],\text{Res}_{\{\mathcal{G}_i\}}X^{**}_{1,1,2}[(\ell_1\cdot k_3)]) &= (1,0)\ ,\\
\mathcal{M}_2\cdot(\text{Res}_{\{\mathcal{G}_i\}}X^{**}_{1,1,2}[1],\text{Res}_{\{\mathcal{G}_i\}}X^{**}_{1,1,2}[(\ell_1\cdot k_3)]) &= (0,1)\ .
\end{aligned} \tag{3.52}$$

In fact, $\mathcal{M}_1$ and $\mathcal{M}_2$ are characterized by the 10-tuples,

$$\mathcal{M}_1 = 2\chi(1+\chi)s_{12}^3(-2,1,1,-2,1,1,1,1,1,1)\ , \tag{3.53}$$

$$\begin{aligned}
\mathcal{M}_2 = 4s_{12}^2(&2(1+2\chi),1-2\chi,-3-2\chi,2(1+2\chi),1-2\chi,\\
&-3-2\chi,1-2\chi,-3-2\chi,1-2\chi,-3-2\chi)\ .
\end{aligned} \tag{3.54}$$

Applying the projectors to the augmented hepta-cut of the basis expansion of the two-loop amplitude provides us with an equation for two unknowns,

$$\begin{aligned}
&\sum_{i\in\{1,2,5,6\}}\oint_{\Gamma_i}\frac{dz}{z(z-\chi)(z-\chi-1)}\sum_{\substack{\text{particles}\\ \text{helicities}}}\prod_{j=1}^{6}A^{\rm tree}_{(j)}(z)\big|_{\mathcal{S}_i} =\\
&\qquad c_1\sum_{i\in\{1,2,5,6\}}\oint_{\Gamma_i}\frac{dz}{z(z-\chi)(z-\chi-1)} + c_2\sum_{i\in\{1,2,5,6\}}\oint_{\Gamma_i}dz\frac{(\ell_1\cdot k_3)|_{\mathcal{S}_i}}{z(z-\chi)(z-\chi-1)}\ .
\end{aligned} \tag{3.55}$$

Thanks to the projectors we can immediately obtain a surprisingly compact formula for the desired coefficients c_1 and c_2 [59],

$$\boxed{c_i = \oint_{\mathcal{M}_i}\frac{dz}{z(z-\chi)(z-\chi-1)}\sum_{\substack{\text{particles}\\ \text{helicities}}}\prod_{j=1}^{6}A^{\rm tree}_{(j)}(z)\ .} \tag{3.56}$$

We stress that this formula applies to any gauge theory, in particular QCD. For the benefit of the interested reader, we provide a more explicit expression for c_1 and c_2 in terms of the residues computed by the contour integrals. Here it is [59]:

$$\begin{aligned} c_1 = & \frac{1}{4} \sum_{i=1,2} \operatorname*{Res}_{z=0} \frac{1}{z} \sum_{\substack{\text{particles} \\ \text{helicities}}} \prod_{j=1}^{6} A_{(j)}^{\text{tree}}(z)\big|_{\mathcal{S}_i} \\ & + \frac{1+\chi}{8} \sum_{i=1,2,5,6} \operatorname*{Res}_{z=\chi} \frac{1}{z-\chi} \sum_{\substack{\text{particles} \\ \text{helicities}}} \prod_{j=1}^{6} A_{(j)}^{\text{tree}}(z)\big|_{\mathcal{S}_i} \\ & - \frac{\chi}{8} \sum_{i=1,2,5,6} \operatorname*{Res}_{z=\chi+1} \frac{1}{z-\chi-1} \sum_{\substack{\text{particles} \\ \text{helicities}}} \prod_{j=1}^{6} A_{(j)}^{\text{tree}}(z)\big|_{\mathcal{S}_i} , \end{aligned} \tag{3.57}$$

$$\begin{aligned} c_2 = & -\frac{1+2\chi}{2s_{12}\chi(\chi+1)} \sum_{i=1,2} \operatorname*{Res}_{z=0} \frac{1}{z} \sum_{\substack{\text{particles} \\ \text{helicities}}} \prod_{j=1}^{6} A_{(j)}^{\text{tree}}(z)\big|_{\mathcal{S}_i} \\ & + \frac{1-2\chi}{4s_{12}\chi} \sum_{i=1,2,5,6} \operatorname*{Res}_{z=\chi} \frac{1}{z-\chi} \sum_{\substack{\text{particles} \\ \text{helicities}}} \prod_{j=1}^{6} A_{(j)}^{\text{tree}}(z)\big|_{\mathcal{S}_i} \\ & + \frac{3+2\chi}{4s_{12}(\chi+1)} \sum_{i=1,2,5,6} \operatorname*{Res}_{z=\chi+1} \frac{1}{z-\chi-1} \sum_{\substack{\text{particles} \\ \text{helicities}}} \prod_{j=1}^{6} A_{(j)}^{\text{tree}}(z)\big|_{\mathcal{S}_i} . \end{aligned} \tag{3.58}$$

3.2.4 Examples

We demonstrate the nonplanar double-box master formula by computing the basis integral coefficients for some specific helicity configurations. Contributions to the intermediate state sums are efficiently tracked via Grassmann variables [97–99]. In particular, we exploit that the transition from $\mathcal{N}=4$ to fewer supersymmetries is very straightforward; we simply apply the replacement

$$\begin{aligned} & \sum_{\substack{\mathcal{N}=4 \\ \text{multiplet}}} \prod_{i=1}^{k} A_{(i)}^{\text{tree}} = \Delta^{-1}(A+B+C+\cdots)^4 \longrightarrow \\ & \qquad \sum_{\substack{\mathcal{N}<4 \\ \text{multiplet}}} \prod_{i=1}^{k} A_{(i)}^{\text{tree}} = \Delta^{-1}(A+B+C+\cdots)^{\mathcal{N}}(A^{4-\mathcal{N}}+B^{4-\mathcal{N}}+C^{4-\mathcal{N}}+\cdots) . \end{aligned} \tag{3.59}$$

Here $A, B, C, \ldots$ contain spin dependence for each kinematically valid assignment of helicities on the internal lines with only gluons propagating in the loops whereas Δ is the denominator. Suppose that we only have two gluonic contributions A and B. For instance this case is relevant for quadruple cuts of one-loop amplitudes and hepta-cuts of two-loop amplitudes. A neat trick allows us to calculate the constant of proportionality between the $\mathcal{N} \leq 4$ and $\mathcal{N}=4$ state sums. Indeed, expanding around $A=-B$ yields

the desired expression [55]

$$\sum_{\substack{\mathcal{N}\leq 4\\ \text{multiplet}}} \prod_{j=1}^{6} A_{(j)}^{\text{tree}} = \frac{A^{4-\mathcal{N}}+B^{4-\mathcal{N}}}{(A+B)^{4-\mathcal{N}}}(1-\tfrac{1}{2}\delta_{\mathcal{N},4}) \sum_{\substack{\mathcal{N}=4\\ \text{multiplet}}} \prod_{j=1}^{6} A_{(j)}^{\text{tree}}$$
$$= \left\{1-(4-\mathcal{N})\left(\frac{A}{A+B}\right)+(4-\mathcal{N})\left(\frac{A}{A+B}\right)^2\right\} \sum_{\substack{\mathcal{N}=4\\ \text{multiplet}}} \prod_{j=1}^{6} A_{(j)}^{\text{tree}} \,. \tag{3.60}$$

We will apply this formula to the $--++$ helicity amplitude. Our starting point is the tree-level data in $\mathcal{N}=4$ theory,

$$\sum_{\substack{\mathcal{N}=4\\ \text{multiplet}}} \prod_{j=1}^{6} A_{(j)}^{\text{tree}}(z)\big|_{\mathcal{S}_i} = -s_{12}^2 s_{14} A_{--++}^{\text{tree}} \,, \tag{3.61}$$

which is independent of the loop momenta. Inserting the spin factors worked out in ref. [59] into eq. (3.60) produces

$$\sum_{\substack{\mathcal{N}\leq 4\\ \text{multiplet}}} \prod_{j=1}^{6} A_{(j)}^{\text{tree}}(z)\big|_{\mathcal{S}_2} = -s_{12}^2 s_{14} A_{--++}^{\text{tree}} \left\{1-(4-\mathcal{N})(z-\chi)+(4-\mathcal{N})(z-\chi)^2\right\} \,. \tag{3.62}$$

Now, feeding this expression into the master formula gives

$$A_4^{(2)}(1^-,1^-,1^+,1^+) =$$
$$-s_{12}^2 s_{14} A_{--++}^{\text{tree}} \Bigg\{ \left[1+(4-\mathcal{N})\frac{s_{14}}{4s_{12}}\left(1+\frac{s_{14}}{s_{12}}\right)\right] X_{1,1,2}^{**}[1]$$
$$+ (4-\mathcal{N})\frac{s_{13}-s_{14}}{2s_{12}^2} X_{1,1,2}^{**}[(\ell_1\cdot k_3)] \Bigg\} \,. \tag{3.63}$$

3.2.5 Massive Hepta-Cut Equations

It is desireable to investigate whether the simple results obtained in the nonplanar sector for massless external particles can be generalized to massive configurations. We are particularly interested in extracting information from the global structure of the hepta-cut. From now on we will consider maximal cuts of the nonplanar double-box integral $X_{2,1,1}$ in the presence of one, two, three or four massive legs. Refer to eq. (3.35) and fig. 3.10 for an outline of the conventions for the momentum flow. The rest of this chapter follows paper II.

Massive unitarity cut equations are conveniently manipulated using mutually projected kinematics [15, 18]. The idea is to obtain massless momenta $(k_i^\flat, k_j^\flat)$ from a pair of massive momenta (k_i, k_j). We will consider four-point kinematics with mutually projecting pairs (k_1,k_2) and (k_3,k_4). For each pair we define

$$k_{j,1}^{\flat,\mu} = k_{j,1}^\mu - \frac{k_{j,1}^2}{2k_{j,1}\cdot k_{j,2}^\flat} k_{j,2}^{\flat,\mu} \,, \quad k_{j,2}^{\flat,\mu} = k_{j,2}^\mu - \frac{k_{j,2}^2}{2k_{j,2}\cdot k_{j,1}^\flat} k_{j,1}^{\flat,\mu} \,. \tag{3.64}$$

Hence, $(k_{j,1}^{\flat,\mu}, k_{j,2}^{\flat,\mu})$ are massless by construction. Note that

$$k_{j,1} \cdot k_{j,2}^{\flat} = k_{j,1}^{\flat} \cdot k_{j,2} = k_{j,1}^{\flat} \cdot k_{j,2}^{\flat} \,. \tag{3.65}$$

Notation may be streamlined if we define the frequently occurring quantity,

$$\gamma_{j,12} = 2k_{j,1}^{\flat} \cdot k_{j,2}^{\flat} \,, \tag{3.66}$$

which upon identification in eq. (3.64) immediately leads to a quadratic equation with the solutions

$$\gamma_{j,12}^{\pm} = k_{j,1} \cdot k_{j,2} \pm \left[(k_{j,1} \cdot k_{j,2})^2 - k_{j,1}^2 k_{j,2}^2 \right]^{1/2} . \tag{3.67}$$

Throughout this calculation we will use the loop-momentum parametrization

$$\ell_1^{\mu} = \frac{1}{2}\langle \lambda_1^- | \gamma^{\mu} | \tilde{\lambda}_1^{\prime -}] = \frac{1}{2}\langle \lambda_1 | \gamma^{\mu} | \tilde{\lambda}_1^{\prime}] \,, \quad \ell_2^{\mu} = \frac{1}{2}\langle \lambda_2^- | \gamma^{\mu} | \tilde{\lambda}_2^{\prime -}] = \frac{1}{2}\langle \lambda_2 | \gamma^{\mu} | \tilde{\lambda}_2^{\prime}] \,. \tag{3.68}$$

Note that the on-shell conditions $\ell_1^2 = \ell_2^2 = 0$ are automatically satisfied. This point will be addressed shortly. We construct the various loop spinors from the spinors associated with the two mutually projecting pairs,

$$\begin{aligned}
|\lambda_1^+\rangle &= \xi_1 |1^{\flat,+}\rangle + \xi_2 \frac{\langle 4^{\flat} 1^{\flat} \rangle}{\langle 4^{\flat} 2^{\flat} \rangle} |2^{\flat,+}\rangle \,, \quad |\tilde{\lambda}_1^{\prime -}\rangle = \xi_1^{\prime} |1^{\flat,-}\rangle + \xi_2^{\prime} \frac{[4^{\flat} 1^{\flat}]}{[4^{\flat} 2^{\flat}]} |2^{\flat,-}\rangle \,, \\
|\lambda_2^+\rangle &= \xi_3 \frac{\langle 1^{\flat} 4^{\flat} \rangle}{\langle 1^{\flat} 3^{\flat} \rangle} |3^{\flat,+}\rangle + \xi_4 |4^{\flat,+}\rangle \,, \quad |\tilde{\lambda}_2^{\prime -}\rangle = \xi_3^{\prime} \frac{[1^{\flat} 4^{\flat}]}{[1^{\flat} 3^{\flat}]} |3^{\flat,-}\rangle + \xi_4^{\prime} |4^{\flat,-}\rangle \,.
\end{aligned} \tag{3.69}$$

All parameters are in general complex. We may expand ℓ_1^{μ} and ℓ_2^{μ} explicitly in the basis of four-vectors, with the result

$$\begin{aligned}
\ell_1^{\mu}(\xi_i, \xi_i^{\prime}) \;=\; & \xi_1 \xi_1^{\prime} k_1^{\flat,\mu} + \xi_2 \xi_2^{\prime} \frac{k_1^{\flat} \cdot k_4^{\flat}}{k_2^{\flat} \cdot k_4^{\flat}} k_2^{\flat,\mu} \\
& + \frac{\xi_1 \xi_2^{\prime}}{2} \frac{[1^{\flat} 4^{\flat}]}{[2^{\flat} 4^{\flat}]} \langle 1^{\flat,-} | \gamma^{\mu} | 2^{\flat,-}] + \frac{\xi_2 \xi_1^{\prime}}{2} \frac{\langle 1^{\flat} 4^{\flat} \rangle}{\langle 2^{\flat} 4^{\flat} \rangle} \langle 2^{\flat,-} | \gamma^{\mu} | 1^{\flat,-}] \,,
\end{aligned} \tag{3.70}$$

$$\begin{aligned}
\ell_2^{\mu}(\xi_i, \xi_i^{\prime}) \;=\; & \xi_3 \xi_3^{\prime} \frac{k_1^{\flat} \cdot k_4^{\flat}}{k_1^{\flat} \cdot k_3^{\flat}} k_3^{\flat,\mu} + \xi_4 \xi_4^{\prime} k_4^{\flat,\mu} \\
& + \frac{\xi_3 \xi_4^{\prime}}{2} \frac{\langle 1^{\flat} 4^{\flat} \rangle}{\langle 1^{\flat} 3^{\flat} \rangle} \langle 3^{\flat,-} | \gamma^{\mu} | 4^{\flat,-}] + \frac{\xi_4 \xi_3^{\prime}}{2} \frac{[1^{\flat} 4^{\flat}]}{[1^{\flat} 3^{\flat}]} \langle 4^{\flat,-} | \gamma^{\mu} | 3^{\flat,-}] \,.
\end{aligned} \tag{3.71}$$

It follows that we are able to eventually fix two of the complex parameters without loss of generality. This freedom amounts to some sort of a gauge choice. However, we emphasize that this choice is not necessarily the same for all cut solutions.

We assume that all four corners are massive. Three of the on-shell equations are very simple as they involve only one of the two loop momenta,

$$(\ell_1 - k_1)^2 = 0 \implies m_1^2 (1 - \xi_1 \xi_1^{\prime}) - \frac{k_1^{\flat} \cdot k_4^{\flat}}{k_2^{\flat} \cdot k_4^{\flat}} \xi_2 \xi_2^{\prime} \gamma_{12} = 0 \,, \tag{3.72}$$

$$(\ell_1 - k_1 - k_2)^2 = 0 \implies s_{12} - m_1^2 - \gamma_{12} \xi_1 \xi_1^{\prime} - \frac{k_1^{\flat} \cdot k_4^{\flat}}{k_2^{\flat} \cdot k_4^{\flat}} m_2^2 \xi_2 \xi_2^{\prime} = 0 \,, \tag{3.73}$$

$$(\ell_2 - k_4)^2 = 0 \implies m_4^2 (1 - \xi_4 \xi_4^{\prime}) - \frac{k_1^{\flat} \cdot k_4^{\flat}}{k_1^{\flat} \cdot k_3^{\flat}} \xi_3 \xi_3^{\prime} \gamma_{34} = 0 \,. \tag{3.74}$$

Lorentz products involving flattened momenta appear frequently in the remainder of this calculation. Therefore we collect the expressions:

$$\begin{aligned} k_1^\flat \cdot k_3^\flat = \gamma_{12}\gamma_{34} &\left(2(\gamma_{12}^2 - m_1^2 m_2^2)(\gamma_{34}^2 - m_3^2 m_4^2)\right)^{-1} \\ &\times \left\{ m_1^2 \left[\gamma_{34}(m_2^2 + m_3^2 - s_{14}) + m_3^2(m_1^2 + m_3^2 - s_{12} - s_{14})\right] \right. \\ &\left. + \gamma_{12}\left[m_3^2(m_1^2 + m_4^2 - s_{14}) + \gamma_{34}(m_2^2 + m_4^2 - s_{12} - s_{14})\right] \right\} , \end{aligned} \tag{3.75}$$

$$\begin{aligned} k_1^\flat \cdot k_4^\flat = \gamma_{12}\gamma_{34} &\left(2(\gamma_{12}^2 - m_1^2 m_2^2)(\gamma_{34}^2 - m_3^2 m_4^2)\right)^{-1} \\ &\times \left\{ m_1^2 \left[\gamma_{34}(m_1^2 + m_3^2 - s_{12} - s_{14}) + m_4^2(m_2^2 + m_3^2 - s_{14})\right] \right. \\ &\left. + \gamma_{12}\left[m_4^2(m_2^2 + m_4^2 - s_{12} - s_{14}) + \gamma_{34}(m_1^2 + m_4^2 - s_{14})\right] \right\} , \end{aligned} \tag{3.76}$$

$$\begin{aligned} k_2^\flat \cdot k_3^\flat = \gamma_{12}\gamma_{34} &\left(2(\gamma_{12}^2 - m_1^2 m_2^2)(\gamma_{34}^2 - m_3^2 m_4^2)\right)^{-1} \\ &\times \left\{ m_2^2 \left[m_3^2(m_1^2 + m_4^2 - s_{14}) + \gamma_{34}(m_2^2 + m_4^2 - s_{12} - s_{14})\right] \right. \\ &\left. + \gamma_{12}\left[m_3^2(m_1^2 + m_3^2 - s_{12} - s_{14}) + \gamma_{34}(m_2^2 + m_3^2 - s_{14})\right] \right\} , \end{aligned} \tag{3.77}$$

$$\begin{aligned} k_2^\flat \cdot k_4^\flat = \gamma_{12}\gamma_{34} &\left(2(\gamma_{12}^2 - m_1^2 m_2^2)(\gamma_{34}^2 - m_3^2 m_4^2)\right)^{-1} \\ &\times \left\{ m_2^2 \left[\gamma_{34}(m_1^2 + m_4^2 - s_{14}) + m_4^2(m_2^2 + m_4^2 - s_{12} - s_{14})\right] \right. \\ &\left. + \gamma_{12}\left[m_4^2(m_2^2 + m_3^2 - s_{14}) + \gamma_{34}(m_1^2 + m_3^2 - s_{12} - s_{14})\right] \right\} . \end{aligned} \tag{3.78}$$

We also have trivial identity $m_i^2 = 2k_i^\flat \cdot k_i$ along with the tedious expressions,

$$k_1^\flat \cdot k_3 = + \frac{\gamma_{12}[m_1^2(m_2^2 + m_3^2 - s_{14}) + \gamma_{12}(m_2^2 + m_4^2 - s_{12} - s_{14})]}{2(\gamma_{12}^2 - m_1^2 m_2^2)} , \tag{3.79}$$

$$k_2^\flat \cdot k_3 = - \frac{\gamma_{12}[\gamma_{12}(m_2^2 + m_3^2 - s_{14}) + m_2^2(m_2^2 + m_4^2 - s_{12} - s_{14})]}{2(\gamma_{12}^2 - m_1^2 m_2^2)} . \tag{3.80}$$

Finally, we also need the quantities

$$\tau \equiv \frac{\langle 1^\flat 4^\flat \rangle \langle 2^\flat 3^\flat \rangle}{\langle 2^\flat 4^\flat \rangle \langle 1^\flat 3^\flat \rangle} , \quad \bar{\tau} \equiv \frac{[1^\flat 4^\flat][2^\flat 3^\flat]}{[2^\flat 4^\flat][1^\flat 3^\flat]} . \tag{3.81}$$

Note that τ and $\bar{\tau}$ are complex conjugates of each other for real external momenta as indicated. But in fact $\tau = \bar{\tau}$. For the sake of completeness we provide the explicit expression,

$$\begin{aligned} \tau = \bar{\tau} = &- \frac{\gamma_{34}(\gamma_{12} + m_1^2)}{(\gamma_{34} + m_3^2)[(\gamma_{12}\gamma_{34} - m_1^2 m_3^2)(\gamma_{12}\gamma_{34} - m_2^2 m_4^2) + \gamma_{12}\gamma_{34} s_{12} s_{14}]} \\ &\times \Big[(\gamma_{12} + m_2^2)(\gamma_{34} + m_3^2)(m_2^2 + m_3^2 - s_{14}) + 2m_2^2 m_3^2 s_{12} + \\ &\quad (\gamma_{12} + m_2^2) m_3^2 (m_1^2 - m_2^2 - s_{12}) + (\gamma_{34} + m_3^2) m_2^2 (m_4^2 - m_3^2 - s_{12}) \Big] . \end{aligned} \tag{3.82}$$

Now, returning to the hepta-cut equations for loop momentum ℓ_1, we obtain for general masses $m_1 \neq 0 \neq m_2$ the solution

$$\xi_1 \xi_1' = \frac{\gamma_{12} s_{12} - (\gamma_{12} + m_2^2) m_1^2}{\gamma_{12}^2 - m_1^2 m_2^2} \equiv \bar{\xi}_1 , \tag{3.83}$$

$$\xi_2 \xi_2' = \frac{m_1^2(m_1^2 + \gamma_{12} - s_{12}) k_2^\flat \cdot k_4^\flat}{(\gamma_{12}^2 - m_1^2 m_2^2) k_1^\flat \cdot k_4^\flat} \equiv \bar{\xi}_2 . \tag{3.84}$$

If we then rewrite eq. (3.74) such that

$$\xi_3\xi_3' + \mu(\xi_4\xi_4' - 1) = 0\ , \quad \mu \equiv \frac{m_4^2 k_1^\flat \cdot k_3^\flat}{\gamma_{34} k_1^\flat \cdot k_4^\flat}\ , \tag{3.85}$$

it is clear that $\xi_3\xi_3' = 0$ if $m_4 = 0$ or $\xi_4\xi_4' = 1$.

The coupled on-shell equations are actually also quite straightforward to solve thanks to the loop-momentum parametrization. One of the equations factorizes completely,

$$(\ell_1 + \ell_2)^2 \ = \ 0 \implies (\xi_1(\xi_3 + \xi_4) + \xi_2(\tau\xi_3 + \xi_4)) \times (\xi_1'(\xi_3' + \xi_4') + \xi_2'(\tau\xi_3' + \xi_4')) = 0\ , \tag{3.86}$$

whereas the other can be brought to the form

$$\begin{aligned}(\ell_1 + \ell_2 + k_3)^2 \ = \ 0 \implies \\ m_3^2 + 2\Bigg\{ k_1^\flat \cdot k_3 \xi_1\xi_1' + \left[\tau k_1^\flat \cdot k_3^\flat + \frac{m_3^2 k_1^\flat \cdot k_4^\flat}{\gamma_{34}}\right](\xi_1\xi_2' + \xi_1'\xi_2) \\ + \frac{m_3^2 k_1^\flat \cdot k_4^\flat}{2k_1^\flat \cdot k_3^\flat}\xi_3\xi_3' + \frac{k_1^\flat \cdot k_4^\flat k_2^\flat \cdot k_3}{k_2^\flat \cdot k_4^\flat}\xi_2\xi_2' + \frac{\gamma_{34}}{2}\xi_4\xi_4'\Bigg\} = 0\ .\end{aligned} \tag{3.87}$$

Inserting eqs. (3.84) and (3.85) into eq. (3.87) yields

$$\begin{aligned}\xi_4\xi_4' = -\left(\gamma_{34} - \frac{m_3^2 m_4^2}{\gamma_{34}}\right)^{-1}\Bigg\{ m_3^2\left(1 + \frac{m_4^2}{\gamma_{34}}\right) + 2\Bigg[k_1^\flat \cdot k_3 \bar\xi_1 + \frac{k_1^\flat \cdot k_4^\flat}{k_2^\flat \cdot k_4^\flat} k_2^\flat \cdot k_3 \bar\xi_2 \\ + \left(\tau k_1^\flat \cdot k_3^\flat + \frac{m_3^2 k_1^\flat \cdot k_4^\flat}{\gamma_{34}}\right)(\xi_1\xi_2' + \xi_1'\xi_2)\Bigg]\Bigg\}\ .\end{aligned} \tag{3.88}$$

Taking advantage of the relations,

$$\frac{\tau}{(\tau - 1)(\bar\xi_1 - \tau\bar\xi_2)} = \frac{2k_1^\flat \cdot k_4^\flat}{\gamma_{34}^2 - m_3^2 m_4^2}\left[m_3^2 + \gamma_{34}\tau\frac{k_1^\flat \cdot k_3^\flat}{k_1^\flat \cdot k_4^\flat}\right]\ , \tag{3.89}$$

$$\frac{\bar\xi_1 + \tau^2\bar\xi_2}{(\tau - 1)(\bar\xi_1 - \tau\bar\xi_2)} = \frac{\gamma_{34}}{\gamma_{34}^2 - m_3^2 m_4^2}\left[m_3^2\left(1 + \frac{m_4^2}{\gamma_{34}}\right) + 2\left(k_1^\flat \cdot k_3 \bar\xi_1 + \frac{k_1^\flat \cdot k_4^\flat}{k_2^\flat \cdot k_4^\flat} k_2^\flat \cdot k_3 \bar\xi_2\right)\right]\ , \tag{3.90}$$

allows us to rewrite eq. (3.88), with the simplified result

$$\xi_4\xi_4' = 1 + \frac{\tau(\bar\xi_1 + \bar\xi_2 + \xi_1\xi_2' + \xi_1'\xi_2)}{(1 - \tau)(\bar\xi_1 - \tau\bar\xi_2)}\ . \tag{3.91}$$

We invite the reader to verify these identities through eqs. (3.75)-(3.80) and (3.82) along with expressions for $\bar\xi_1$ and $\bar\xi_2$ given in eq. (3.84). It is a rather unwieldy task, though.

The hepta-cut solutions form three pairs of parity conjugates $(\mathcal{S}_1, \mathcal{S}_2)$, $(\mathcal{S}_3, \mathcal{S}_4)$, $(\mathcal{S}_5, \mathcal{S}_6)$. In terms of the kinematic quantities $\bar\xi_1$, $\bar\xi_2$, τ and μ, see eqs. (3.82)-(3.85),

the explicit solutions take the form,

$$\begin{aligned}
\mathcal{S}_1 \,:\, (\xi_1,\xi_2,\xi_3,\xi_4) &= \left(1, z, \frac{\mu\tau(1+z)}{1+\tau z}, 1\right) \\
(\xi_1',\xi_2',\xi_3',\xi_4') &= \left(\bar\xi_1, \frac{\bar\xi_2}{z}, -\frac{(\bar\xi_2+\bar\xi_1 z)(1+\tau z)}{z(1-\tau)(\bar\xi_1-\tau\bar\xi_2)}, \frac{(\bar\xi_2+\bar\xi_1 z)(1+\tau z)}{z(1-\tau)(\bar\xi_1-\tau\bar\xi_2)}\right) ,
\end{aligned} \tag{3.92}$$

$$\begin{aligned}
\mathcal{S}_2 \,:\, (\xi_1,\xi_2,\xi_3,\xi_4) &= \left(\bar\xi_1, \frac{\bar\xi_2}{z}, -\frac{(\bar\xi_2+\bar\xi_1 z)(1+\tau z)}{z(1-\tau)(\bar\xi_1-\tau\bar\xi_2)}, \frac{(\bar\xi_2+\bar\xi_1 z)(1+\tau z)}{z(1-\tau)(\bar\xi_1-\tau\bar\xi_2)}\right) \\
(\xi_1',\xi_2',\xi_3',\xi_4') &= \left(1, z, \frac{\mu\tau(1+z)}{1+\tau z}, 1\right) ,
\end{aligned} \tag{3.93}$$

$$\mathcal{S}_3 \,:\, (\xi_1,\xi_2,\xi_3,\xi_4) = \left(1, -\frac{\bar\xi_2}{\bar\xi_1}, z, 1\right) , \quad (\xi_1',\xi_2',\xi_3',\xi_4') = \left(\bar\xi_1, -\bar\xi_1, 0, 1\right) , \tag{3.94}$$

$$\mathcal{S}_4 \,:\, (\xi_1,\xi_2,\xi_3,\xi_4) = \left(\bar\xi_1, -\bar\xi_1, 0, 1\right) , \quad (\xi_1',\xi_2',\xi_3',\xi_4') = \left(1, -\frac{\bar\xi_2}{\bar\xi_1}, z, 1\right) , \tag{3.95}$$

$$\mathcal{S}_5 \,:\, (\xi_1,\xi_2,\xi_3,\xi_4) = \left(\bar\xi_1, -\tau\bar\xi_2, \mu, z\right) , \quad (\xi_1',\xi_2',\xi_3',\xi_4') = (1, -1/\tau, 1, 0) , \tag{3.96}$$

$$\mathcal{S}_6 \,:\, (\xi_1,\xi_2,\xi_3,\xi_4) = (1, -1/\tau, 1, 0) , \quad (\xi_1',\xi_2',\xi_3',\xi_4') = \left(\bar\xi_1, -\tau\bar\xi_2, \mu, z\right) . \tag{3.97}$$

Defining

$$w(z) = \frac{1+z}{1+\tau z} \iff z(w) = -\frac{1-w}{1-\tau w} , \tag{3.98}$$

the on-shell loop momenta read

$$\begin{aligned}
\ell_1^\mu|_{\mathcal{S}_1} &= \bar\xi_1 k_1^{\flat,\mu} + \bar\xi_2 \frac{k_1^\flat\cdot k_4^\flat}{k_2^\flat\cdot k_4^\flat} k_2^{\flat,\mu} + \frac{\bar\xi_2}{2z}\frac{[1^\flat 4^\flat]}{[2^\flat 4^\flat]}\langle 1^{\flat,-}|\gamma^\mu|2^{\flat,-}] + \frac{\bar\xi_1 z}{2}\frac{\langle 1^\flat 4^\flat\rangle}{\langle 2^\flat 4^\flat\rangle}\langle 2^{\flat,-}|\gamma^\mu|1^{\flat,-}] , \\
\ell_2^\mu|_{\mathcal{S}_1} &= -\frac{1+\tau z}{(1-\tau)(\bar\xi_1-\tau\bar\xi_2)z}\Big\{\mu\tau w(z)(\bar\xi_1 z+\bar\xi_2)\frac{k_1^\flat\cdot k_4^\flat}{k_1^\flat\cdot k_3^\flat}k_3^{\flat,\mu} - (\bar\xi_1 z+\tau\bar\xi_2)k_4^{\flat,\mu} \\
&\quad - \frac{1}{2}\mu\tau w(z)(\bar\xi_1 z+\tau\bar\xi_2)\frac{\langle 1^\flat 4^\flat\rangle}{\langle 1^\flat 3^\flat\rangle}\langle 3^{\flat,-}|\gamma^\mu|4^{\flat,-}] + \frac{1}{2}(\bar\xi_1 z+\bar\xi_2)\frac{[1^\flat 4^\flat]}{[1^\flat 3^\flat]}\langle 4^{\flat,-}|\gamma^\mu|3^{\flat,-}]\Big\} ,
\end{aligned} \tag{3.99}$$

$$\begin{aligned}
\ell_1^\mu|_{\mathcal{S}_2} &= \bar\xi_1 k_1^{\flat,\mu} + \bar\xi_2 \frac{k_1^\flat\cdot k_4^\flat}{k_2^\flat\cdot k_4^\flat} k_2^{\flat,\mu} + \frac{\bar\xi_1 z}{2}\frac{[1^\flat 4^\flat]}{[2^\flat 4^\flat]}\langle 1^{\flat,-}|\gamma^\mu|2^{\flat,-}] + \frac{\bar\xi_2}{2z}\frac{\langle 1^\flat 4^\flat\rangle}{\langle 2^\flat 4^\flat\rangle}\langle 2^{\flat,-}|\gamma^\mu|1^{\flat,-}] , \\
\ell_2^\mu|_{\mathcal{S}_2} &= -\frac{1+\tau z}{(1-\tau)(\bar\xi_1-\tau\bar\xi_2)z}\Big\{\mu\tau w(z)(\bar\xi_1 z+\bar\xi_2)\frac{k_1^\flat\cdot k_4^\flat}{k_1^\flat\cdot k_3^\flat}k_3^{\flat,\mu} - (\bar\xi_1 z+\tau\bar\xi_2)k_4^{\flat,\mu} \\
&\quad - \frac{1}{2}\mu\tau w(z)(\bar\xi_1 z+\tau\bar\xi_2)\frac{\langle 1^\flat 4^\flat\rangle}{\langle 1^\flat 3^\flat\rangle}\langle 3^{\flat,-}|\gamma^\mu|4^{\flat,-}] + \frac{1}{2}(\bar\xi_1 z+\bar\xi_2)\frac{[1^\flat 4^\flat]}{[1^\flat 3^\flat]}\langle 4^{\flat,-}|\gamma^\mu|3^{\flat,-}]\Big\} ,
\end{aligned} \tag{3.100}$$

$$\begin{aligned}
\ell_1^\mu|_{\mathcal{S}_3} &= \bar\xi_1 k_1^{\flat,\mu} + \bar\xi_2 \frac{k_1^\flat\cdot k_4^\flat}{k_2^\flat\cdot k_4^\flat} k_2^{\flat,\mu} - \frac{\bar\xi_1}{2}\frac{[1^\flat 4^\flat]}{[2^\flat 4^\flat]}\langle 1^{\flat,-}|\gamma^\mu|2^{\flat,-}] - \frac{\bar\xi_2}{2}\frac{\langle 1^\flat 4^\flat\rangle}{\langle 2^\flat 4^\flat\rangle}\langle 2^{\flat,-}|\gamma^\mu|1^{\flat,-}] , \\
\ell_2^\mu|_{\mathcal{S}_3} &= k_4^{\flat,\mu} + \frac{z}{2}\frac{\langle 1^\flat 4^\flat\rangle}{\langle 1^\flat 3^\flat\rangle}\langle 3^{\flat,-}|\gamma^\mu|4^{\flat,-}] ,
\end{aligned} \tag{3.101}$$

$$\ell_1^\mu|_{\mathcal{S}_4} = \bar\xi_1 k_1^{\flat,\mu} + \bar\xi_2 \frac{k_1^\flat\cdot k_4^\flat}{k_2^\flat\cdot k_4^\flat} k_2^{\flat,\mu} - \frac{\bar\xi_2}{2}\frac{[1^\flat 4^\flat]}{[2^\flat 4^\flat]}\langle 1^{\flat,-}|\gamma^\mu|2^{\flat,-}] - \frac{\bar\xi_1}{2}\frac{\langle 1^\flat 4^\flat\rangle}{\langle 2^\flat 4^\flat\rangle}\langle 2^{\flat,-}|\gamma^\mu|1^{\flat,-}] ,$$

$$\ell_2^\mu|_{\mathcal{S}_4} = k_4^{\flat,\mu} + \frac{z}{2}\frac{[1^\flat 4^\flat]}{[1^\flat 3^\flat]}\langle 4^{\flat,-}|\gamma^\mu|3^{\flat,-}] \,, \tag{3.102}$$

$$\ell_1^\mu|_{\mathcal{S}_5} = \bar{\xi}_1 k_1^{\flat,\mu} + \bar{\xi}_2\frac{k_1^\flat\cdot k_4^\flat}{k_2^\flat\cdot k_4^\flat}k_2^{\flat,\mu} - \frac{\bar{\xi}_1}{2\tau}\frac{[1^\flat 4^\flat]}{[2^\flat 4^\flat]}\langle 1^{\flat,-}|\gamma^\mu|2^{\flat,-}] - \frac{\bar{\xi}_2\tau}{2}\frac{\langle 1^\flat 4^\flat\rangle}{\langle 2^\flat 4^\flat\rangle}\langle 2^{\flat,-}|\gamma^\mu|1^{\flat,-}] \,,$$

$$\ell_2^\mu|_{\mathcal{S}_5} = \mu\frac{k_1^\flat\cdot k_4^\flat}{k_1^\flat\cdot k_3^\flat}k_3^{\flat,\mu} + \frac{z}{2}\frac{[1^\flat 4^\flat]}{[1^\flat 3^\flat]}\langle 4^{\flat,-}|\gamma^\mu|3^{\flat,-}] \,, \tag{3.103}$$

$$\ell_1^\mu|_{\mathcal{S}_6} = \bar{\xi}_1 k_1^{\flat,\mu} + \bar{\xi}_2\frac{k_1^\flat\cdot k_4^\flat}{k_2^\flat\cdot k_4^\flat}k_2^{\flat,\mu} - \frac{\tau\bar{\xi}_2}{2}\frac{[1^\flat 4^\flat]}{[2^\flat 4^\flat]}\langle 1^{\flat,-}|\gamma^\mu|2^{\flat,-}] - \frac{\bar{\xi}_1}{2\tau}\frac{\langle 1^\flat 4^\flat\rangle}{\langle 2^\flat 4^\flat\rangle}\langle 2^{\flat,-}|\gamma^\mu|1^{\flat,-}] \,,$$

$$\ell_2^\mu|_{\mathcal{S}_6} = \mu\frac{k_1^\flat\cdot k_4^\flat}{k_1^\flat\cdot k_3^\flat}k_3^{\flat,\mu} + \frac{z}{2}\frac{\langle 1^\flat 4^\flat\rangle}{\langle 1^\flat 3^\flat\rangle}\langle 3^{\flat,-}|\gamma^\mu|4^{\flat,-}] \,. \tag{3.104}$$

3.2.6 Less Massive Hepta-Cut Equations

Nonplanar double-box integrals with one, two and three massive legs are important for higher-multiplicity scattering processes, starting already at five external massless particles. Accordingly, we will also study such contributions here.

In order to specify the discussion we focus on the two momenta in the crossed end of the diagram and assume that $m_1 m_2 \neq 0$. Note that the only dependence on m_3 is implicitly through e.g. τ and μ. All hepta-cut equations behave correctly for $m_3 \to 0$. Furthermore, $\mu \to 0$ for $m_4 \to 0$ so that eq. (3.85) becomes $\xi_3\xi_3' = 0$. The number of hepta-cut solutions remains six and the explicit solutions are inherited from the four-mass case in the limit $\mu \to 0$. The kinematic configurations covered by this class of kinematics are depicted in fig. 3.12.

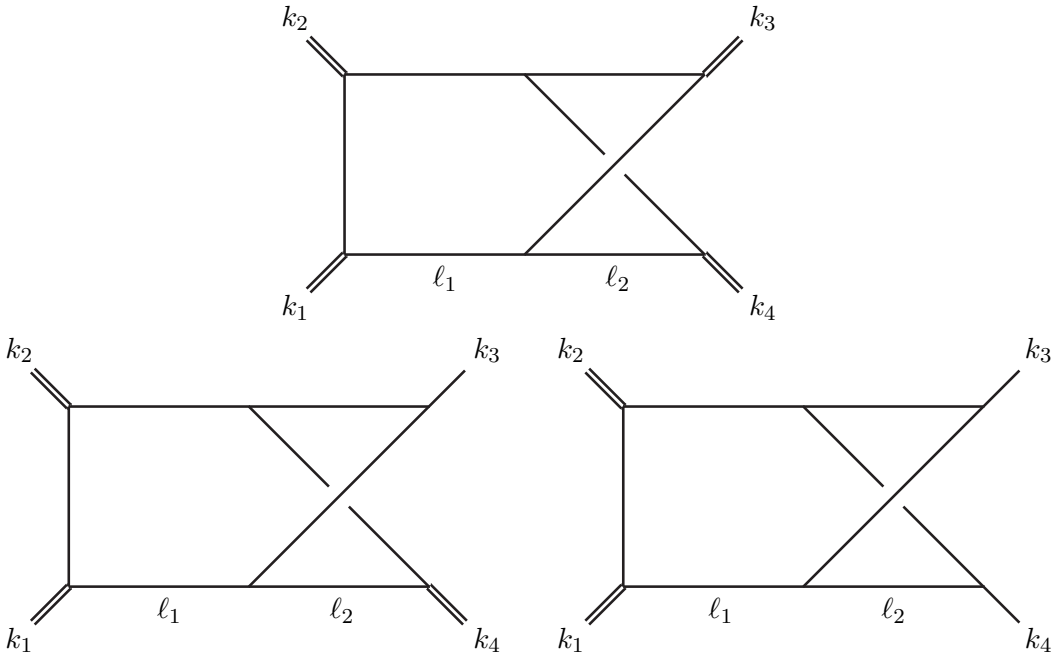

Figure 3.12: The first class of nonplanar double-box integrals includes the four-mass, three-mass and short-side two-mass diagrams with $m_1 m_2 \neq 0$. Massive external legs are indicated by doubled lines.

The situation is slightly more complicated if we allow one of both of the momenta k_1 and k_2 in the planar end to become massless. The problem is that the massless limits are no longer smooth and must be treated carefully. It can be seen that $\bar{\xi}_1 \to 1$ as $m_2 \to 0$ with m_1 arbitrary. Moreover, $\bar{\xi}_1 \to 1 + m_2^2/\gamma_{12}$ as $m_1 \to 0$. Consequently, the equation $\xi_1\xi_1' - \bar{\xi}_1 = 0$ is not branched. But $\bar{\xi}_2 = 0$ if $m_1 m_2 = 0$ and we instead get the equation $\xi_2\xi_2' = 0$. This implies that eq. (3.84) must be replaced by a pair of solutions, namely $\xi_2 = 0$ with ξ_2' free or vice versa. This class of kinematics supports eight distinct solutions that can be parametrized as follows,

$$\begin{aligned}
\widetilde{\mathcal{S}}_1 &: (\xi_1,\xi_2,\xi_3,\xi_4) = \left(1, z, \frac{\mu\tau(1+z)}{1+\tau z}, 1\right), \quad (\xi_1',\xi_2',\xi_3',\xi_4') = \left(\bar{\xi}_1, 0, -\frac{1+\tau z}{1-\tau}, \frac{1+\tau z}{1-\tau}\right), \\
\widetilde{\mathcal{S}}_2 &: (\xi_1,\xi_2,\xi_3,\xi_4) = \left(\bar{\xi}_1, 0, -\frac{1+\tau z}{1-\tau}, \frac{1+\tau z}{1-\tau}\right), \quad (\xi_1',\xi_2',\xi_3',\xi_4') = \left(1, z, \frac{\mu\tau(1+z)}{1+\tau z}, 1\right), \\
\widetilde{\mathcal{S}}_3 &: (\xi_1,\xi_2,\xi_3,\xi_4) = \left(1, z, -\frac{1+z}{1+\tau z}, 1\right), \quad (\xi_1',\xi_2',\xi_3',\xi_4') = \left(\bar{\xi}_1, 0, \frac{\mu\tau(1+\tau z)}{\tau-1}, \frac{1+\tau z}{1-\tau}\right), \\
\widetilde{\mathcal{S}}_4 &: (\xi_1,\xi_2,\xi_3,\xi_4) = \left(\bar{\xi}_1, 0, \frac{\mu\tau(1+\tau z)}{\tau-1}, \frac{1+\tau z}{1-\tau}\right), \quad (\xi_1',\xi_2',\xi_3',\xi_4') = \left(1, z, -\frac{1+z}{1+\tau z}, 1\right), \\
\widetilde{\mathcal{S}}_5 &: (\xi_1,\xi_2,\xi_3,\xi_4) = (1, 0, z, 1), \quad (\xi_1',\xi_2',\xi_3',\xi_4') = \left(\bar{\xi}_1, -\bar{\xi}_1, 0, 1\right), \\
\widetilde{\mathcal{S}}_6 &: (\xi_1,\xi_2,\xi_3,\xi_4) = \left(\bar{\xi}_1, -\bar{\xi}_1, 0, 1\right), \quad (\xi_1',\xi_2',\xi_3',\xi_4') = (1, 0, z, 1), \\
\widetilde{\mathcal{S}}_7 &: (\xi_1,\xi_2,\xi_3,\xi_4) = \left(\bar{\xi}_1, 0, \mu, z\right), \quad (\xi_1',\xi_2',\xi_3',\xi_4') = (1, -1/\tau, 1, 0), \\
\widetilde{\mathcal{S}}_8 &: (\xi_1,\xi_2,\xi_3,\xi_4) = (1, -1/\tau, 1, 0), \quad (\xi_1',\xi_2',\xi_3',\xi_4') = \left(\bar{\xi}_1, 0, \mu, z\right).
\end{aligned} \tag{3.105}$$

The covered kinematic configurations are shown in fig. 3.13.

We remark that six of the tilded solutions are inherited from the four-mass case by letting $\bar{\xi}_2 \to 0$. The new branches are named $\widetilde{\mathcal{S}}_3$ and $\widetilde{\mathcal{S}}_4$. For a lengthy calculation of the explicit forms of the loop momenta evaluated on each of the hepta-cut solutions, refer to ref. [62].

3.2.7 Residues and Topological Structure

Before we can evaluate the hepta-cut nonplanar double-box integrals, it is necessary to figure out how to impose the automatically satisfied constraints $\ell_1^2 = \ell_2^2 = 0$ by localization. The trick is to introduce new parameters $\zeta_1, \zeta_2 \in \mathbb{C}$ and two null-vectors η_1, η_2 with the properties [55],

$$\not{\eta}_1^{\mu}|\lambda_1^+\rangle \neq 0 \neq \not{\eta}_1^{\mu}|\tilde{\lambda}_1'^-\rangle, \quad \not{\eta}_2^{\mu}|\lambda_2^+\rangle \neq 0 \neq \not{\eta}_1^{\mu}|\tilde{\lambda}_2'^-\rangle, \tag{3.106}$$

and then alter the loop-momentum parametrization such that

$$\ell_1^{\mu} = \frac{1}{2}\langle\lambda_1|\gamma^{\mu}|\tilde{\lambda}_1'] + \zeta_1\eta_1^{\mu}, \tag{3.107}$$

$$\ell_2^{\mu} = \frac{1}{2}\langle\lambda_2|\gamma^{\mu}|\tilde{\lambda}_2'] + \zeta_2\eta_2^{\mu}. \tag{3.108}$$

Intermediate calculations simplify if we use the massless legs because; take for example $\eta_1 = k_2^{\flat}$ and $\eta_2 = k_3^{\flat}$. Then for $\mathcal{S}_1, \ldots, \mathcal{S}_4$,

$$\ell_1^2 = \gamma_{12}\xi_1\xi_1'\zeta_1 = 0, \quad \ell_2^2 = \gamma_{34}\xi_4\xi_4'\zeta_2 = 0, \tag{3.109}$$

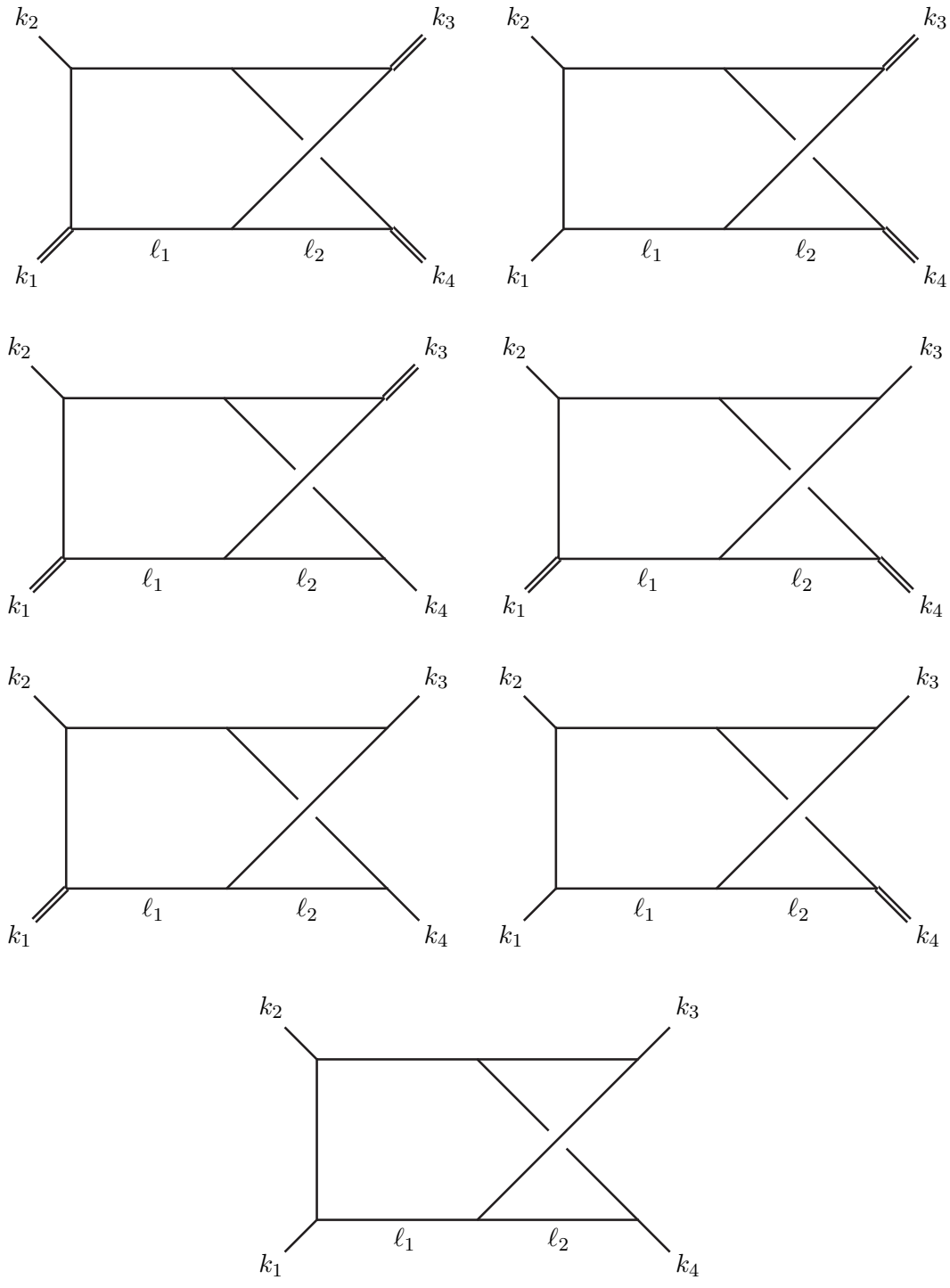

Figure 3.13: The second class of nonplanar double-box integrals includes the three-mass and the two-mass short-side diagrams with massless legs in the planar end of the diagram together with diagonal and long-side two-mass diagrams, all one-mass diagrams and finally the zero-mass diagram.

hence desired behavior is achieved for $\zeta_1 = \zeta_2 = 0$ as $\xi_1\xi_1' \neq 0 \neq \xi_4\xi_4'$ for general kinematics. Similarly, $\eta_1 = k_2^\flat$ and $\eta_2 = k_4^\flat$ are valid choices for solutions $\mathcal{S}_5$ and $\mathcal{S}_6$ is $\eta_1 = k_2^\flat$ and $\eta_2 = k_4^\flat$.

The Jacobians associated with the coordinate transformation from loop four-momenta to parameter space vary from solution to solution and are no longer constants. The reason is that our parametrization is not linear. For $\mathcal{S}_1$ and $\mathcal{S}_3$ we fix $\xi_1 = \xi_4' = 1$ and thus keep the variables $\alpha = (\zeta_1, \xi_1', \xi_2, \xi_2')$ and $\beta = (\zeta_2, \xi_3, \xi_3', \xi_4)$. Then,

$$J^L_{\mathcal{S}_{1,3}} = \det_{\mu,i} \frac{\partial \ell_1^\mu}{\partial \alpha_i} = i\frac{\gamma_{12}^2 k_1^\flat \cdot k_4^\flat \xi_1'}{4k_2^\flat \cdot k_4^\flat} \ , \quad J^R_{\mathcal{S}_{1,3}} = \det_{\mu,i} \frac{\partial \ell_2^\mu}{\partial \beta_i} = i\frac{\gamma_{34}^2 k_1^\flat \cdot k_4^\flat \xi_4'}{4k_1^\flat \cdot k_3^\flat} \ . \tag{3.110}$$

For $\mathcal{S}_2$ and $\mathcal{S}_4$ we keep the variables $\alpha = (\zeta_1, \xi_1, \xi_2, \xi_2')$ and $\beta = (\zeta_2, \xi_3, \xi_3', \xi_4')$ so that the Jacobians become

$$J^L_{\mathcal{S}_{2,4}} = \det_{\mu,i} \frac{\partial \ell_1^\mu}{\partial \alpha_i} = i\frac{\gamma_{12}^2 k_1^\flat \cdot k_4^\flat \xi_1}{4k_2^\flat \cdot k_4^\flat} \ , \quad J^R_{\mathcal{S}_{2,4}} = \det_{\mu,i} \frac{\partial \ell_2^\mu}{\partial \beta_i} = i\frac{\gamma_{34}^2 k_1^\flat \cdot k_4^\flat \xi_4}{4k_1^\flat \cdot k_3^\flat} \ . \tag{3.111}$$

Finally, for solutions $\mathcal{S}_5$ and $\mathcal{S}_6$,

$$J^L_{\mathcal{S}_5} = \det_{\mu,i} \frac{\partial \ell_1^\mu}{\partial \alpha_i} = i\frac{\gamma_{12}^2 k_1^\flat \cdot k_4^\flat \xi_1}{4k_2^\flat \cdot k_4^\flat} \ , \quad J^R_{\mathcal{S}_5} = \det_{\mu,i} \frac{\partial \ell_2^\mu}{\partial \beta_i} = i\gamma_{34}^2 \left(\frac{k_1^\flat \cdot k_4^\flat}{k_1^\flat \cdot k_3^\flat}\right)^2 \xi_3 \ , \tag{3.112}$$

$$J^L_{\mathcal{S}_6} = \det_{\mu,i} \frac{\partial \ell_1^\mu}{\partial \alpha_i} = i\frac{\gamma_{12}^2 k_1^\flat \cdot k_4^\flat \xi_1'}{4k_2^\flat \cdot k_4^\flat} \ , \quad J^R_{\mathcal{S}_6} = \det_{\mu,i} \frac{\partial \ell_2^\mu}{\partial \beta_i} = i\gamma_{34}^2 \left(\frac{k_1^\flat \cdot k_4^\flat}{k_1^\flat \cdot k_3^\flat}\right)^2 \xi_3' \ . \tag{3.113}$$

Changing integration variables as explained above, replacing the real slice integration contours by a multidimensional torus encircling one of the joint solutions of the heptacut equations and finally carrying out the seven of the contour integrals produces a total Jacobian J_i. Schematically,

$$X^{**}_{1,1,2}[1]_{\mathcal{S}_i} \equiv \oint_{\Gamma_i} dz J_i(z) \ . \tag{3.114}$$

The Jacobians are obtained by direct calculation without complication. We will spare the reader for extraneous details and simply state the resulting expressions:

$$X^{**}_{1,1,2}[1]_{\mathcal{S}_{1,2}} = +\frac{\gamma_\star(1-\tau)(\bar\xi_1 - \tau\bar\xi_2)}{\tau\bar\xi_1^2(1+\mu\tau)} \oint dz \frac{z}{(z+1)\left(z+\frac{1}{\tau}\right)\left(z+\frac{\bar\xi_2}{\bar\xi_1}\right)\left(z+\frac{\tau\bar\xi_2}{\bar\xi_1}\right)} \ , \tag{3.115}$$

$$X^{**}_{1,1,2}[1]_{\mathcal{S}_{3,4}} = -\frac{\gamma_\star}{\bar\xi_1 - \tau\bar\xi_2} \oint \frac{dz}{\left(z+\frac{\bar\xi_1-\bar\xi_2}{\bar\xi_1-\tau\bar\xi_2}\right)\left(z-\frac{\mu\tau(\bar\xi_1-\bar\xi_2)}{\bar\xi_1-\tau\bar\xi_2}\right)} \ , \tag{3.116}$$

$$X^{**}_{1,1,2}[1]_{\mathcal{S}_{5,6}} = +\frac{\gamma_\star}{\bar\xi_1 - \tau\bar\xi_2} \oint \frac{dz}{\left(z-\frac{\bar\xi_1-\tau^2\bar\xi_2}{\tau(\bar\xi_1-\tau\bar\xi_2)}\right)\left(z+\frac{\mu(\bar\xi_1-\tau^2\bar\xi_2)}{\bar\xi_1-\tau\bar\xi_2)}\right)} \ . \tag{3.117}$$

In these equations, (see also ref. [58])

$$\gamma_\star \equiv \frac{\gamma_{12}\gamma_{34}}{32(\gamma_{12}^2 - m_1^2m_2^2)(\gamma_{34}^2 - m_3^2m_4^2)k_1^\flat \cdot k_4^\flat} \ . \tag{3.118}$$

We invite the reader to consult e.g. refs. [55, 59, 60] for related examples.

For the sake of clarity below, let us denote each of the z-pole locations as follows (see eqs.(3.115)-(3.117)),

$$\{z_{1;1},\ldots,z_{1;4}\} = \left\{-1,-\frac{1}{\tau},-\frac{\bar\xi_2}{\bar\xi_1},-\frac{\tau\bar\xi_2}{\bar\xi_1}\right\} = \{z_{2;1},\ldots,z_{2;4}\}\ ,$$
$$\{z_{3;1},z_{3;2}\} = \left\{-\frac{\bar\xi_1-\bar\xi_2}{\bar\xi_1-\tau\bar\xi_2},\frac{\mu\tau(\bar\xi_1-\bar\xi_2)}{\bar\xi_1-\tau\bar\xi_2}\right\} = \{z_{4;1},z_{4;2}\}\ ,$$
$$\{z_{5;1},z_{5;2}\} = \left\{\frac{\bar\xi_1-\tau^2\bar\xi_2}{\tau(\bar\xi_1-\tau\bar\xi_2)},-\frac{\mu(\bar\xi_1-\tau^2\bar\xi_2)}{\bar\xi_1-\tau\bar\xi_2}\right\} = \{z_{6;1},z_{6;2}\}\ . \tag{3.119}$$

Additional singularities are associated with solutions $\mathcal{S}_1$ and $\mathcal{S}_2$; either of the loop momenta may become infinite for a finite value of z. Also, in each solution there is a pole at $z=\infty$. We conclude that the union of the singular point loci for all six branches has 24 points in total.

We will write the augmented hepta-cut as

$$\begin{aligned} X^{**}_{1,1,2}[\Phi(\ell_1(z),\ell_2(z)]\big|_{\rm aug} &\equiv \sum_{i=1}^{6}\oint_{\Gamma_i} dz J_i(z)\Phi(\ell_1(z),\ell_2(z)) \\ &= \sum_{i=1}^{|\mathcal{S}|}\sum_{\xi\in\text{poles}}\omega(i,\xi)\operatorname*{Res}_{z=\xi} J_i(z)\Phi(z)\big|_{\mathcal{S}_i}\ . \end{aligned} \tag{3.120}$$

where Γ_i is a linear combination of small z-circles around the poles, so that the integral extracts the residues of the loop integrand. Here we adopted the notation that the weight of the residue evaluated at $z=\xi$ at the ith branch is denoted by $\omega(i,\xi)$.

Inspecting the global structure of the hepta-cut [56, 79] reveals that not all of these residues are linearly independent. To see this, consider an arbitrary integrand test function $\Phi(\ell_1(z),\ell_2(z))$ and assume that Φ is regular on the Jacobian poles. Then,

$$\operatorname*{Res}_{\mathcal{S}_i\cap S_j} J(z)\Phi(\ell_1(z),\ell_2(z))\big|_{\mathcal{S}_i} = -\operatorname*{Res}_{\mathcal{S}_i\cap S_j} J(z)\Phi(\ell_1(z),\ell_2(z))\big|_{\mathcal{S}_j}\ . \tag{3.121}$$

In this equation, the left and right hand sides of the equation are understood to be evaluated in local coordinates on solutions $\mathcal{S}_i$ and $\mathcal{S}_j$ respectively. Other choices are equally valid. The complete list of such identities reads

$$\begin{aligned}
\operatorname*{Res}_{z=z_{1,1}} J_1(z)\Phi(z)|_{\mathcal{S}_1} &= -\operatorname*{Res}_{z=z_{4,1}} J_4(z)\Phi(z)|_{\mathcal{S}_4}\ ,\\
\operatorname*{Res}_{z=z_{1,2}} J_1(z)\Phi(z)|_{\mathcal{S}_1} &= -\operatorname*{Res}_{z=z_{6,2}} J_6(z)\Phi(z)|_{\mathcal{S}_6}\ ,\\
\operatorname*{Res}_{z=z_{1,3}} J_1(z)\Phi(z)|_{\mathcal{S}_1} &= -\operatorname*{Res}_{z=z_{3,2}} J_3(z)\Phi(z)|_{\mathcal{S}_3}\ ,\\
\operatorname*{Res}_{z=z_{1,4}} J_1(z)\Phi(z)|_{\mathcal{S}_1} &= -\operatorname*{Res}_{z=z_{5,1}} J_5(z)\Phi(z)|_{\mathcal{S}_5}\ ,\\
\operatorname*{Res}_{z=z_{2,1}} J_2(z)\Phi(z)|_{\mathcal{S}_2} &= -\operatorname*{Res}_{z=z_{3,1}} J_3(z)\Phi(z)|_{\mathcal{S}_3}\ ,\\
\operatorname*{Res}_{z=z_{2,2}} J_2(z)\Phi(z)|_{\mathcal{S}_2} &= -\operatorname*{Res}_{z=z_{5,2}} J_5(z)\Phi(z)|_{\mathcal{S}_5}\ ,\\
\operatorname*{Res}_{z=z_{2,3}} J_2(z)\Phi(z)|_{\mathcal{S}_2} &= -\operatorname*{Res}_{z=z_{4,2}} J_4(z)\Phi(z)|_{\mathcal{S}_4}\ ,\\
\operatorname*{Res}_{z=z_{2,4}} J_2(z)\Phi(z)|_{\mathcal{S}_2} &= -\operatorname*{Res}_{z=z_{6,1}} J_6(z)\Phi(z)|_{\mathcal{S}_6}\ .
\end{aligned} \tag{3.122}$$

This intersection pattern exactly confirms the global topological structure of the hepta-cut in fig. 3.15. This picture is generated by pinching the tubes of the genus-3 surface six

times along the indicated horizontal and vertical lines passing through the center of the surface as illustrated in fig. 3.14. This identification reduces the number of independent residues to 16. The residues at infinity and in numerator insertions are not shared. But all residues on each of the Riemann spheres are bound to vanish by the one-dimensional global residue theorem, hence we can further remove six residues.

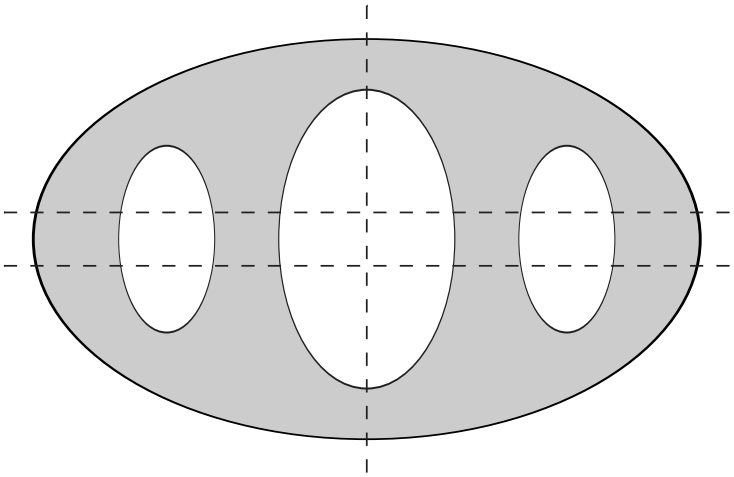

Figure 3.14: The hepta-cut of the nonplanar double-box diagram defines a genus-3 algebraic curve. The one-dimensional complex curve should be understood as the filled two-dimensional real surface. Specific kinematics lead to degeneracies that can be viewed as contractions of tubes along straight horizontal and vertical lines in the paper plane through the handles of the surface.

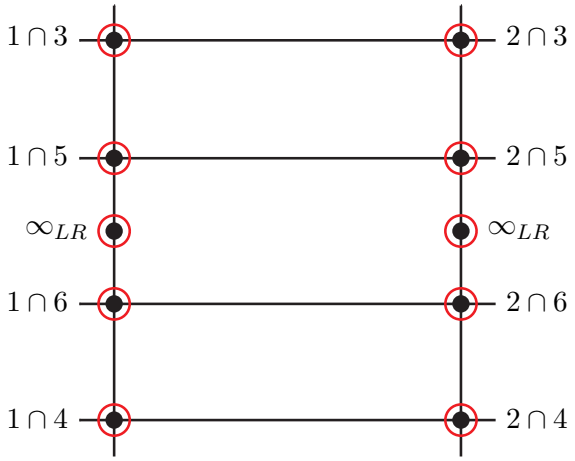

Figure 3.15: Global structure of the hepta-cut of the nonplanar double-box with four massive external legs. The figure illustrates the intersections of the irreducible components of the algebraic curve defined by the zero locus of the polynomial ideal generated by the inverse propagators. All degenerate configurations considered in this paper fall within this topological picture and that of fig. 3.16. The straight lines are drawn for simplicity and should be interpreted as $\mathbb{CP}^1$.

The upshot of the above consideration is that it suffices to encircle 10 global poles in order to produce a complete basis of homology for $\mathcal{S}_1 \cup \cdots \cup \mathcal{S}_6$. What is more, the

contributions from branches $\mathcal{S}_3, \ldots, \mathcal{S}_6$ turn out to be redundant, because each of them only has a single pole (at $z = \infty$) in addition to those located at the intersections with $\mathcal{S}_1$ and $\mathcal{S}_2$. An overcomplete basis is minimized by setting extraneous residue weights to zero. We find it natural to encircle all Jacobian poles along with poles in numerator insertions where both loop momenta become infinite simultaneously. Following the notation of ref. [56], the weights of the ten global poles can be written

$$\boldsymbol{\Omega} = (\omega_{1\cap4}, \omega_{1\cap6}, \omega_{1\cap3}, \omega_{1\cap5}, \omega_{1,\infty_{LR}}, \omega_{2\cap3}, \omega_{2\cap5}, \omega_{2\cap4}, \omega_{2\cap6}, \omega_{1,\infty_{LR}}) \equiv (\omega_1, \ldots, \omega_{10}) \,. \tag{3.123}$$

In our convention, a residue with weight $\omega_{i\cap j}$ is evaluated on the ith branch. We can not deny that it will likely be convenient to instead encircle infinity poles later on, since the scalar integrals have simpler or even vanishing residues there.

We will now relax the condition $m_1 m_2 \neq 0$ and turn to the analytic structure of the loop integrand under these circumstances. As will become clear in a moment, the topological picture is that of an octuply pinched genus-3 surface, where tubes have been contracted along one vertical and two horizontal lines passing through the center; the setting in mind is sketched in fig. 3.14.

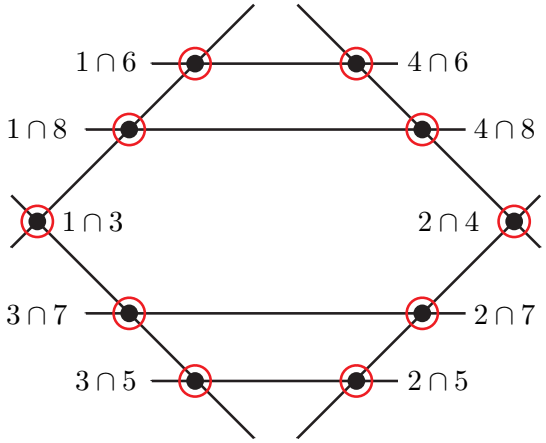

Figure 3.16: Global structure of the hepta-cut of the nonplanar double-box integrals in class (b). The straight lines are drawn for simplicity and represent the Riemann spheres associated with each of the eight solutions to the hepta-cut equations. See also fig. 3.15.

The topological structure is easy to reproduce from sharing of global poles and coincidence of residues. According to ref. [62],

$$X^{**}_{1,1,2}[1]_{\widetilde{\mathcal{S}}_{1,2}} = +\frac{\gamma_\star(1-\tau)}{\tau\bar{\xi}_1(1+\mu\tau)} \oint \frac{dz}{z(z+1)(z+1/\tau)} \,, \tag{3.124}$$

$$X^{**}_{1,1,2}[1]_{\widetilde{\mathcal{S}}_{3,4}} = -\frac{\gamma_\star(1-\tau)}{\tau\bar{\xi}_1(1+\mu\tau)} \oint \frac{dz}{z(z+1)(z+1/\tau)} \,, \tag{3.125}$$

$$X^{**}_{1,1,2}[1]_{\widetilde{\mathcal{S}}_{5,6}} = -\frac{\gamma_\star}{\bar{\xi}_1} \oint \frac{dz}{(z+1)(z-\mu\tau)} \,, \tag{3.126}$$

$$X^{**}_{1,1,2}[1]_{\widetilde{\mathcal{S}}_{7,8}} = +\frac{\gamma_\star}{\bar{\xi}_1} \oint \frac{dz}{(z+\mu)(z-1/\tau)} \,. \tag{3.127}$$

The residues at the poles in eqs. (3.124)-(3.127) again satisfy numerous linear relations analogous to those in eq. (3.122). The global structure is precisely reflected by the following pattern,

$$\begin{aligned}
\operatorname*{Res}_{z=0} \widetilde{J}_1(z)\Phi(z)|_{\widetilde{\mathcal{S}}_1} &= -\operatorname*{Res}_{z=0} \widetilde{J}_3(z)\Phi(z)|_{\widetilde{\mathcal{S}}_3}\,, \\
\operatorname*{Res}_{z=-1} \widetilde{J}_1(z)\Phi(z)|_{\widetilde{\mathcal{S}}_1} &= -\operatorname*{Res}_{z=-1} \widetilde{J}_6(z)\Phi(z)|_{\widetilde{\mathcal{S}}_6}\,, \\
\operatorname*{Res}_{z=-1/\tau} \widetilde{J}_1(z)\Phi(z)|_{\widetilde{\mathcal{S}}_1} &= -\operatorname*{Res}_{z=-\mu} \widetilde{J}_8(z)\Phi(z)|_{\widetilde{\mathcal{S}}_8}\,, \\
\operatorname*{Res}_{z=-1} \widetilde{J}_3(z)\Phi(z)|_{\widetilde{\mathcal{S}}_3} &= -\operatorname*{Res}_{z=\mu\tau} \widetilde{J}_5(z)\Phi(z)|_{\widetilde{\mathcal{S}}_5}\,, \\
\operatorname*{Res}_{z=-1/\tau} \widetilde{J}_3(z)\Phi(z)|_{\widetilde{\mathcal{S}}_3} &= -\operatorname*{Res}_{z=1/\tau} \widetilde{J}_7(z)\Phi(z)|_{\widetilde{\mathcal{S}}_7}\,, \\
\operatorname*{Res}_{z=0} \widetilde{J}_2(z)\Phi(z)|_{\widetilde{\mathcal{S}}_2} &= -\operatorname*{Res}_{z=0} \widetilde{J}_4(z)\Phi(z)|_{\widetilde{\mathcal{S}}_4}\,, \\
\operatorname*{Res}_{z=-1} \widetilde{J}_2(z)\Phi(z)|_{\widetilde{\mathcal{S}}_2} &= -\operatorname*{Res}_{z=-1} \widetilde{J}_5(z)\Phi(z)|_{\widetilde{\mathcal{S}}_5}\,, \\
\operatorname*{Res}_{z=-1/\tau} \widetilde{J}_2(z)\Phi(z)|_{\widetilde{\mathcal{S}}_2} &= -\operatorname*{Res}_{z=-\mu} \widetilde{J}_7(z)\Phi(z)|_{\widetilde{\mathcal{S}}_7}\,, \\
\operatorname*{Res}_{z=-1} \widetilde{J}_4(z)\Phi(z)|_{\widetilde{\mathcal{S}}_4} &= -\operatorname*{Res}_{z=\mu\tau} \widetilde{J}_6(z)\Phi(z)|_{\widetilde{\mathcal{S}}_6}\,, \\
\operatorname*{Res}_{z=-1/\tau} \widetilde{J}_4(z)\Phi(z)|_{\widetilde{\mathcal{S}}_4} &= -\operatorname*{Res}_{z=1/\tau} \widetilde{J}_8(z)\Phi(z)|_{\widetilde{\mathcal{S}}_8}\,.
\end{aligned} \tag{3.128}$$

3.2.8 Master Integral Projectors

We fix a basis $e = (k_1, k_2, k_4, \omega)$ of the four-dimensional momentum space. The spurious direction is necessary as usual since only three of the four momenta are independent. All contractions between internal and external vectors can be written in terms of the eight fundamental scalar products, $\ell_i \cdot e_j$. An analysis similar to that of the double box shows that only two of the dot products are irreducible. A general numerator polynomial may be parametrized as follows,

$$N = \sum_{\{\alpha_1,\ldots,\alpha_4\}} c_{\alpha_1\cdots\alpha_4} (\ell_1\cdot k_4)^{\alpha_1} (\ell_2\cdot k_1)^{\alpha_2} (\ell_1\cdot\omega)^{\alpha_3} (\ell_2\cdot\omega)^{\alpha_4}\,. \tag{3.129}$$

We impose renormalization conditions and perform the multivariate polynomial division of N towards a Gröbner basis constructed from the seven nonplanar double-box propagators using `BasisDet` [71]. The integrand contains 19 parity-odd and 19 parity-even elements (see also ref. [68]). The 19 nonplanar double-box integrals of the form,

$$X^{**}_{1,1,2}[n,m] \equiv X^{**}_{1,1,2}\left[\left(\frac{(\ell_1+k_4)^2}{2}\right)^n \left(\frac{(\ell_2+k_1)^2}{2}\right)^m\right] \tag{3.130}$$

are related by 16 or 17 IBP identities depending on the kinematic configuration in question. For class (a) there are three master integrals. The masters will again be the scalar integral along with a rank-1 tensor integral. The third master is a rank-2 tensor integral. More precisely,

$$X^{**}_{1,1,2}[n,m] = c_1 X^{**}_{1,1,2}[1] + c_2 X^{**}_{1,1,2}[(\ell_1\cdot k_4)] + c_3 X^{**}_{1,1,2}[(\ell_1\cdot k_4)^2] + \cdots\,, \tag{3.131}$$

and in particular,

$$A^{(1)}_4 = c_1 X^{**}_{1,1,2}[1] + c_2 X^{**}_{1,1,2}[(\ell_1\cdot k_4)] + c_3 X^{**}_{1,1,2}[(\ell_1\cdot k_4)^2] + \cdots\,. \tag{3.132}$$

In class (b), the rank-2 integral becomes reducible, leaving only two masters. For this project we used the Mathematica package `FIRE` [103] to generate the IBP relations, some of which are included below for illustration purposes. We found two relations that hold for arbitrary values of the external masses,

$$X^{**}_{1,1,2}[0,-1] = \frac{1}{4}\left(s_{14}+\frac{m_1^2m_3^2-m_2^2m_4^2}{s_{12}}\right)X^{**}_{1,1,2}[0,0]-\frac{1}{2}\left(1+\frac{m_1^2-m_2^2}{s_{12}}\right)X^{**}_{1,1,2}[-1,0]\,, \tag{3.133}$$

$$X^{**}_{1,1,2}[-1,-1] = \frac{1}{4}\left(s_{14}+\frac{m_1^2m_3^2-m_2^2m_4^2}{s_{12}}\right)X^{**}_{1,1,2}[-1,0]-\frac{1}{2}\left(1+\frac{m_1^2-m_2^2}{s_{12}}\right)X^{**}_{1,1,2}[-2,0]\,. \tag{3.134}$$

If, say, $m_2 = m_3 = m_4 = 0$ but $m_1 \neq 0$, there is an additional linear relation among these integrals, namely

$$X^{**}_{1,1,2}[-2,0] = -\frac{s_{12}^2 s_{14}}{16(m_1^2-s_{12})}X^{**}_{1,1,2}[0,0]-\frac{1}{8}\left(3+\frac{2s_{14}}{m_1^2-s_{12}}\right)X^{**}_{1,1,2}[-1,0]\,. \tag{3.135}$$

In order to ensure that the unitarity cut prescription yields consistent results, we must demand that all integral reduction identities remain satisfied; that is

$$X^{**}_{1,1,2}[\Phi(\ell_1,\ell_2)] = 0 \implies X^{**}_{1,1,2}[\Phi(\ell_1,\ell_2)]\big|_{8-\text{cut}} = 0\,. \tag{3.136}$$

For the problem at hand the requirement can be formulated as

$$X^{**}_{1,1,2}[N(\ell_1,\ell_2]]\big|_{\text{aug}} = X^{**}_{1,1,2}[c_1+c_2(\ell_1\cdot k_4)]\big|_{\text{aug}} \tag{3.137}$$

for N given by eq. (3.129). Equivalently, regarding the parity-odd terms, it suffices to require that the full variety of integrals with Levi-Civita insertions, after invoking momentum conservations, continue to integrate to zero on general contours.

The goal of the rest of this section is to turn the two-loop master equation into algebraic equations for the nonplanar double-box master integral coefficients. We will present two example that are representative for each of the two classes of hepta-cut; after all the calculations are rather self-similar and take up several pages. All cases including the principal kinematic configuration with four distinct external masses are treated in vast detail in ref. [62]. Our first example here is the one-mass diagram with $m_1 \neq 0$. We decide to encircle the following ten global poles,

$$\{\widetilde{\mathcal{G}}_i\} = (\widetilde{\mathcal{G}}_{1\cap6},\,\widetilde{\mathcal{G}}_{1\cap8},\,\widetilde{\mathcal{G}}_{3\cap5},\,\widetilde{\mathcal{G}}_{3\cap7},\,\widetilde{\mathcal{G}}_{1\cap3},\,\widetilde{\mathcal{G}}_{2\cap5},\,\widetilde{\mathcal{G}}_{2\cap7},\,\widetilde{\mathcal{G}}_{4\cap6},\,\widetilde{\mathcal{G}}_{4\cap8},\,\widetilde{\mathcal{G}}_{2\cap4}) \equiv (\widetilde{\mathcal{G}}_1,\ldots,\widetilde{\mathcal{G}}_{10})\,, \tag{3.138}$$

and denote by $\widetilde{\mathbf{\Omega}}$ the corresponding contour weights,

$$\widetilde{\mathbf{\Omega}} = (\widetilde{\omega}_{1\cap6},\,\widetilde{\omega}_{1\cap8},\,\widetilde{\omega}_{3\cap5},\,\widetilde{\omega}_{3\cap7},\,\widetilde{\omega}_{1\cap3},\,\widetilde{\omega}_{2\cap5},\,\widetilde{\omega}_{2\cap7},\,\widetilde{\omega}_{4\cap6},\,\widetilde{\omega}_{4\cap8},\,\widetilde{\omega}_{2\cap4}) \equiv (\widetilde{\omega}_1,\ldots,\widetilde{\omega}_{10})\,. \tag{3.139}$$

Eq. (3.124) reduces to

$$X^{**}_{1,1,2}[1]_{\widetilde{\mathcal{S}}_{1,2}} \longrightarrow -\frac{m_1^2-s_{12}}{\chi s_{12}}\oint\frac{dz}{z(z+1)(z+(s_{12}(1+\chi)-m_1^2)/(\chi s_{12}))}\,, \tag{3.140}$$

$$X^{**}_{1,1,2}[1]_{\widetilde{\mathcal{S}}_{3,4}} \longrightarrow +\frac{m_1^2-s_{12}}{\chi s_{12}}\oint\frac{dz}{z(z+1)(z+(s_{12}(1+\chi)-m_1^2)/(\chi s_{12}))}\,. \tag{3.141}$$

Note that we stripped off the overall factor. The parity-odd requirements translate into five linearly independent constraints,

$$\begin{pmatrix} 1 & 0 & 0 & 0 & 0 & -1 & 0 & 0 & 0 & 0 \\ 0 & 1 & 0 & 0 & 0 & 0 & -1 & 0 & 0 & 0 \\ 0 & 0 & 1 & 0 & 0 & 0 & 0 & -1 & 0 & 0 \\ 0 & 0 & 0 & 1 & 0 & 0 & 0 & 0 & -1 & 0 \\ 0 & 0 & 0 & 0 & 1 & 0 & 0 & 0 & 0 & -1 \end{pmatrix} \begin{pmatrix} \widetilde{\omega}_{1\cap 6} \\ \widetilde{\omega}_{1\cap 8} \\ \widetilde{\omega}_{3\cap 5} \\ \widetilde{\omega}_{3\cap 7} \\ \widetilde{\omega}_{1\cap 3} \\ \widetilde{\omega}_{2\cap 5} \\ \widetilde{\omega}_{2\cap 7} \\ \widetilde{\omega}_{4\cap 6} \\ \widetilde{\omega}_{4\cap 8} \\ \widetilde{\omega}_{2\cap 4} \end{pmatrix} = 0 \,. \tag{3.142}$$

Finally we find three linearly independent IBP equations,

$$\widetilde{\mathbf{\Omega}} \cdot (0,\, 1,\, 0,\, 1,\, 0,\, 0,\, 1,\, 0,\, 1,\, 0) = 0 \,, \tag{3.143}$$

$$\widetilde{\mathbf{\Omega}} \cdot (1,\, -1,\, 1,\, -1,\, 0,\, 1,\, -1,\, 1,\, -1,\, 0) = 0 \,, \tag{3.144}$$

$$\widetilde{\mathbf{\Omega}} \cdot (1,\, 1,\, -1,\, -1,\, 2,\, 1,\, 1,\, -1,\, -1,\, 2) = 0 \,. \tag{3.145}$$

The residues computed by the master integrals at the global poles are

$$\begin{aligned} &\mathrm{Res}_{\{\widetilde{\mathcal{G}}_i\}} X^{**}_{1,1,2}[1] = \\ &\qquad \Bigg(-1,\, -\frac{\chi s_{12}}{m_1^2-(1+\chi)s_{12}},\, 1,\, \frac{\chi s_{12}}{m_1^2-(1+\chi)s_{12}},\, \frac{\chi s_{12}}{m_1^2-(1+\chi)s_{12}}, \\ &\qquad\quad -1,\, -\frac{\chi s_{12}}{m_1^2-(1+\chi)s_{12}},\, 1,\, \frac{\chi s_{12}}{m_1^2-(1+\chi)s_{12}},\, \frac{\chi s_{12}}{m_1^2-(1+\chi)s_{12}} \Bigg) \,, \\ &\mathrm{Res}_{\{\widetilde{\mathcal{G}}_i\}} X^{**}_{1,1,2}[\ell_1 \cdot k_4] = \\ &\qquad \frac{\chi s_{12}^2}{2(m_1^2-(1+\chi)s_{12})} (0,\, 1,\, 0,\, -1,\, -1,\, 0,\, 1,\, 0,\, -1,\, -1) \,. \end{aligned} \tag{3.146}$$

Imposing the integral reduction constraints leaves us with two undetermined winding numbers. This fits perfectly with the two projectors defined by

$$\mathcal{M}_1 \cdot \big(\operatorname*{Res}_{\{\widetilde{\mathcal{G}}_i\}} X^{**}_{1,1,2}[1],\, \operatorname*{Res}_{\{\widetilde{\mathcal{G}}_i\}} X^{**}_{1,1,2}[\ell_1 \cdot k_4] \big) = (1, 0) \,, \tag{3.147}$$

$$\mathcal{M}_2 \cdot \big(\operatorname*{Res}_{\{\widetilde{\mathcal{G}}_i\}} X^{**}_{1,1,2}[1],\, \operatorname*{Res}_{\{\widetilde{\mathcal{G}}_i\}} X^{**}_{1,1,2}[\ell_1 \cdot k_4] \big) = (0, 1) \,. \tag{3.148}$$

In words, $\mathcal{M}_1$ and $\mathcal{M}_2$ are just particular choices of the contour weights with the property that contribution from only one of the master integrals is picked up, and further normalized to unity.

Practically speaking, the eight contour constraints together with either of the projectors are arranged as 10×10 matrices. The rank is 10, so the equations have a unique solution. A short calculation shows that the projectors are characterized by the following

winding numbers,

$$\mathcal{M}_1 = \frac{1}{16}(-3,\, 1,\, 3,\, -1,\, 2,\, -3,\, 1,\, 3,\, -1,\, 2)\,, \tag{3.149}$$

$$\begin{aligned}\mathcal{M}_2 = \frac{1}{8\chi s_{12}^2}(&-m_1^2 + (1-2\chi)s_{12},\, 3m_1^2 - (3+2\chi)s_{12},\, m_1^2 - (1-2\chi)s_{12},\\ &-3m_1^2 + (3+2\chi)s_{12},\, 2(-m_1^2 + (1+2\chi)s_{12}),\, -m_1^2 + (1-2\chi)s_{12},\\ &3m_1^2 - (3+2\chi)s_{12},\, m_1^2 - (1-2\chi)s_{12},\, -3m_1^2 + (3+\chi)s_{12},\\ &2(-m_1^2 + (1+2\chi)s_{12}))\,.\end{aligned} \tag{3.150}$$

We thus immediately arrive at a very compact and general formula for the one-mass master integral coefficients

$$c_i = \oint_{\mathcal{M}_i} dz\, \widetilde{J}(z) \sum_{\substack{\text{helicities}\\ \text{particles}}} \prod_{k=1}^{6} A_{(k)}^{\text{tree}}(z)\,, \tag{3.151}$$

where the rescaled Jacobian for this configuration takes the form

$$\widetilde{J}(z) \equiv \pm\frac{m_1^2 - s_{12}}{\chi s_{12}} \frac{1}{z(z+1)(z + (s_{12}(1+\chi) - m_1^2)/(\chi s_{12})}\,. \tag{3.152}$$

The results presented here agree with the purely massless calculation reported in ref. [59] when we take $m_1 \to 0$.

The next example is the three-mass diagram with $m_4 = 0$ which is smoothly connected to the two-mass short-side diagram with $m_1 m_2 \neq 0$. The master equation for this problem is

$$A_4^{(2)} = c_1 X_{1,1,2}^{**}[1] + c_2 X_{1,1,2}^{**}[(\ell_1 + k_4)^2/2] + c_3 X_{1,1,2}^{**}[((\ell_1 + k_4)^2/2)^2] + \cdots\,, \tag{3.153}$$

and we use the singular point locus,

$$\{\mathcal{G}_i\} = (\mathcal{G}_{1\cap 4},\, \mathcal{G}_{1\cap 6},\, \mathcal{G}_{1\cap 3},\, \mathcal{G}_{1\cap 5},\, \mathcal{G}_{1,\infty_{LR}},\, \mathcal{G}_{2\cap 3},\, \mathcal{G}_{2\cap 5},\, \mathcal{G}_{2\cap 4},\, \mathcal{G}_{2\cap 6},\, \mathcal{G}_{2,\infty_{LR}}) \equiv (\mathcal{G}_1, \ldots, \mathcal{G}_{10})\,. \tag{3.154}$$

Setting $\mu = 0$ and stripping off the overall factor of $\gamma_\star$ from eq. (3.115) leaves us with

$$X_{1,1,2}^{**}[1]_{\mathcal{S}_{1,2}} \longrightarrow \frac{(1-\tau)(\bar{\xi}_1 - \tau\bar{\xi}_2)}{\tau\bar{\xi}_1^2} \oint dz \frac{z}{(z+1)(z+1/\tau)(z+\bar{\xi}_2/\bar{\xi}_1)(z+\tau\bar{\xi}_2/\bar{\xi}_1)}\,. \tag{3.155}$$

For this problem we prefer quantities constructed from flat momenta, $\bar{\xi}_1$, $\bar{\xi}_2$ and τ, instead of the usual Mandelstam variables and external masses. In this way, it is possible

to express the residues in a rather clean form,

$$\begin{aligned}\mathrm{Res}_{\{\mathcal{G}_i\}}\, X^{**}_{1,1,2}[1] = \\ \Bigg(&-\frac{1}{\bar\xi_1-\bar\xi_2}, \frac{\tau}{\bar\xi_1-\tau^2\bar\xi_2}, \frac{1}{\bar\xi_1-\bar\xi_2}, -\frac{\tau}{\bar\xi_1-\tau^2\bar\xi_2}, 0, \\ &-\frac{1}{\bar\xi_1-\bar\xi_2}, \frac{\tau}{\bar\xi_1-\tau^2\bar\xi_2}, \frac{1}{\bar\xi_1-\bar\xi_2}, -\frac{\tau}{\bar\xi_1-\tau^2\bar\xi_2}, 0\Bigg)\,, \end{aligned} \tag{3.156}$$

$$\begin{aligned}\mathrm{Res}_{\{\mathcal{G}_i\}}\, X^{**}_{1,1,2}[(\ell_1+k_4)^2/2] = \\ \Bigg(0, &-\frac{(1-\tau)(\bar\xi-\tau\bar\xi_2)k_1^\flat\cdot k_4^\flat}{\bar\xi_1-\tau^2\bar\xi_2}, 0, \frac{(1-\tau)(\bar\xi-\tau\bar\xi_2)k_1^\flat\cdot k_4^\flat}{\bar\xi_1-\tau^2\bar\xi_2}, 0, \\ 0, &-\frac{(1-\tau)(\bar\xi-\tau\bar\xi_2)k_1^\flat\cdot k_4^\flat}{\bar\xi_1-\tau^2\bar\xi_2}, 0, \frac{(1-\tau)(\bar\xi-\tau\bar\xi_2)k_1^\flat\cdot k_4^\flat}{\bar\xi_1-\tau^2\bar\xi_2}, 0\Bigg)\,, \end{aligned} \tag{3.157}$$

$$\begin{aligned}\mathrm{Res}_{\{\mathcal{G}_i\}}\, X^{**}_{1,1,2}[((\ell_1+k_4)^2/2)^2] = \\ \Bigg(0, &\frac{(1-\tau)^2(\bar\xi-\tau\bar\xi_2)^2(k_1^\flat\cdot k_4^\flat)^2}{\tau(\bar\xi_1-\tau^2\bar\xi_2)}, 0, -\frac{(1-\tau)^2(\bar\xi-\tau\bar\xi_2)^2(k_1^\flat\cdot k_4^\flat)^2}{\tau(\bar\xi_1-\tau^2\bar\xi_2)}, \\ &\frac{(1-\tau)(\bar\xi-\tau\bar\xi_2)(k_1^\flat\cdot k_4^\flat)^2}{\tau}, 0, \frac{(1-\tau)^2(\bar\xi-\tau\bar\xi_2)^2(k_1^\flat\cdot k_4^\flat)^2}{\tau(\bar\xi_1-\tau^2\bar\xi_2)}, 0, \\ &-\frac{(1-\tau)^2(\bar\xi-\tau\bar\xi_2)^2(k_1^\flat\cdot k_4^\flat)^2}{\tau(\bar\xi_1-\tau^2\bar\xi_2)}, \frac{(1-\tau)(\bar\xi-\tau\bar\xi_2)(k_1^\flat\cdot k_4^\flat)^2}{\tau}\Bigg)\,. \end{aligned} \tag{3.158}$$

The correct projectors are

$$\mathcal{M}_1 = N_1(1,\,0,\,-1,\,0,\,0,\,1,\,0,\,-1,\,0,\,0)\,, \tag{3.159}$$

$$\mathcal{M}_2 = N_2(q_1,\,q_2,\,q_3,\,q_4,\,q_5,\,q_1,\,q_2,\,q_3,\,q_4,\,q_5)\,, \tag{3.160}$$

$$\mathcal{M}_3 = N_3(1,\,1,\,1,\,1,\,2,\,1,\,1,\,1,\,1,\,2)\,, \tag{3.161}$$

where

$$N_1 \equiv \frac{\gamma_{12}m_1^2m_3^2 - \chi(\gamma_{12}+m_1^2)(\gamma_{12}+m_2^2)s_{12}}{4m_1^2(m_2^2(\gamma_{12}+m_1^2)-\gamma_{12}m_3^2)+4\chi\gamma_{12}s_{12}(\gamma_{12}+m_1^2)}\,, \tag{3.162}$$

$$\begin{aligned}N_2 \equiv &\frac{1}{2(\gamma_{12}^2+m_1^2m_2^2+\gamma_{12}(m_1^2+m_2^2-m_3^2))} \\ &\times\frac{1}{m_1^2(m_2^2(\gamma_{12}+m_1^2)-\gamma_{12}m_3^2)+\chi\gamma_{12}(\gamma_{12}+m_1^2)s_{12}}\,, \end{aligned} \tag{3.163}$$

$$\begin{aligned}N_3 \equiv &\frac{\gamma_{12}(\gamma_{12}^2-m_1^2m_2^2)}{\gamma_{12}^2+m_1^2m_2^2+\gamma_{12}(m_1^2+m_2^2-m_3^2)} \\ &\times\frac{1}{m_1^4m_2^2+\chi\gamma_{12}^2s_{12}+\gamma_{12}m_1^2(m_2^2-m_3^2+\chi s_{12})}\,, \end{aligned} \tag{3.164}$$

and

$$\begin{aligned}q_1 \equiv &\gamma_{12}^4-m_1^4m_2^4+\gamma_{12}^3(m_1^2+m_2^2-m_3^2-\chi s_{12}) \\ &-\gamma_{12}m_1^2m_2^2(m_1^2+m_2^2-m_3^2+\chi s_{12})+\gamma_{12}^2(m_1^2m_3^2-\chi(m_1^2+m_2^2)s_{12})\,, \end{aligned} \tag{3.165}$$

$$\begin{aligned}q_2 \equiv &m_1^2(-2(\gamma_{12}+m_1^2)m_2^2(\gamma_{12}+m_2^2) \\ &+\gamma_{12}(\gamma_{12}+2m_2^2)m_3^2)-\chi\gamma_{12}(\gamma_{12}+m_1^2)(\gamma_{12}+m_2^2)s_{12}\,, \end{aligned} \tag{3.166}$$

$$q_3 \equiv \gamma_{12}^4 - m_1^4 m_2^4 + \gamma_{12}^3(m_1^2 + m_2^2 - m_3^2 + \chi s_{12}) \\ - \gamma_{12} m_1^2 m_2^2 (m_1^2 + m_2^2 - m_3^2 - \chi s_{12}) - \gamma_{12}^2 (m_1^2 m_3^2 - \chi(m_1^2 + m_2^2) s_{12}) \,, \tag{3.167}$$

$$q_4 \equiv q_1 - q_2 + q_3 \,, \tag{3.168}$$

$$q_5 \equiv q_1 + q_3 \,. \tag{3.169}$$

We have verified that the projectors (3.159)-(3.161) respect all of the parity-odd constraints provided that

$$\begin{pmatrix} 1 & 0 & 0 & 0 & 0 & -1 & 0 & 0 & 0 & 0 \\ 0 & 1 & 0 & 0 & 0 & 0 & -1 & 0 & 0 & 0 \\ 0 & 0 & 1 & 0 & 0 & 0 & 0 & -1 & 0 & 0 \\ 0 & 0 & 0 & 1 & 0 & 0 & 0 & 0 & -1 & 0 \\ 0 & 0 & 0 & 0 & 1 & 0 & 0 & 0 & 0 & -1 \end{pmatrix} \begin{pmatrix} \omega_{1\cap 4} \\ \omega_{1\cap 6} \\ \omega_{1\cap 3} \\ \omega_{1\cap 5} \\ \omega_{1,\infty_{LR}} \\ \omega_{2\cap 3} \\ \omega_{2\cap 5} \\ \omega_{2\cap 4} \\ \omega_{2\cap 6} \\ \omega_{2,\infty_{LR}} \end{pmatrix} = 0 \,. \tag{3.170}$$

Moreover, we found two linearly independent constraints imposed by IBP identities,

$$\boldsymbol{\Omega} \cdot (0,\, 1,\, 0,\, 1,\, -1,\, 0,\, 1,\, 0,\, 1,\, -1) = 0 \,, \tag{3.171}$$

$$\boldsymbol{\Omega} \cdot (1,\, -1,\, 1,\, -1,\, 0,\, 1,\, -1,\, 1,\, -1,\, 0) = 0 \,. \tag{3.172}$$

Multivariate Residues and Maximal Unitarity 4

A method is more important than a discovery, since the right method will lead to new and even more important discoveries.
— Lev Landau (1908–1968)

Three-loop amplitudes contain a widespread of planar and nonplanar integral topologies. At four external particles, the basis integrals have at most ten propagators. A few examples are the planar tennis court and the double-crossed ladder in fig. 4.1. Neglecting

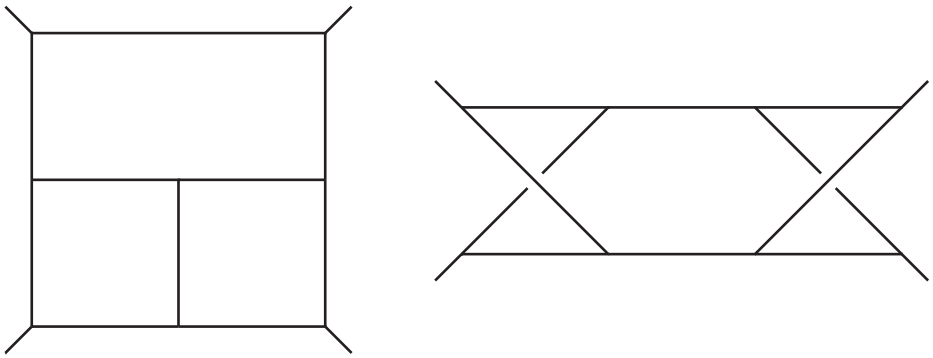

Figure 4.1: The three-loop planar tennis court and the double-crossed triple-box diagram.

the (-2ϵ)-dimensional components of the regularized loop momenta, the integrand of such integrals has a total of $3 \times 4 = 12$ degrees of freedom. In particular, the maximal cut – in this case a *deca-cut* – which promotes all internal lines to on-shell values leaves two integration variables unfrozen and thus a multidimensional contour integral to be evaluated. The integrals in fig. 4.1 belong to a larger class of multiloop integrals, whose maximal cuts, in the language of algebraic geometry, define multidimensional algebraic varieties. At two loops this class of integrals include subleading topologies[1] such as the bowtie and slashed-box integrals shown in fig. 4.2.

In this chapter we present the extension of the maximal unitarity formalism to three-loop amplitudes. We formulate the problem in terms of degenerate and nondegenerate

[1]Integrals with a sub-bubble, e.g. the two-loop box-bubble and even the bubble itself at one loop, appearently have no leading singularity and hence require special treatment.

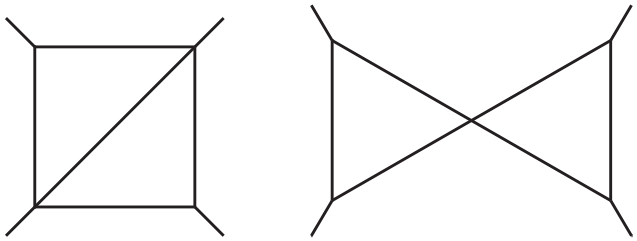

Figure 4.2: The two-loop slashed-box $P_{1,1}$ (left) and bowtie $A^*_{2,2}$ (right) diagrams (in the notation of ref. [53]). The four-dimensional maximal cuts leave $8-5=3$ and $8-6=2$ loop-momentum degrees of freedom unfrozen respectively, and hence define multidimensional algebraic varieties rather than algebraic curves or discrete set of points as encountered in the previous one- and two-loop examples.

multivariate residues and solve it by means of computational algebraic geometry. In the process of developing the method, we concentrate on the the planar triple box, although we expect our method to generalize to more complicated examples including nonplanar diagrams. The technique is applied in gauge theories with an arbitrary number of adjoint fermion and scalar particles. Our principal result is a surprisingly compact set of unique projectors for all three triple-box master integral coefficients.

Curiously, degenerate multivariate residues also appear in connection with multi-loop integrals with doubled or higher powers of propagators. It is possible to almost effortlessly extend the notion of generalized unitarity cuts to accommodate such integrals. We stress out that all IBP identities (involving integrals with and without doubled propagators) can be derived from the set of IBPs without doubled propagators.

4.1 Multivariate Residues

Residues in higher dimensions can in many cases be evaluated straightforwardly using a generalization of Cauchy's theorem via Jacobian determinants. We have already seen plenty examples of such *nondegenerate* multivariate residues in generalized unitarity cuts in the previous chapters. More generally, multivariate residues can be *degenerate* as alluded in sec. 2.3. Here we briefly review the concepts and explain how to calculate degenerate residue via computational algebraic geometry methods. For a more rigorous and comprehensive treatment, consult refs. [113–115].

The quantum field theory Feynman rules dictate that any loop integrand is a rational function that of the loop momenta. We will therefore restrict our attention to rational functions of several complex variables. Consider a differential form $\omega(z)$ of n complex variables $z \equiv (z_1, \ldots, z_n)$,

$$\omega(z) = \frac{h(z) dz_1 \wedge \cdots \wedge dz_n}{f_1(z) \cdots f_n(z)} \,, \tag{4.1}$$

constructed from the holomorphic functions $h : \mathbb{C}^n \to \mathbb{C}$ and $f : \mathbb{C}^n \to \mathbb{C}^n$ with $f(z) = (f_1(z), \ldots, f_n(z))$. Suppose that $\xi \in \mathbb{C}^n$ is an isolated zero of f, i.e. $f_1(\xi) = \cdots = f_n(\xi) = 0$ and $f^{-1}(0) \cap U = \{\xi\}$ for a sufficiently small neighborhood U of ξ. The residue of ω at $z = \xi$ with respect to the list of divisors $\{f_1, \ldots, f_n\}$ is defined to be

$$\mathrm{Res}_{\{f_1,\ldots,f_n\},\xi}(\omega) \equiv \left(\frac{1}{2\pi i}\right)^n \oint_\Gamma \frac{h(z) dz_1 \wedge \cdots \wedge dz_n}{f_1(z) \cdots f_n(z)} \,, \tag{4.2}$$

where $\Gamma = \{z : |f_i(z)| = \delta_i\}$ for infinitesimal real values δ_i.

Multivariate residues that are either *factorizable* or *nondegenerate* are almost trivial to calculate.

(i) The multivariate residue is *factorizable* if the f_is are univariate polynomials, namely, $f_i(z) = f_i(z_i)$. In these circumstances, the n-dimensional contour is factorized onto the product of n univariate circles and the residue is given by

$$\text{Res}_{\{f_1,\ldots,f_n\},\xi}(\omega) = \left(\frac{1}{2\pi i}\right)^n \oint_{|f_1(z_1)|=\epsilon_1} \frac{dz_1}{f_1(z_1)} \cdots \oint_{|f_n(z_n)|=\epsilon_n} \frac{dz_n}{f_n(z_n)} h(z) \; . \quad (4.3)$$

In particular, the residue is evaluated by applying the univariate residue formula iteratively.

(i) The multivariate residue is *non-degenerate* if and only if the Jacobian of the f_i's evaluated at $z = \xi$ is nonvanishing, i.e.,

$$J(\xi) = \det_{i,j} \frac{\partial f_i}{\partial z_j}\bigg|_{z=\xi} \neq 0 \; . \quad (4.4)$$

Invoking the multidimensional version of Cauchy's theorem yields [111]

$$\text{Res}_{\{f_1,\ldots,f_n\},\xi}(\omega) = \frac{h(\xi)}{J(\xi)} \; . \quad (4.5)$$

In some cases a multivariate residue is neither nondegenerate nor factorizable. For example, consider the meromorphic differential form,

$$\omega(z_1, z_2) = \frac{z_2}{z_1^2(z_2 - z_1)} \; , \quad (4.6)$$

which has a pole at $\xi = (0, 0)$. This residue is not factorizable as the denominator factors are obviously not univariate polynomials. Furthermore, the Jacobian vanishes at $z = \xi$, hence the above prescription does not apply. We say that the residue at $z = \xi$ is *degenerate*. Fortunately, degenerate residues can be evaluated thanks to the transformation law [111] in algebraic geometry.

> **(The Transformation Law)** Assume that $I = \langle f_1(z), \ldots, f_n(z)\rangle$ and $J = \langle u_1(z), \ldots, u_n(z)\rangle$ are zero-dimensional ideals generated by finite sets of holomorphic functions $f_i, u_i : \mathbb{CP}^n \to \mathbb{C}$. Suppose that $J \subseteq I$ such that $u_i(z) = \sum_{i=1}^n a_{ij}(z) f_j(z)$ for polynomials $a_{ij}(z)$. Denoting the conversion matrix by $A(z) = (a_{ij}(z))_{i,j=1,\ldots,n}$, the multivariate residue at $z = \xi$ satisfies,

$$\text{Res}_{\{f_1,\ldots,f_n\},\xi}\left(\frac{h(z)dz_1 \wedge \cdots \wedge dz_n}{f_1(z)\cdots f_n(z)}\right) = \text{Res}_{\{u_1,\ldots,u_n\},\xi}\left(\frac{h(z)dz_1 \wedge \cdots \wedge dz_n}{u_1(z)\cdots u_n(z)} \det A\right) . \quad (4.7)$$

The transformation law is valid for both nondegenerate and degenerate residues. There is a particularly advantageous set of generators that may be used to transform degenerate residues to factorizable residues. The trick is to choose the u_is to be univariate and this can be achieved via Gröbner bases [60]:

1. Calculate the Gröbner basis $\{g_1, \ldots, g_k\}$ of $\{f_1, \ldots, f_n\}$ using the *DegreeLexicographic* order and record the converting matrix r_{ij}, such that $g_i = r_{ij} f_j$.

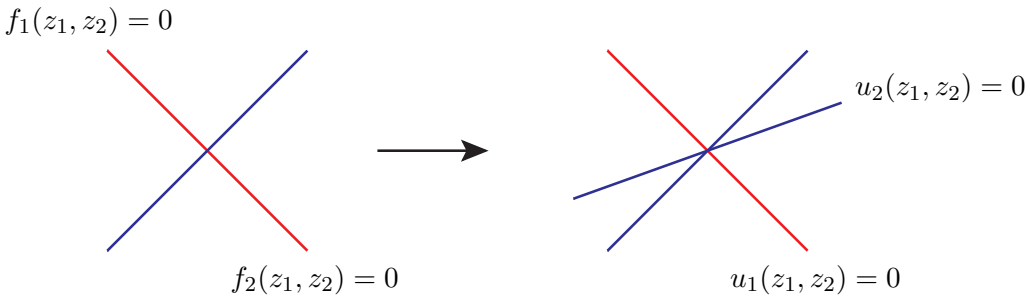

Figure 4.3: Calculating multivariate residues involves disentangling denominator factors whose first approximations are linearly dependent.

2. For $1 \leq i \leq n$, calculate the Gröbner basis of $\{f_1, \ldots, f_n\}$ using the *Lexicographic* order of $z_{i+1} \succ \cdots \succ z_n \succ z_1 \succ \cdots z_i$. Pick the univariate polynomial of z_i from this Gröbner basis and call it u_i.

3. Divide each of the u_is towards $\{g_1, \ldots, g_k\}$ so $u_i = s_{ij} g_j$.

4. The transformation matrix is $a_{ij} = s_{ik} r_{kj}$. By the transformation law, the degenerate residue is converted to a factorizable residue with the matrix $A = (a_{ij})_{i,j=1,\ldots,n}$.

4.1.1 Gröbner Basis Examples

We demonstrate the Gröbner basis algorithm for calculating degenerate multivariate residues by a few simple examples.

Let us take $\{f_1, f_2\} = \{z_1, (z_1 + z_2)(z_1 - z_2)\}$ and $h = z_2$. Clearly, there is a degenerate residue at the origin. In fact, all three factors are zero at the pole, so the Jacobian also vanishes there. The Gröbner basis G_1 for $I = \langle z_1, (z_1 - z_2)(z_1 + z_2)\rangle$ in lexicographic order $z_2 \succ z_1$ is $G_1 = \{z_1, z_2^2\}$, hence we pick up $u_1 = z_1$. Similarly, the Gröbner basis G_2 for I in the lexicographic order $z_1 \succ z_2$ is $G_2 = \{z_2^2, z_1\}$, so we set $u_2 = z_2^2$. The two set of generators are related by the conversion matrix A,

$$\begin{pmatrix} u_1 \\ u_2 \end{pmatrix} = A \begin{pmatrix} f_1 \\ f_2 \end{pmatrix} , \quad A = \begin{pmatrix} 1 & 0 \\ z_1 & -1 \end{pmatrix} , \tag{4.8}$$

whence $\det A = -1$. By the transformation law (4.7),

$$\mathrm{Res}_{\{f_1,f_2\},(0,0)} \left(\frac{z_2 dz_1 \wedge dz_2}{z_1(z_1 + z_2)(z_1 - z_2)} \right) = \mathrm{Res}_{\{u_1,u_2\},(0,0)} \left(- \frac{z_2 dz_1 \wedge dz_2}{z_1 z_2^2} \right) = -1 . \tag{4.9}$$

Our next example is slightly more general, yet still two-dimensional. Consider the differential form,

$$\omega(z_1, z_2) = \frac{z_1 dz_1 \wedge dz_2}{z_2(a_1 z_1 + a_2 z_2)(b_1 z_1 + b_2 z_2)} , \tag{4.10}$$

for nonzero constants a_1, a_2, b_1, b_2. There is a single pole at finite values of z_1 and z_2, namely $\xi = (0, 0)$. The associated residue is degenerate by inspection. We may partition the denominator factors,

$$f_1(z_1, z_2) = z_2 , \tag{4.11}$$
$$f_2(z_1, z_2) = a_1 z_1 + a_2 z_2 , \tag{4.12}$$
$$f_3(z_1, z_2) = b_1 z_1 + b_2 z_2 , \tag{4.13}$$

in three inequivalent ways, namely $\{f_1, f_2 f_3\}$, $\{f_2, f_3 f_1\}$ and $\{f_3, f_1 f_2\}$. To set the stage, let us evaluate the residue for the denominator partitioning $\{f_1, f_2 f_3\}$. The Gröbner basis of $\{f_1, f_2 f_3\}$ in the lexicographic order $z_2 \succ z_1$ is $G_1 = \{a_1 b_1 z_1^2, z_2\}$ and for the lexicographic order $z_1 \succ z_2$ we find $G_2 = \{z_2, a_1 b_1 z_1^2\}$. Thus, we pick $u_1 = a_1 b_1 z_1^2$ and $u_2 = z_2$. Dividing u_1 and u_2 towards a Gröbner basis constructed from the $\{f_1, f_2 f_3\}$ yields the relation

$$\begin{pmatrix} u_1 \\ u_2 \end{pmatrix} = \begin{pmatrix} -(a_1 b_2 + a_2 b_1) z_1 - a_2 b_2 z_2 & 1 \\ 1 & 0 \end{pmatrix} \begin{pmatrix} f_1 \\ f_2 f_3 \end{pmatrix} . \tag{4.14}$$

A direct calculation now shows that

$$\mathrm{Res}_{\{f_1, f_2 f_3\}, \xi}(\omega) = \mathrm{Res}_{\{u_1, u_2\}, \xi} \frac{z_1 \det A dz_1 \wedge dz_2}{u_1(z_1) u_2(z_2)} = - \operatorname*{Res}_{z_1=0} \operatorname*{Res}_{z_2=0} \frac{1}{a_1 b_1 z_1 z_2} = - \frac{1}{a_1 b_1} . \tag{4.15}$$

The residues for the other two denominator partitionings are computed in a similar manner, with the results[2] [64]

$$\rho_1 \equiv \mathrm{Res}_{\{f_1, f_2 f_3\}, \xi}(\omega) = - \frac{1}{a_1 b_1} , \tag{4.16}$$

$$\rho_2 \equiv \mathrm{Res}_{\{f_2, f_3 f_1\}, \xi}(\omega) = - \frac{a_2}{a_1 (a_1 b_2 - a_2 b_1)} , \tag{4.17}$$

$$\rho_3 \equiv \mathrm{Res}_{\{f_3, f_1 f_2\}, \xi}(\omega) = + \frac{b_2}{b_1 (a_1 b_2 - a_2 b_1)} . \tag{4.18}$$

In particular, note that the sum of the residues vanishes,

$$\rho_1 + \rho_2 + \rho_3 = 0 . \tag{4.19}$$

More generally, we have the following lemma [60]:

> **(Lemma)** Let $f_1(z_1, z_2)$, $f_2(z_1, z_2)$ and $f_3(z_1, z_2)$ be linear functions with a simultaneous zero at $z = \xi$ such that $\langle f_1, f_2 \rangle$, $\langle f_2, f_3 \rangle$ and $\langle f_3, f_1 \rangle$ are all zero-dimensional ideals. Assume that $h(z_1, z_2)$ is a holomorphic function in a neighborhood of ξ and let the differential form ω be given by $\omega = h dz_1 \wedge dz_2 / (f_1 f_2 f_3)$. Then,
>
> $$\mathrm{Res}_{\{f_1 f_2, f_3\}, \xi}(\omega) + \mathrm{Res}_{\{f_2 f_3, f_1\}, \xi}(\omega) + \mathrm{Res}_{\{f_3 f_1, f_2\}, \xi}(\omega) = 0 . \tag{4.20}$$

The lemma is easy to prove by direct computation. Without loss of generality we set $\xi = (0, 0)$, $f_1 = a_1 z_1 + b_1 z_2$, $f_2 = a_2 z_1 + b_2 z_2$ and $f_3 = a_3 z_1 + b_3 z_2$. Using the Gröbner basis method, we find

$$\begin{pmatrix} z_1^2 \\ z_2^2 \end{pmatrix} = A_1 \begin{pmatrix} f_1 f_2 \\ f_3 \end{pmatrix} , \quad \begin{pmatrix} z_1^2 \\ z_2^2 \end{pmatrix} = A_2 \begin{pmatrix} f_2 f_3 \\ f_1 \end{pmatrix} , \quad \begin{pmatrix} z_1^2 \\ z_2^2 \end{pmatrix} = A_3 \begin{pmatrix} f_3 f_1 \\ f_2 \end{pmatrix} , \tag{4.21}$$

where A_1 and A_2 and A_3 are the appropriate conversion matrices. The corresponding determinants are

$$\det A_1 = \frac{\begin{vmatrix} z_2 & z_1 \\ a_3 & b_3 \end{vmatrix}}{\begin{vmatrix} a_3 & b_3 \\ a_1 & b_1 \end{vmatrix} \begin{vmatrix} a_3 & b_3 \\ a_2 & b_2 \end{vmatrix}} , \quad \det A_2 = \frac{\begin{vmatrix} z_2 & z_1 \\ a_1 & b_1 \end{vmatrix}}{\begin{vmatrix} a_1 & b_1 \\ a_2 & b_2 \end{vmatrix} \begin{vmatrix} a_1 & b_1 \\ a_3 & b_3 \end{vmatrix}} , \quad \det A_3 = \frac{\begin{vmatrix} z_2 & z_1 \\ a_2 & b_2 \end{vmatrix}}{\begin{vmatrix} a_2 & b_2 \\ a_1 & b_1 \end{vmatrix} \begin{vmatrix} a_2 & b_2 \\ a_3 & b_3 \end{vmatrix}} . \tag{4.22}$$

[2] Yes, we again forgot to put in factors of $1/(2\pi i)$.

All determinants in the denominators are nonzero by the assumption of zero-dimensionality of the ideals $\langle f_1, f_2\rangle$, $\langle f_2, f_3\rangle$ and $\langle f_3, f_1\rangle$. A short explicit calculation shows that

$$\det A_1 + \det A_2 + \det A_3 = 0 \,. \tag{4.23}$$

The proof is completed by invoking the transformation law (4.7).

4.2 Global Residue Theorem

A well known theorem of univariate complex analysis states that the sum of all residues of a meromorphic differential form on $\mathbb{CP}^1$ vanishes. Here we review the multivariate version – the global residue theorem. It relates residues in $\mathbb{C}^n$ and residues at complex infinity and thus plays a crucial role for studying the global structure of residues from generalized unitarity cuts.

> **(Global Residue Theorem)** Let M be an n-dimensional compact complex manifold with divisors $D_1, \ldots, D_n$ and let ω be a differential n-form on $M - D_1 \cup \cdots \cup D_n$. Suppose that the intersection $S = D_1 \cap \cdots \cap D_n$ is a discrete set. Then, with respect to the the divisor list $\{D_1, \ldots, D_n\}$,
>
> $$\sum_{P\in S} \mathrm{Res}_P(\omega) = 0 \,. \tag{4.24}$$

The proof of the Global Residue Theorem can be found in ref. [111]. For the sake of definiteness, we provide further explanation of the theorem: M is locally isomorphic to $\mathbb{C}^n$, thus we may choose a local coordinate system $(z_1, \ldots, z_n)$. Locally, each divisor D_i is a hypersurface defined by the equation $f_i(z_1, \ldots, z_n)$. The residue regarding $\{D_1, \ldots, D_n\}$ can thus be translated to the local residue at P regarding $\{f_1, \ldots, f_n\}$.

A slight complication is that the manifold $\mathbb{C}^n$ is not compact. Instead we consider projective space $\mathbb{CP}^n$ with homogeneous coordinates $[w_0, w_1, \ldots, w_n]$. Indeed, $\mathbb{CP}^n$ is a compact manifold. Recall that $\mathbb{CP}^n$ is covered by patches,

$$U_i = \{[w_0, w_1, \ldots, w_n] \mid w_i \neq 0\} \,. \tag{4.25}$$

In particular, $\mathbb{C}^n$ is embedded inside $\mathbb{CP}^n$ as U_0,

$$(z_1, \ldots, z_n) = \left(\frac{w_1}{w_0}, \ldots, \frac{w_n}{w_0}\right) . \tag{4.26}$$

Points at complex infinity form a subspace $\mathbb{CP}^{n-1}$ specified by $w_0 = 0$.

4.2.1 Multivariate Residues at Infinity

Before we return to the three-loop problem, let us work through a simple example demonstrating the GRT for multivariate residues. In contrast to the univariate case, there are several different residue identities for the same differential form. We will show how to relate residues at infinity to residues in $\mathbb{C}^n$.

Consider on $\mathbb{CP}^2$ the differential form

$$\omega(z_1, z_2) = \frac{dz_1 \wedge dz_2}{z_1 z_2} \,. \tag{4.27}$$

Reexpressed on U_1 and U_2 we have $\omega = -(dw_0 \wedge dw_2)/(w_0 w_2)$ and $\omega = (dw_0 \wedge dw_1)/(w_0 w_1)$ and respectively. Consequently, ω is defined on $\mathbb{CP}^2$ excluding the irreducible hyperspaces $w_0 = 0$, $w_1 = 0$ and w_2. We may define the divisors $D_1 = \{w_0 w_1 = 0\}$ and $D_2 = \{w_2 = 0\}$ so that $D_1 \cap D_2 = \{[1,0,0],[0,1,0]\}$. Then,

$$\text{Res}_{\{D_1,D_2\},[1,0,0]}(\omega) + \text{Res}_{\{D_1,D_2\},[0,1,0]}(\omega) = (+1) + (-1) = 0 \,, \tag{4.28}$$

as implied by the GRT. Alternatively, for $D'_1 = \{w_1\}$ and $D'_2 = \{w_0 w_2 = 0\}$ we have $D'_1 \cap D'_2 = \{[1,0,0],[0,0,1]\}$. By the GRT,

$$\text{Res}_{\{D'_1,D'_2\},[1,0,0]}(\omega) + \text{Res}_{\{D'_1,D'_2\},[0,1,0]}(\omega) = (+1) + (-1) = 0 \,. \tag{4.29}$$

In words, there is one residue at the origin and two residues at complex infinity. Repeated application of the GRT reveals that the values of the two residues at infinity are both the opposite of that at the origin.

4.3 Maximal Cuts of Planar Triple-Box Integrals

After a complex detour we are now returning to the primary object of interest, namely the four-point planar triple-box integral,

$$I_{\square\square\square}[\Phi(\ell_1,\ell_2,\ell_3)] \equiv \left(\prod_{j=1}^{3} \int \frac{d^D \ell_j}{(2\pi)^D}\right) \frac{\Phi(\{\ell_i\})}{\prod_{i=1}^{10} f_i(\{\ell_i\}} \,, \tag{4.30}$$

where the inverse propagators $\{f_i\}$ according to the momentum flow conventions outlined in fig. 4.4 are given by[3]

$$\begin{aligned} &f_1 = \ell_1^2 \,, && f_2 = \ell_2^2 \,, && f_3 = \ell_3^2 \,, && f_4 = (\ell_1 + k_1)^2 \,, \\ &f_5 = (\ell_1 - k_2)^2 \,, && f_6 = (\ell_2 + k_3)^2 \,, && f_7 = (\ell_2 - k_4)^2 \,, && f_8 = (\ell_3 + K_{12})^2 \,, \\ &f_9 = (\ell_1 - \ell_3 - k_2)^2 \,, && f_{10} = (\ell_3 - \ell_2 - k_3)^2 \,. \end{aligned} \tag{4.31}$$

The external momenta are for simplicity assumed to be massless. External masses can be treated using flattened momenta as described in sec. 3.2.5. We consider generalized unitarity cuts in strictly four dimensions and therefore reconstruct the master integral coefficients to leading order in the dimensional regularization parameter. The analytic expression of the scalar master integral has been computed in dimensional regularization [102].

We will be interested in the algebraic variety defined by imposing on-shell constraints for all triple-box propagators. The set of solutions is

$$\mathcal{S} = \left\{(\ell_1,\ell_2,\ell_3) \in (\mathbb{CP}^4)^{\otimes 3} \mid f_i(\ell_1,\ell_2,\ell_3) = 0\right\} \,. \tag{4.32}$$

The deca-cut results in 10 equations for 12 unknowns. In other words, $\mathcal{S}$ is a two-dimensional algebraic variety (or equivalently, a four-dimensional real surface). Following a the method proposed by Zhang [71], the polynomial system of equations can be reduced by primary decomposition into an intersection of 14 primary ideals. The

[3]Note that our definition of the triple box integral is related to that in ref. [70] by the linear transformation of the three loop momenta, $\tilde{\ell}_1 = \ell_1 + k_1$, $\tilde{\ell}_2 = -\ell_2 + k_4$ and $\ell_3 = -\ell_3 - K_{12}$. The deca-cut Jacobians are clearly invariant under such rearrangements of the momenta.

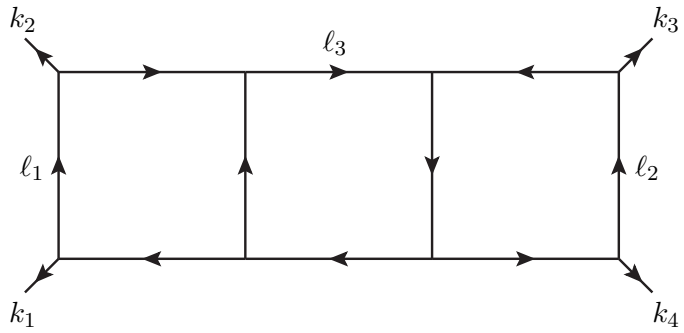

Figure 4.4: Momentum flow for the planar triple box with four external legs.

local form of the 14 deca-cut solutions was worked out in ref. [70] in terms of the loop-momentum parametrization

$$\begin{aligned}
\ell_1^\mu &= \alpha_1 k_1^\mu + \alpha_2 k_2^\mu + \frac{\alpha_3}{2}\frac{\langle 23\rangle}{\langle 13\rangle}\langle 1^-|\gamma^\mu|2^-] + \frac{\alpha_4}{2}\frac{\langle 13\rangle}{\langle 23\rangle}\langle 2^-|\gamma^\mu|1^-] \,, \\
\ell_2^\mu &= \beta_1 k_3^\mu + \beta_2 k_4^\mu + \frac{\beta_3}{2}\frac{\langle 14\rangle}{\langle 13\rangle}\langle 3^-|\gamma^\mu|4^-] + \frac{\beta_4}{2}\frac{\langle 13\rangle}{\langle 14\rangle}\langle 4^-|\gamma^\mu|3^-] \,. \\
\ell_3^\mu &= \gamma_1 k_2^\mu + \gamma_2 k_3^\mu + \frac{\gamma_3}{2}\frac{\langle 34\rangle}{\langle 24\rangle}\langle 2^-|\gamma^\mu|3^-] + \frac{\gamma_4}{2}\frac{\langle 24\rangle}{\langle 34\rangle}\langle 3^-|\gamma^\mu|2^-] \,.
\end{aligned} \tag{4.33}$$

The parameters $\{\alpha_i\}$, $\{\beta_i\}$ and $\{\gamma_i\}$ are in general complex valued. However, at specifically four external points we are able to find normalization factors for the basis elements as in eq. (4.33) such that all parameters are rotated onto the real axis. We will not go into specific details about how the deca-cut equations are solved algebraically. All solutions were presented in ref. [70], so we merely quote the result in tables 4.1-4.2. None of the solutions are related to each other by any kind of parameter redefinitions. For compactness we only explicitly display solutions that are not related to each other by parity. The parity conjugate solutions denoted with primes are easy to construct using the following relations

$$\begin{aligned}
&\alpha_1' = 0 \,, \qquad \alpha_2' = 0 \,, \qquad \alpha_3' = -\frac{1+\chi}{\chi}\alpha_4 \,, \qquad \alpha_4' = -\frac{\chi}{1+\chi}\alpha_3 \,, \\
&\beta_1' = 0 \,, \qquad \beta_2' = 0 \,, \qquad \beta_3' = -\frac{1+\chi}{\chi}\beta_4 \,, \qquad \beta_4' = -\frac{\chi}{1+\chi}\beta_3 \,, \\
&\gamma_1' = \gamma_1 \,, \qquad \gamma_2' = \gamma_2 \,, \qquad \gamma_3' = -(1+\chi)\gamma_4 \,, \qquad \gamma_4' = -\frac{1}{1+\chi}\gamma_3 \,.
\end{aligned} \tag{4.34}$$

It has been explicitly verified that the 14 deca-cut solutions are in one-to-one correspondence with the generically valid configurations of chiral and antichiral three-point vertices, see fig. 4.5.

The four-dimensional momentum space is again spanned by three of the four external momentum vectors (remember that $k_1+k_2+k_3+k_4=0$) together with a perpendicular direction ω. We denote the basis by $e \equiv (k_1, k_2, k_4, \omega)$. The fundamental scalar products are $\tilde{\ell}_i \cdot e_j$ for $1 \leq i \leq 3$ and $1 \leq j \leq 4$, whereas there are four parity-even and three parity-odd ISPs, namely,

$$\{\, \tilde{\ell}_1 \cdot k_4 \,,\ \tilde{\ell}_2 \cdot k_1 \,,\ \tilde{\ell}_3 \cdot k_4 \,,\ \tilde{\ell}_3 \cdot k_1 \,,\ \tilde{\ell}_1 \cdot \omega \,,\ \tilde{\ell}_2 \cdot \omega \,,\ \tilde{\ell}_3 \cdot \omega \,\} \,. \tag{4.35}$$

	α_1	α_2	α_3	α_4	β_1	β_2	β_3	β_4
$\mathcal{S}_1$	0	0	$1-\frac{1}{\chi}\frac{1+z_1}{z_2}$	0	0	0	$1+z_2$	0
$\mathcal{S}_2$	0	0	$\left(1+\frac{1}{\chi}\right)(1+z_1)$	0	0	0	0	$-1-\frac{1}{1+\chi}\frac{1}{z_1}$
$\mathcal{S}_3$	0	0	z_2	0	0	0	0	$-1-z_1$
$\mathcal{S}_4$	0	0	$\left(1+\frac{1}{\chi}\right)(1+z_1)$	0	0	0	0	z_2
$\mathcal{S}_5$	0	0	z_2	0	0	0	1	0
$\mathcal{S}_6$	0	0	1	0	0	0	z_2	0
$\mathcal{S}_7$	0	0	z_1	0	0	0	z_2	0

Table 4.1: The deca-cut freezes the parameters $\alpha_1,\ldots,\alpha_4$ and $\beta_1,\ldots,\beta_4$ of the outer loop momenta ℓ_1 and ℓ_2 to the displayed values. The solutions are written as functions of the two unfrozen parameters $(z_1,z_2)\in\mathbb{C}^2$.

	γ_1	γ_2
$\mathcal{S}_1$	$\frac{1}{\chi}\left(1+\frac{1}{z_1}\right)\left(1+\frac{1}{z_2}\right)$	$-\frac{1}{\chi}\left(1+\frac{1}{z_1}\right)+\frac{z_2}{z_1}$
$\mathcal{S}_2$	$\frac{1}{\chi}(1+z_2)(1+(1+\chi)z_1)$	$\frac{1}{\chi}\left(1+\frac{1}{z_1}\right)z_2$
$\mathcal{S}_3$	$\frac{1}{\chi}\left(1+\frac{1}{z_1}\right)$	0
$\mathcal{S}_4$	0	$-\frac{1}{\chi}\left(1+\frac{1}{z_1}\right)$
$\mathcal{S}_5$	z_1	0
$\mathcal{S}_6$	0	z_1
$\mathcal{S}_7$	0	0

	γ_3	γ_4
$\mathcal{S}_1$	$\frac{1+\chi}{\chi}\left(1+\frac{1}{z_1}\right)$	$-\frac{1}{\chi(1+\chi)}\left(1+\frac{1}{z_1}\right)\left(1+\frac{1}{z_2}\right)+\frac{1}{1+\chi}\frac{1+z_2}{z_1}$
$\mathcal{S}_2$	$-\left(\frac{1+\chi}{\chi}+\frac{1}{\chi}\frac{1}{z_1}\right)z_2$	$-\frac{1}{\chi}(1+z_1)(1+z_2)$
$\mathcal{S}_3$	0	$-\frac{1}{\chi}\left(1+\frac{1}{1+\chi}\frac{1}{z_1}\right)$
$\mathcal{S}_4$	$\frac{1}{\chi}\frac{1}{z_1}+\frac{1+\chi}{\chi}$	0
$\mathcal{S}_5$	0	$-\frac{1}{1+\chi}(1+z_1)$
$\mathcal{S}_6$	0	$-\frac{1}{1+\chi}(1-z_1)$
$\mathcal{S}_7$	0	$-\frac{1}{1+\chi}$

Table 4.2: Values of the parameters $\gamma_1,\ldots,\gamma_4$ of loop-momentum ℓ_3 defined in eq. (4.33) specified by the seven deca-cut solutions $\mathcal{S}_1,\ldots,\mathcal{S}_7$. The parity conjugate solutions $\mathcal{S}_8,\ldots,\mathcal{S}_{14}$ are obtained by applying the rules in eq. (4.34). All solutions were borrowed from ref. [70].

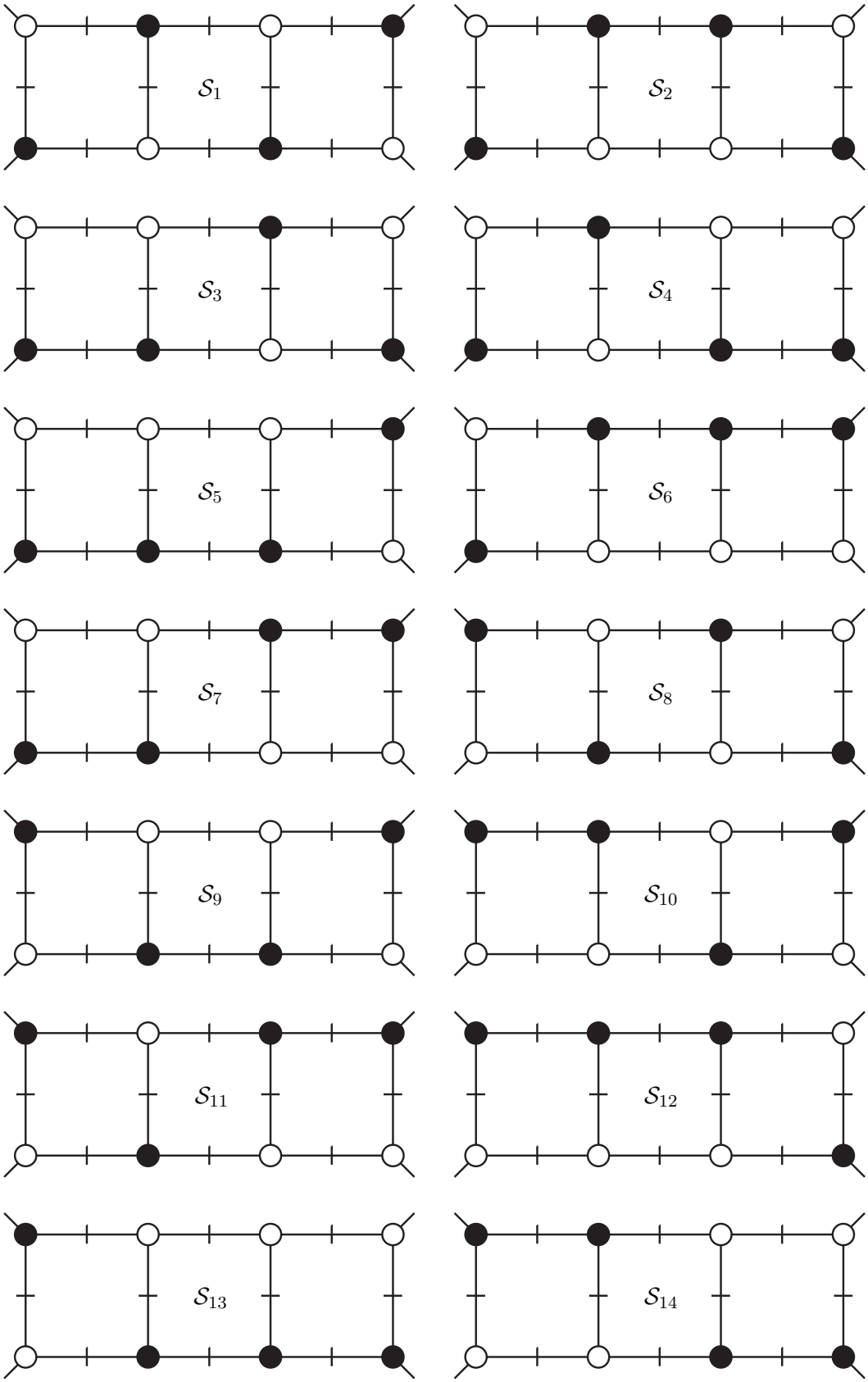

Figure 4.5: The 14 inequivalent solutions to the deca-cut equations for the massless four-point triple-box diagram. The white and black blobs denote chiral and antichiral three-vertices respectively.

Now we can parametrize the most general form of the integrand. The numerator naturally splits into a parity-odd (S) and a parity-even (NS) part,

$$\begin{aligned} N(\tilde{\ell}_1,\tilde{\ell}_2,\tilde{\ell}_3) = & \sum_{\{\alpha_1,\ldots,\alpha_7\}} c_{\alpha_1\cdots\alpha_7}(\tilde{\ell}_1\cdot k_4)^{\alpha_1}(\tilde{\ell}_2\cdot k_1)^{\alpha_2}(\tilde{\ell}_3\cdot k_4)^{\alpha_3}(\tilde{\ell}_3\cdot k_1)^{\alpha_4} \\ & \qquad \times (\tilde{\ell}_1\cdot\omega)^{\alpha_5}(\tilde{\ell}_2\cdot\omega)^{\alpha_6}(\tilde{\ell}_3\cdot\omega)^{\alpha_7} \\ = & \sum_{\{\alpha_1,\ldots,\alpha_4\}} (\tilde{\ell}_1\cdot k_4)^{\alpha_1}(\tilde{\ell}_2\cdot k_1)^{\alpha_2}(\tilde{\ell}_3\cdot k_4)^{\alpha_3}(\tilde{\ell}_3\cdot k_1)^{\alpha_4} \\ & \qquad \times \Big\{ c^{\mathrm{NS}}_{\alpha_1\cdots\alpha_4 0} + c^{\mathrm{NS}}_{\alpha_1\cdots\alpha_4 1}(\tilde{\ell}_1\cdot\omega)(\tilde{\ell}_2\cdot\omega) \\ & \qquad\qquad + c^{\mathrm{S}}_{\alpha_1\cdots\alpha_4 0}(\tilde{\ell}_1\cdot\omega) + c^{\mathrm{S}}_{\alpha_1\cdots\alpha_4 1}(\tilde{\ell}_2\cdot\omega) + c^{\mathrm{S}}_{\alpha_1\cdots\alpha_4 2}(\tilde{\ell}_3\cdot\omega)\Big\} \end{aligned} \tag{4.36}$$

where the additional orthogonal direction as usual is defined by

$$\omega \equiv \frac{1}{2s_{12}}\left(\langle 2|3|1]\langle 1|\gamma^\mu|2] - \langle 1|3|2]\langle 2|\gamma^\mu|1]\right) . \tag{4.37}$$

The exponents in eq. (4.36) are constrained by renormalizability conditions and the integrand-level reduction is then completed by multivariate polynomial division of N modulo a Gröbner basis constructed from the inverse propagators using `BasisDet` [71] as usual. The integrand contains 199 parity-even and 199 parity-odd elements [70].

The reduction to master integrals is eventually achieved by applying IBP relations generated by `Reduze2` [104, 105] and vanishing of parity-odd integrands upon integration over real Minkowski space. A few examples of the IBP identities are included below for reference; the remaining IBPs are available from the author upon request. For compactness we state the IBPs in terms of the ISPs $x_{ij} \equiv \tilde{\ell}_i\cdot v_j$ with $v = (k_1, k_2, k_4, \omega)$. In this notation,

$$\begin{aligned} I_{\square\square\square}[x_{13}^2] &= +\frac{1}{2}\chi s_{12} I_{10}[x_{13}] + \cdots \\ I_{\square\square\square}[x_{13}^2 x_{21} x_{31}] &= +\frac{1}{32}\chi s_{12}^4 I_{10}[1] - \frac{1}{8} s_{12}^3 I_{10}[x_{13}] \\ I_{\square\square\square}[x_{13}^2 x_{21}^3 x_{33}] &= -\frac{1}{128}\chi(3+\chi(3+\chi)) s_{12}^6 I_{10}[1] + \frac{1}{32}(3+\chi(3+\chi)) s_{12}^5 I_{10}[x_{13}] + \cdots . \end{aligned} \tag{4.38}$$

It is convenient to choose an integral basis which allows us to directly compare coefficients with the results obtained by Badger, Frellesvig and Zhang [70]. The three-loop amplitude can be written

$$A_4^{(3)} = c_1 I_{\square\square\square}[1] + c_2 I_{\square\square\square}[(\tilde{\ell}_1 + k_4)^2] + c_3 I_{\square\square\square}[(\tilde{\ell}_3 - k_4)^2] + \cdots . \tag{4.39}$$

The trailing dots hide terms which are not probed by the triple-box maximal cut. Note that since the external legs are massless, e.g.,

$$I_{\square\square\square}[(\tilde{\ell}_1 + k_4)^2] = 2 I_{\square\square\square}[\ell_1\cdot k_4] + \cdots . \tag{4.40}$$

The changes of integration variables $\ell_1^\mu \to \alpha_i$ and similarly for the remaining two loop momenta are compensated by three independent Jacobians. Since the loop-momentum parametrization (4.33) is linear, these Jacobians are constant factors of external invariants and can therefore be canceled on either side of the deca-cut master equation in what

follows. For the sake of completeness we nevertheless worked out the explicit expressions and found that

$$J_\alpha = \det_{\mu,i} \frac{\partial \ell_1^\mu}{\partial \alpha_i} = \frac{s_{12}^2}{4i} \ , \quad J_\beta = \det_{\mu,i} \frac{\partial \ell_2^\mu}{\partial \beta_i} = \frac{s_{12}^2}{4i} \ , \quad J_\gamma = \det_{\mu,i} \frac{\partial \ell_3^\mu}{\partial \gamma_i} = \frac{s_{14}^2}{4i} \ . \tag{4.41}$$

The deca-cut involves fourteen nondegenerate residues associated with the poles of the integrand where all propagators go on-shell simultaneously. It is fairly easy to express the inverse propagators using the loop-momentum parametrization (4.33) and then calculate the residues via the transformation law (4.7). The relatively compact results read [60]

$$I_{\square\square\square}[1]_{\mathcal{S}_1} = +\frac{1}{\chi^2 s_{12}^{10}} \oint \frac{dz_1 \wedge dz_2}{(1+z_1)(1+z_2)(1+z_1-\chi z_2)} \ , \tag{4.42}$$

$$I_{\square\square\square}[1]_{\mathcal{S}_2} = -\frac{1}{\chi^2 s_{12}^{10}} \oint \frac{dz_1 \wedge dz_2}{(1+z_1)(1+z_2)(1+(1+\chi)z_1)z_2} \ , \tag{4.43}$$

$$I_{\square\square\square}[1]_{\mathcal{S}_3} = -\frac{1}{\chi^2 s_{12}^{10}} \oint \frac{dz_1 \wedge dz_2}{(1+z_1)z_2(1+z_1[1+\chi(1-z_2)])} \ , \tag{4.44}$$

$$I_{\square\square\square}[1]_{\mathcal{S}_4} = -\frac{1}{\chi^2 s_{12}^{10}} \oint \frac{dz_1 \wedge dz_2}{(1+z_1)z_2(1+(1+\chi)z_1(1+z_2))} \ , \tag{4.45}$$

$$I_{\square\square\square}[1]_{\mathcal{S}_5} = -\frac{1}{\chi^3 s_{12}^{10}} \oint \frac{dz_1 \wedge dz_2}{z_1 z_2(1+z_1-z_2)} \ , \tag{4.46}$$

$$I_{\square\square\square}[1]_{\mathcal{S}_6} = +\frac{1}{\chi^3 s_{12}^{10}} \oint \frac{dz_1 \wedge dz_2}{z_1 z_2(1-z_1-z_2)} \ , \tag{4.47}$$

$$I_{\square\square\square}[1]_{\mathcal{S}_7} = -\frac{1}{\chi^3 s_{12}^{10}} \oint \frac{dz_1 \wedge dz_2}{z_1 z_2(1-z_1)(1-z_2)} \ . \tag{4.48}$$

The singularity structure for the parity conjugate branches is exactly the same as we would expect from experience. For $i = 1, \ldots, 7$,

$$I_{\square\square\square}[1]_{\mathcal{S}_i} \propto I_{\square\square\square}[1]_{\mathcal{S}_{i+7}} \ . \tag{4.49}$$

4.3.1 Global Poles and Residue Relations

The products of on-shell tree-level amplitudes evaluated in the kinematics specified by the deca-cut solutions define fourteen multivariate Laurent polynomials. Schematically,

$$\sum_{\substack{\text{helicities} \\ \text{particles}}} \prod_{j=1}^{8} A_{(j)}^{\text{tree}}(z_1, z_2)\big|_{\mathcal{S}_i} = \sum_{j,k} d_{i;jk} z_1^j z_2^k \ . \tag{4.50}$$

It can be shown that all coefficients $d_{i,jk}$ with $|j|$ or $|k| > 4$ vanish for all i in all gauge theories even though higher order terms are not ruled out by renormalization conditions [70]. Evaluated on solution $\mathcal{S}_1$ and its complex conjugate $\mathcal{S}_8$, the products of trees will contain terms with negative powers of z_1 and z_2 in the numerator. This follows easily from the shape of the deca-cut solutions. Also, solutions $\mathcal{S}_2$, $\mathcal{S}_3$ and $\mathcal{S}_4$ and their complex conjugates will give rise to negative powers of z_1 cf. tables 4.1-4.2.

The poles contributed by the numerators must be treated on equal footing with the Jacobian poles. We therefore write down 14 lists of poles based on all combinations of two vanishing polynomial factors in the deca-cut Jacobians and the possible extra denominators z_1, z_2. The poles are labeled by the number of the branch in Roman numerals, and its order counted within this branch. More precisely, in $(\dots)$ we specify the location of the pole, and in $\{\dots\}$ we list the particular denominators vanishing for the residue in question.

- Branch $\mathcal{S}_1$: 8 residues for finite z_1, z_2:
  I1 $(-1,-1)$, $\{1+z_1, 1+z_2\}$ I2 $(-1,0)$, $\{(1+z_1)z_2, 1+z_1-\chi z_2\}$
  I3 $(-1,0)$, $\{z_2(1+z_1-\chi z_2), 1+z_1\}$ I4 $(-1,0)$, $\{(1+z_1)(1+z_1-\chi z_2), z_2\}$
  I5 $(0,-1)$, $\{z_1, 1+z_2\}$ I6 $(0,0)$, $\{z_1, z_2\}$
  I7 $(0,1/\chi)$, $\{z_1, 1+z_1-\chi z_2\}$ I8 $(-1-\chi,-1)$, $\{1+z_2, 1+z_1-\chi z_2\}$
- Branch $\mathcal{S}_2$: 6 residues for finite z_1, z_2:
  II1 $(-1,-1)$, $\{1+z_1, 1+z_2\}$ II2 $(-1,0)$, $\{1+z_1, z_2\}$
  II3 $(0,-1)$, $\{z_1, 1+z_2\}$ II4 $(0,0)$, $\{z_1, z_2\}$
  II5 $(-1/(1+\chi),-1)$, $\{1+(1+\chi)z_1, 1+z_2\}$ II6 $(-1/(1+\chi),0)$, $\{1+(1+\chi)z_1, z_2\}$
- Branch $\mathcal{S}_3$: 4 residues for finite z_1, z_2:
  III1 $(-1,0)$, $\{1+z_1, z_2\}$ III2 $(-1,1)$, $\{1+z_1, 1+z_1(1+\chi(1-z_2))\}$
  III3 $(0,0)$, $\{z_2, z_1\}$ III4 $(-1/(1+\chi),0)$, $\{z_2, 1+z_1(1+\chi(1-z_2))\}$
- Branch $\mathcal{S}_4$: 4 residues for finite z_1, z_2:
  IV1 $(-1,0)$, $\{1+z_1, z_2\}$ IV2 $(-1,-\chi/(1+\chi))$, $\{1+z_1, 1+(1+\chi)z_1(1+z_2)\}$
  IV3 $(0,0)$, $\{z_1, z_2\}$ IV4 $(-(1/(1+\chi),0)$, $\{z_2, 1+(1+\chi)z_1(1+z_2)\}$
- Branch $\mathcal{S}_5$: 3 residues for finite z_1, z_2:
  V1 $(-1,0)$, $\{1+z_1-z_2, z_2\}$ V2 $(0,0))$, $\{z_1, z_2\}$
  V3 $(0,1)$, $\{z_1, 1+z_1-z_2\}$
- Branch $\mathcal{S}_6$: 3 residues for finite z_1, z_2:
  VI1 $(0,0)$, $\{z_1, z_2\}$ VI2 $(0,1)$, $\{z_1, z_1+z_2-1\}$
  VI3 $(1,0)$, $\{z_2, z_1+z_2-1\}$
- Branch $\mathcal{S}_7$: 4 residues for finite z_1, z_2:
  VII1 $(0,0)$, $\{z_1, z_2\}$ VII2 $(0,1)$, $\{z_1, z_2-1\}$
  VII3 $(1,0)$, $\{z_1-1, z_2\}$ VII4 $(1,1)$, $\{z_1-1, z_2-1\}$
- Branch $\mathcal{S}_8$: 8 residues for finite z_1, z_2:
  VIII1 $(-1,-1)$, $\{1+z_1, 1+z_2\}$ VIII2 $(-1,0)$, $\{(1+z_1)z_2, 1+z_1-\chi z_2\}$
  VIII3 $(-1,0)$, $\{z_2(1+z_1-\chi z_2), 1+z_1\}$ VIII4 $(-1,0)$, $\{(1+z_1)(1+z_1-\chi z_2), z_2\}$
  VIII5 $(0,-1)$, $\{z_1, 1+z_2\}$ VIII6 $(0,0)$, $\{z_1, z_2\}$
  VIII7 $(0,1/\chi)$, $\{z_1, 1+z_1-\chi z_2\}$ VIII8 $(-1-\chi,-1)$, $\{1+z_2, 1+z_1-\chi z_2\}$
- Branch $\mathcal{S}_9$: 6 residues for finite z_1, z_2:
  IX1 $(-1,-1)$, $\{1+z_1, 1+z_2\}$ IX2 $(-1,0)$, $\{1+z_1, z_2\}$
  IX3 $(0,-1)$, $\{z_1, 1+z_2\}$ IX4 $(0,0)$, $\{z_1, z_2\}$
  IX5 $(-1/(1+\chi),-1)$, $\{1+(1+\chi)z_1, 1+z_2\}$ IX6 $(-1/(1+\chi),0)$, $\{1+(1+\chi)z_1, z_2\}$
- Branch $\mathcal{S}_{10}$: 4 residues for finite z_1, z_2:
  X1 $(-1,0)$, $\{1+z_1, z_2\}$ X2 $(-1,1)$, $\{1+z_1, 1+z_1(1+\chi(1-z_2))\}$
  X3 $(0,0)$, $\{z_2, z_1\}$ X4 $(-1/(1+\chi),0)$, $\{z_2, 1+z_1(1+\chi(1-z_2))\}$

- Branch $\mathcal{S}_{11}$: 4 residues for finite z_1, z_2:
  XI1 $(-1,0)\,,\ \{1+z_1,z_2\}$ XI2 $(-1,-\chi/(1+\chi))\,,\ \{1+z_1,1+(1+\chi)z_1(1+z_2)\}$
  XI3 $(0,0)\,,\ \{z_1,z_2\}$ XI4 $(-(1/(1+\chi),0)\,,\ \{z_2,1+(1+\chi)z_1(1+z_2)\}$

- Branch $\mathcal{S}_{12}$: 3 residues for finite z_1, z_2:
  XII1 $(-1,0)\,,\ \{1+z_1-z_2,z_2\}$ XII2 $(0,0))\,,\ \{z_1,z_2\}$
  XII3 $(0,1)\,,\ \{z_1,1+z_1-z_2\}$

- Branch $\mathcal{S}_{13}$: 3 residues for finite z_1, z_2:
  XIII1 $(0,0)\,,\ \{z_1,z_2\}$ XIII2 $(0,1)\,,\ \{z_1,z_1+z_2-1\}$
  XIII3 $(1,0)\,,\ \{z_2,z_1+z_2-1\}$

- Branch $\mathcal{S}_{14}$: 4 residues for finite z_1, z_2:
  XIV1 $(0,0)\,,\ \{z_1,z_2\}$ XIV2 $(0,1)\,,\ \{z_1,z_2-1\}$
  XIV3 $(1,0)\,,\ \{z_1-1,z_2\}$ XIV4 $(1,1)\,,\ \{z_1-1,z_2-1\}$

We also have to consider residues at complex infinity. However, the GRT implies that every single residue at infinity is linearly related to residues evaluated at finite values of z_1 and z_2. The proof is sketched in an appendix in ref. [60].

Apparently, 64 two-dimensional residues at finite values of z_1 and z_2 are left to be calculated. Thankfully, many of them are actually redundant. The first few residues are eliminated by the above lemma. For instance, the three residues I2, I3 and I3 at $(z_1,z_2)=(-1,0)$ sum to zero. Similarly we discard residue VIII4. We are able to disregard more than half of the residues as they are evaluated at intersections between the 14 deca-cut branches. Exhausting all relations leads to the conclusion that only 23 of the 64 residues are linearly independent. Our choice is summarized by the list:

$$\begin{aligned}\{\mathcal{R}_i\} = \{&\text{I1, I2, I3, I5, I6, I7, I8, II1, II3, II4, II6, III1, III3, V2,}\\ &\text{VIII1, VIII2, VIII3, VIII5, VIII6, IX3, IX4, IX6, XI2}\}\ .\end{aligned} \tag{4.51}$$

The next step is to actually calculate the values of all terms in the numerator on these residues. We calculate the nondegenerate residues directly by means of the Jacobian, while the degenerate residues are obtained via the transformation law (4.7). The whole calculation is automated by a program powered by the algebraic geometry software Macaulay2 [112]. For example, the residues computed by the three master integrals, namely $I_{10}[1]$, $I_{10}[(\tilde{\ell}_1+k_4)^2]$ and $I_{10}[(\tilde{\ell}_3-k_4)^2]$, are

$$\begin{aligned}&\text{Res}_{\{\mathcal{R}_i\}}\, I_{10}[1] =\\ &\quad\frac{1}{\chi^3 s_{12}^{10}}\{-1,1,-1,0,0,0,-1,-1,0,0,-1,1,0,1,1,-1,1,0,0,0,0,-1,1\}\ ,\end{aligned} \tag{4.52}$$

$$\begin{aligned}&\text{Res}_{\{\mathcal{R}_i\}}\, I_{10}[(\tilde{\ell}_1+k_4)^2] =\\ &\quad\frac{1}{\chi^2 s_{12}^{9}}\{0,1,0,0,0,0,-1,-1,0,0,0,1,0,1,0,-1,0,0,0,0,0,0,1\}\ ,\end{aligned} \tag{4.53}$$

$$\begin{aligned}&\text{Res}_{\{\mathcal{R}_i\}}\, I_{10}[(\tilde{\ell}_3-k_4)^2] =\\ &\quad\frac{1}{\chi^2 s_{12}^{9}}\{0,1,0,0,1,-1,0,0,0,0,0,0,-1,0,0,-1,0,0,-1,0,0,0,0\}\ ,\end{aligned} \tag{4.54}$$

where the values are listed in the same order as in (4.51). Note that we actually calculated the values of all terms on all 64 residues and explicitly verified the linear relations among them, for example the relation in eq. (4.20).

4.4 Integral Reduction and Projectors

The task is now to extract the three master integral coefficients in eq. (4.39) from the augmented deca-cut. In advance of calculations below, we pull out a universal prefactor and define the dimensionless coefficients $\hat{c}_i$,

$$c_i = s_{12}^3 s_{14} A_4^{\text{tree}} \hat{c}_i \ , \tag{4.55}$$

where the tree-level amplitude is given by the Parke-Taylor formula (1.4). For instance for external helicities $--++$,

$$A_4^{\text{tree}}(1^-, 2^-, 3^+, 4^+) = i \frac{\langle 12\rangle^4}{\langle 12\rangle\langle 23\rangle\langle 34\rangle\langle 41\rangle} \ . \tag{4.56}$$

4.4.1 Uniqueness of Master Contours

The remaining question to resolve is whether the master integral projectors are uniquely determined or not? In particular, is possible to find three unique linear combinations of the multivariate residues such that all constraints from IBP identities and vanishing of parity-odd terms upon integration over real Minkowski space? To answer this question we organize all constraints as a homogeneous system of equations with a matrix $\tilde{M}$ of size 398×20. A direct calculation shows that $\operatorname{rank} \tilde{M} = 20$. Hence the deformed integration contours are subject to only 20 constraints in order to yield a valid unitarity cut prescription.

The remaining three degrees of freedom that are not fixed by integral reduction consistency requirements leave space for exactly three master integrals. We will define projectors $\mathcal{M}_1$, $\mathcal{M}_2$ and $\mathcal{M}_3$ with the properties that only one of the master integrals are picked up on the cut and normalized to unity. Let M be the 401×23 matrix obtained by extending $\tilde{M}$ with the residues of the three master integrals (4.54). The defining equations for the projectors can thus be phrased as follows,

$$\mathcal{M}_1 : \ M\Omega_1 = (0, \ldots, 0, 1, 0, 0)^T \ , \tag{4.57}$$

$$\mathcal{M}_2 : \ M\Omega_2 = (0, \ldots, 0, 0, 1, 0)^T \ , \tag{4.58}$$

$$\mathcal{M}_3 : \ M\Omega_3 = (0, \ldots, 0, 0, 0, 1)^T \ . \tag{4.59}$$

In this way, the three solutions Ω_1, Ω_2 and Ω_3 correspond to extracting the coefficient in front of $I_{10}[1]$, $I_{10}[(\tilde{\ell}_1 + k_4)^2]$ and $I_{10}[(\tilde{\ell}_3 - k_4)^2]$ respectively.

Since Ω_i is a 23-dimensional vectors and $\operatorname{rank} M = 23$, the solutions for the three projectors are uniquely determined. They can be obtained by standard algebra techniques, with the result

$$\begin{aligned}
\Omega_1 &= \frac{1}{8}\chi^3 s_{12}^{10}(-1, 0, -2, 0, 1, 1, 0, 0, 1, -1, -1, 0, 1, 0, 1, 0, 2, 0, -1, 1, -1, -1, 0) \ , \\
\Omega_2 &= \frac{1}{4}\chi^2 s_{12}^{9}(0, 1, 2, -1, -2, -1, 0, -1, -1, 1, 0, 0, -1, 1, 0, -1, -2, 1, 2, -1, 1, 0, 0) \ , \\
\Omega_3 &= \frac{1}{4}\chi^2 s_{12}^{9}(1, -1, -2, 3, 3, 0, -2, 1, 0, 0, 1, 2, 0, -1, -1, 1, 2, -3, -3, 0, 0, 1, 0) \ .
\end{aligned} \tag{4.60}$$

The associated master contours $\mathcal{M}_i$ can be written down explicitly as linear combinations of weighted infinitesimal toroidal surfaces encircling the global poles. Each master contour receives only contribution from a small subset Λ of the 14 deca-cut branches after redundant residues have been removed. This suggest the decomposition

$\mathcal{M}_i = \sum_{k\in\Lambda} \mathcal{M}_{i;k}$ for $\Lambda = \{\mathrm{I}, \mathrm{II}, \mathrm{III}, \mathrm{V}, \mathrm{VIII}, \mathrm{IX}, \mathrm{XI}\}$. This notation hides the weights implicitly in the contours. Our result for the master integral coefficients can then be written schematically in the very compact form

$$\boxed{c_i = \sum_{k\in\Lambda} \oint_{\mathcal{M}_{i;k}} \frac{dz_1 dz_2}{J_k(z_1, z_2)} \sum_{\substack{\text{helicities} \\ \text{particles}}} \prod_{j=1}^{8} A_{(j)}^{\text{tree}}(z_1, z_2)\big|_{\mathcal{S}_k} .} \tag{4.61}$$

4.5 Examples

In this section we demonstrate how to calculate three-loop master integral coefficients in four-point gluon amplitudes with specific helicity configurations and massless kinematics. We specialize to deca-cuts in the s-channel since the contribution from the t-channel follows by cyclic permutation of external labels.

The input of our computation is the intermediate state sum over the product of the eight tree-level amplitudes which arise by cutting the amplitude on-shell, evaluated on each of the deca-cut branches. We can think of the trees as being a numerator insertion,

$$N|_{\mathcal{S}_i} = \sum_{\substack{\text{helicities} \\ \text{particles}}} \prod_{j=1}^{8} A_{(j)}^{\text{tree}}(z_1, z_2)\big|_{\mathcal{S}_i} , \tag{4.62}$$

and the expression is summed over all internal helicity states and distinct configurations of gluons, fermions and scalars propagating in the loops as usual. The state sum may be obtained in supersymmetric Yang-Mills theories through superspace techniques, see e.g. refs. [97–99], or by direct calculation in a generic gauge theory from the specific distributions of on-shell tree-point MHV and $\overline{\text{MHV}}$ vertices and all possible flavor combinations. For now we simply rely on the fact that the triple-box tree-level data has already been calculated in ref. [70] as explicit Laurent expansions, with n_f fermion and n_s complex scalar flavors in the adjoint representation.

4.5.1 $-+-+$ Helicity Amplitude

Our first example is the $-+-+$ helicity gluon amplitude shown in fig. 4.6. We have

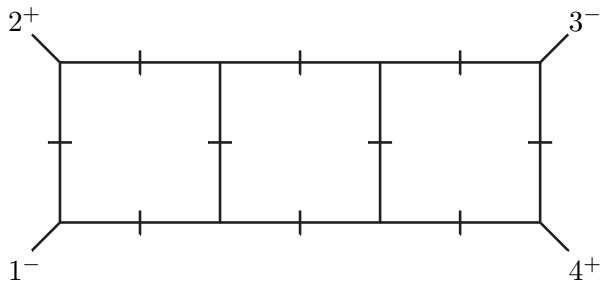

Figure 4.6: The deca-cut planar four-point triple box diagram with alternating external helicity configuration.

computed the 23 independent residues from the Laurent expansions of the products of

tree-level amplitudes. The result can be summarized as the list

$$\begin{aligned}\operatorname{Res}_{\{\mathcal{G}_i\}} \frac{1}{J(z_1,z_2)} \sum_{\substack{\text{helicities}\\ \text{particles}}} \prod_{j=1}^{8} A_{(j)}^{-+-+} \\ = \frac{1}{\chi^3 s_{12}^{10}} (1,-1,1,-r_1,0,r_1,1-r_1,1-r_1,r_1,-r_1,1,-1, \\ 0,-1,-1+r_1,1-r_1,-1+r_1,0,r_2,0,0,1-r_1,-1)\,,\end{aligned} \tag{4.63}$$

where r_1 and r_2 are given by

$$r_1 \equiv \frac{\chi(1+\chi^2)(4-n_f)+2\chi^2(3-n_s)}{(1+\chi)^4}\,, \tag{4.64}$$

$$\begin{aligned}r_2 \equiv \frac{\chi}{(1+\chi)^4}\Big(&8(1-2\chi)(3-n_s)(4-n_f)-(13-(24-\chi)\chi)(4-n_f) \\ &-2\chi(3-n_s)+(1-(4-\chi)\chi)(n_f(3-n_s)^2-2(4-n_f)^2) \\ &-2(1-2\chi)(4-n_f)^2\Big)\,.\end{aligned} \tag{4.65}$$

Note that the integrand in eq. (4.63) is supposed to be evaluated on the branch on which the specific residue actually resides.

In an $\mathcal{N}$-fold supersymmetric theory one has $n_f = \mathcal{N}$ and $n_s = \mathcal{N}-1$. With this in mind, the residues in eqs. (4.64)-(4.65) were brought to a form that exposes the fact that the results simplify dramatically for $\mathcal{N}=4$ and also $\mathcal{N}=2$. Now, plugging the residues into eq. (4.61) produces the normalized master integral coefficients

$$\begin{aligned}\hat{c}_1^{-+-+} = &-1+(4-n_f)\frac{\chi}{(1+\chi)^2}-2(1+n_s-n_f)\frac{\chi^2}{(1+\chi)^4} \\ &-(2(1-2n_s)+n_f)(4-n_f)\frac{(1-2\chi)\chi}{4(1+\chi)^4} \\ &-(n_f(3-n_s)^2-2(4-n_f)^2)\frac{(1-(4-\chi)\chi)\chi}{8(1+\chi)^4}\,,\end{aligned} \tag{4.66}$$

$$\begin{aligned}\hat{c}_2^{-+-+} = &-(4-n_f)\frac{1}{s_{12}(1+\chi)^2}+2(1+n_s-n_f)\frac{\chi}{s_{12}(1+\chi)^4} \\ &+(2(1-2n_s)+n_f)(4-n_f)\frac{1-2\chi}{s_{12}(1+\chi)^4} \\ &+(n_f(3-n_s)^2-2(4-n_f)^2)\frac{1-(4-\chi)\chi}{2s_{12}(1+\chi)^4}\,,\end{aligned} \tag{4.67}$$

$$\begin{aligned}\hat{c}_3^{-+-+} = &-(2(1-2n_s)+n_f)(4-n_f)\frac{3(1-2\chi)}{2s_{12}(1+\chi)^4} \\ &-(n_f(3-n_s)^2-2(4-n_f)^2)\frac{3(1-(4-\chi)\chi)}{4s_{12}(1+\chi)^4}\,.\end{aligned} \tag{4.68}$$

Our results agree with those of Badger, Frellesvig and Zhang [70][4] and Bern, Dixon, Smirnov [89].

[4] Modulo typos.

4.5.2 $--++$ Helicity Amplitude

The planar triple-box contribution to the $--++$ helicity gluon amplitude turns out to be rather trivial. We computed the three master integral coefficients from the deca-cut shown in fig. 4.7 and found the simple results

$$\hat{c}_1^{--++} = -1\,, \tag{4.69}$$
$$\hat{c}_2^{--++} = 0\,, \tag{4.70}$$
$$\hat{c}_3^{--++} = 0\,. \tag{4.71}$$

Needless to say, eq. (4.69)-(4.71) are in agreement with the analysis of Badger, Frellesvig and Zhang [70] and Bern, Dixon and Smirnov [89].

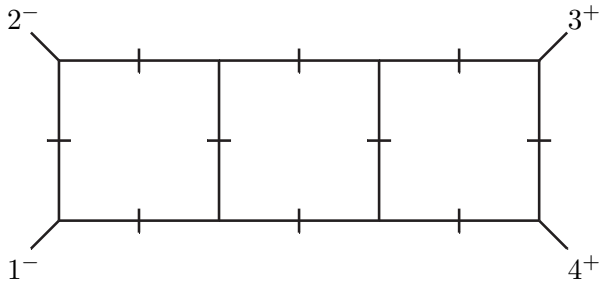

Figure 4.7: The maximally cut planar four-gluon triple box diagram with external helicities $--++$.

4.6 Generalized Cuts and Doubled Propagators

Feynman integrals with doubled propagators arise frequently in connection with IBP identities, Schwinger parametrizations and Mellin-Barnes representations. This section presents a natural extension of generalized unitarity to multiloop integrals that otherwise seem to be incompatible with the usual cut prescription. Naively, if we try to evaluate a generalized unitarity cut of an integral with higher powers of propagators, the immediate result is singular. Nevertheless, integral bases that contain elements with doubled propagators can lead to significant simplifications as argued in ref. [100]. We demonstrate the cuts of integrals with doubled propagators are naturally handled by means of multivariate residue technology.

We will consider dimensionally regularized n-loop Feynman integrals with arbitrary integer powers (referred to as indices) $(\sigma_1, \ldots, \sigma_p)$ of p propagators. In condensed notation,

$$I[\Phi(\ell_1, \ell_2, \ell_3)](\sigma_1, \ldots, \sigma_p) \equiv \left(\prod_{i=1}^{n} \int \frac{d^D \ell_i}{(2\pi)^D} \right) \frac{\Phi(\{\ell_i\})}{\prod_{k=1}^{p} f_k^{\sigma_k}(\{\ell_i\}} \,, \tag{4.72}$$

for linear polynomials f_k with respect to dot products of the n loop momenta $\{\ell_i\}$ and m external momenta $\{k_i\}$. The single-propagator integral is recovered by setting $\sigma_1 = \cdots = \sigma_p = 1$. Note that it is always possible to bring the numerator Φ into the form of negative powers of additional propagators.

Multiloop amplitude calculations typically suffer from a severe proliferation of Feynman integrals. Although a large portion of the integrals can be reduced algebraically

at the level of the integrand, many integrals are nominally irreducible. The aid is to apply IBP identities to express integrals as linear combinations of master integrals. We exploit that total derivatives integrate to zero,

$$\left(\prod_{i=1}^{n}\int\frac{d^D\ell_i}{(2\pi)^D}\right)\frac{\partial}{\partial\ell_a^\mu}\left(k_b^\mu\prod_{k=1}^{p}\frac{1}{f_k^{\sigma_k}(\{\ell_i\})}\right)=0\,, \tag{4.73}$$

$$\left(\prod_{i=1}^{n}\int\frac{d^D\ell_i}{(2\pi)^D}\right)\frac{\partial}{\partial\ell_a^\mu}\left(\ell_b^\mu\prod_{k=1}^{p}\frac{1}{f_k^{\sigma_k}(\{\ell_i\})}\right)=0\,, \tag{4.74}$$

and discard the boundary term produced by the D-dimensional integration. The resulting equations can be cast as linear relations among integrals with shifted exponents,

$$\sum_i \mu_i I(\sigma_1+\rho_{i,1},\ldots,\sigma_n+\rho_{i,n})=0 \tag{4.75}$$

where $\rho_{i,j}\in\{-1,0,1\}$. The IBPs are extremely efficient in practice, reducing hundreds of planar triple-box integrals onto just three masters, for instance.

4.6.1 Simple Example: One-Loop Box

Our first example is the one-loop box integral with four massless external legs and arbitrary powers of propagators. The corresponding Feynman expression is a special case of eq. (2.11), which we shall write as

$$I_4(\sigma_1,\ldots,\sigma_4)[\Phi(\ell)]\equiv\int\frac{d^D\ell}{(2\pi)^D}\prod_{i=1}^{4}\frac{\Phi(\ell)}{f_i^{\sigma_i}(\ell)}\,, \tag{4.76}$$

where $f_1,\ldots,f_4$ are given by

$$f_1=\ell^2\,,\quad f_2=(\ell-k_1)^2\,,\quad f_3=(\ell-K_{12})^2\,,\quad f_4=(\ell+k_4)^2\,. \tag{4.77}$$

Take as an example the box integral $I_4(1,1,1,2)[1]$ which can be reduced into the usual scalar box integral. The Jacobian of $\{f_1,f_2,f_3,f_4^2\}$ vanishes at both branches of the quadruple cut and thus gives rise to degenerate multivariate residues. We therefore transform the inverse propagators into a univariate description,

$$\begin{pmatrix}g_1\\g_2\\g_3\\g_4\end{pmatrix}\equiv\begin{pmatrix}\alpha_1-1\\\alpha_2\\-\alpha_3(\alpha_3+\chi)^2\\-\alpha_4(\alpha_4+\chi)^2\end{pmatrix}=M\begin{pmatrix}f_1\\f_2\\f_3\\f_4^2\end{pmatrix}\,. \tag{4.78}$$

Here, M is a 4×4 matrix whose entries are polynomials in $\alpha_1,\ldots,\alpha_4$. The explicit form of M is not particular illuminating, but we need its determinant,

$$\det M=-\frac{\chi(1+\chi)(\alpha_3-\alpha_4)(\alpha_3+\alpha_4+2\chi)}{s_{12}^5}\,. \tag{4.79}$$

This transformation trivializes the calculation of the quadruple cut residues. Applying the Britto-Cachazo-Feng formula (2.36) immediately leads to the conclusion,

$$I_4(1,1,1,2)[1]=\frac{1}{s_{12}\chi}I_4(1,1,1,1)[1]+\cdots\,. \tag{4.80}$$

Similarly we find the reductions

$$I_4(2,1,1,2)[1] = \frac{2}{s_{12}^2\chi} I_4(1,1,1,1)[1] + \cdots \,, \tag{4.81}$$

$$I_4(3,1,1,1)[1] = \frac{1}{s_{12}^2} I_4(1,1,1,1)[1] + \cdots \,, \tag{4.82}$$

which are all consistent with the known IBP identities in the $\epsilon \to 0$ limit,

$$I_4(1,1,1,2)[1] = \frac{1+2\epsilon}{s_{12}\chi} I_4(1,1,1,1)[1] + \cdots \,, \tag{4.83}$$

$$I_4(2,1,1,2)[1] = \frac{2(1+\epsilon)(1+2\epsilon)}{s_{12}^2\chi} I_4(1,1,1,1)[1] + \cdots \,, \tag{4.84}$$

$$I_4(3,1,1,1)[1] = \frac{(1+\epsilon)(1+2\epsilon)}{s_{12}^2} I_4(1,1,1,1)[1] + \cdots \,. \tag{4.85}$$

4.6.2 Example: Massless Planar Double Box

We now shift gears and proceed to two-loop integrals with doubled propagator. Our first example is the planar double-box integral $P^{**}_{2,2}$ defined in eq. (3.4). We shall rewrite the integral into the more general 9-propagator form,

$$P^{**}_{2,2}(\sigma_1,\ldots,\sigma_9)[\Phi(\ell_1,\ell_2)] \equiv \int \frac{d^D\ell_1}{(2\pi)^D} \int \frac{d^D\ell_2}{(2\pi)^D} \prod_{i=1}^{9} \frac{\Phi(\ell_1,\ell_2)}{f_i^{\sigma_i}(\ell_1,\ell_2)} \,, \tag{4.86}$$

where the seven inverse propagators $\{f_i\}$ are given by

$$\begin{aligned} &f_1 = \ell_1^2 \,, \quad f_2 = (\ell_1 - k_1)^2 \,, \quad f_3 = (\ell_1 - K_{12})^2 \,, \\ &f_4 = \ell_2^2 \,, \quad f_5 = (\ell_2 - k_4)^2 \,, \quad f_6 = (\ell_2 - K_{34})^2 \,, \quad f_7 = (\ell_1 + \ell_2)^2 \end{aligned} \tag{4.87}$$

and $f_8 = \ell_1 \cdot k_4$ and $f_9 = \ell_2 \cdot k_1$ are the nonspurious ISPs.

We will from now on concentrate on integrals that have at least one doubled propagators, e.g.

$$P^{**}_{2,2}(2,1,\ldots,1,0,0) = c_1 P^{**}_{2,2}(1,\ldots,1,0,0) + c_2 P^{**}_{2,2}(1,\ldots,1,-1,0) + \cdots \,, \tag{4.88}$$

$$P^{**}_{2,2}(1,\ldots,1,2,0,0) = c_1' P^{**}_{2,2}(1,\ldots,1,0,0) + c_2' P^{**}_{2,2}(1,\ldots,1,-1,0) + \cdots \,. \tag{4.89}$$

The maximal cut of such integrals clearly involves degenerate multivariate residues by the preceding discussion. Accordingly, we apply the algorithm and transform the residue to a factorized form. We find that

$$P^{**}_{2,2}(2,1,\ldots,1,0,0)_{\mathcal{S}_{1,3}} = -\frac{1}{16 s_{12}^4} \oint \frac{dz}{z(z+\chi)} \,, \tag{4.90}$$

$$P^{**}_{2,2}(2,1,\ldots,1,0,0)_{\mathcal{S}_{2,4,5,6}} = -\frac{1}{16 s_{12}^4} \oint \frac{dz}{z(z+\chi)^2} \,, \tag{4.91}$$

$$P^{**}_{2,2}(1,\ldots,1,2,0,0)_{\mathcal{S}_i} = -\frac{1}{16 s_{12}^4} \oint \frac{dz}{z(z+\chi)^2} \,. \tag{4.92}$$

Now we can take advantage of the master integral projectors in order to reduce double-box integrals with doubled propagators. As an example we will examine the integrals

on the left hand side of eq. (4.88). The residues evaluated at the usual list of global poles are

$$\begin{aligned}\text{Res}_{\{\mathcal{G}_i\}} P^{**}_{2,2}(2,1,\ldots,1,0,0) &= \frac{1}{16\chi s_{12}^4}(1,-1,1,1,-1,1,0,0)\,,\\ \text{Res}_{\{\mathcal{G}_i\}} P^{**}_{2,2}(1,\ldots,1,2,0,0) &= \frac{1}{16\chi^2 s_{12}^4}(1,-1,1,1,-1,1,0,0)\,.\end{aligned} \tag{4.93}$$

The projectors immediately produce the reduction identities

$$P^{**}_{2,2}(2,1,\ldots,1,0,0) = +\frac{1}{s_{12}} P^{**}_{2,2}(1,\ldots,1,0,0) + \cdots\,, \tag{4.94}$$

$$P^{**}_{2,2}(1,\ldots,1,2,0,0) = +\frac{1}{\chi s_{12}} P^{**}_{2,2}(1,\ldots,1,0,0) + \cdots\,. \tag{4.95}$$

Our results are easily verified by considering the four-dimensional limits of the following IBP relations in $D = 4 - 2\epsilon$,

$$\begin{aligned}&P^{**}_{2,2}(2,1,\ldots,1,0,0) =\\ &\qquad \frac{1+2\epsilon}{s_{12}} P^{**}_{2,2}(1,\ldots,1,0,0) + \cdots\end{aligned} \tag{4.96}$$

$$\begin{aligned}&P^{**}_{2,2}(1,\ldots,1,2,0,0) =\\ &\qquad \frac{1+2\epsilon}{1+\epsilon}\left(\frac{1+3\epsilon}{\chi s_{12}} P^{**}_{2,2}(1,\ldots,1,0,0) + \frac{4\epsilon}{\chi s_{12}^2} P^{**}_{2,2}(1,\ldots,1,-1,0)\right) + \cdots\,.\end{aligned} \tag{4.97}$$

Indeed, when $\epsilon \to 0$ the tensor integral is suppressed and the scalar integrals equate up to the factors specified above.

We remark that any other powers of propagators may be treated analogously. A complete list of hepta-cuts of planar double-box integrals with a doubled propagator can be found in ref. [61].

4.6.3 Example: Massless Nonplanar Double Box

The four-point two-loop nonaplanar double-box integral with arbitrary powers of propagators is given by

$$X^{**}_{1,1,2}(\sigma_1,\ldots,\sigma_7) \equiv \int_{\mathbb{R}^D} \frac{d^D\ell_1}{(2\pi)^D} \int_{\mathbb{R}^D} \frac{d^D\ell_2}{(2\pi)^D} \prod_{i=1}^{7} \frac{1}{\tilde{f}_i^{\sigma_i}(\ell_1,\ell_2)}\,, \tag{4.98}$$

where the inverse propagators are

$$\begin{aligned}&\tilde{f}_1 = \ell_1^2\,, \quad \tilde{f}_2 = (\ell_1+k_1)^2\,, \quad \tilde{f}_3 = (\ell_2+k_4)^2\,,\\ &\tilde{f}_4 = \ell_2^2\,, \quad \tilde{f}_5 = (\ell_1-k_3)^2\,, \quad \tilde{f}_6 = (\ell_1+\ell_2-k_3)^2\,, \quad \tilde{f}_7 = (\ell_1+\ell_2-K_{23})^2\end{aligned} \tag{4.99}$$

and $f_8 = \ell_1 \cdot k_3$ and $\ell_2 \cdot k_2$ are the ISPs. We will study integrals with doubled and also tripled propagators,

$$\begin{aligned}&X^{**}_{1,1,2}(2,1,\ldots,1,0,0) =\\ &\qquad c_1 X^{**}_{1,1,2}(1,\ldots,1,0,0) + c_2 X^{**}_{1,1,2}(1,\ldots,1,-1,0) + \cdots\,,\end{aligned} \tag{4.100}$$

$$\begin{aligned}&X^{**}_{1,1,2}(1,\ldots,1,3,0,0) =\\ &\qquad c_1' X^{**}_{1,1,2}(1,\ldots,1,0,0) + c_2' X^{**}_{1,1,2}(1,\ldots,1,-1,0) + \cdots\,,\end{aligned} \tag{4.101}$$

and derive the coefficients at $\mathcal{O}(\epsilon^0)$. The degenerate multivariate residues associated with the hepta-cuts of the displayed integrals are

$$X^{**}_{1,1,2}(2,1,\ldots,1,0,0)_{\mathcal{S}_{3,4}} = +\frac{1}{16s_{12}^4}\oint dz \frac{1+(1+\chi)z}{z^2(z+\chi)^2}\,, \tag{4.102}$$

$$X^{**}_{1,1,2}(2,1,\ldots,1,0,0)_{\mathcal{S}_{7,8}} = +\frac{1}{16s_{12}^4}\oint dz \frac{1+\chi}{z^2(z-\chi-1)}\,, \tag{4.103}$$

$$X^{**}_{1,1,2}(2,1,\ldots,1,0,0)_{\mathcal{S}_{1,2,5,6}} = +\frac{1}{16s_{12}^4}\oint dz \frac{1}{z(z-\chi)^2(z-\chi-1)}\,, \tag{4.104}$$

$$X^{**}_{1,1,2}(1,\ldots,1,3,0,0)_{\mathcal{S}_{3,4}} = -\frac{1}{16s_{12}^5}\oint dz \frac{h(z)}{z(z+\chi)^5}\,, \tag{4.105}$$

$$X^{**}_{1,1,2}(1,\ldots,1,3,0,0)_{\mathcal{S}_{7,8}} = -\frac{1}{16s_{12}^5}\oint dz \frac{(1+\chi)^2}{z(z-\chi-1)^3}\,, \tag{4.106}$$

$$X^{**}_{1,1,2}(1,\ldots,1,3,0,0)_{\mathcal{S}_{1,2,5,6}} = -\frac{1}{16s_{12}^5}\oint dz \frac{1}{z(z-\chi)^3(z-\chi-1)}\,, \tag{4.107}$$

where $h(z)$ is defined by

$$h(z) = \chi^4 - \chi^3(4z+1) + \chi^2(z(z+1)+1) + 2\chi z(z+1) + z^2\,. \tag{4.108}$$

It is easiest to compare results with refs. [59] if we encircle poles at the nodal points of the pinched genus-3 curve and thus eliminate all residues at infinity. The solutions are holomorphically parametrized and there are no additional poles in tensor integrals. We denote the contour weights by

$$\Omega = (\omega_{1\cap 6},\, \omega_{1\cap 3},\, \omega_{1\cap 7}\,, \omega_{2\cap 5},\, \omega_{2\cap 4},\, \omega_{2\cap 8},\, \omega_{5\cap 3},\, \omega_{5\cap 7},\, \omega_{6\cap 4},\, \omega_{6\cap 8})\,, \tag{4.109}$$

so the corresponding residues extracted from the basis integrals read

$$R_1 = \frac{1}{16\chi(1+\chi)s_{12}^3}(-1, 1+\chi, -\chi, -1, 1+\chi, -\chi, 1+\chi, -\chi, 1+\chi, -\chi)\,, \tag{4.110}$$

$$R_2 = \frac{1}{32s_{12}^2}(0, 1, -1, 0, 1, -1, 0, 0, 0, 0)\,. \tag{4.111}$$

We also need to collect the residues computed by the integrals with doubled and tripled propagators,

$$\begin{aligned}&\mathrm{Res}_{\{\mathcal{G}_i\}} X^{**}_{1,1,2}(2,1,\ldots,1,0,0) = \\ &\qquad \frac{1}{16(1+\chi)\chi^2 s_{12}^4}(-1, 1-\chi^2, \chi^2, -1, 1-\chi^2, \chi^2, 1-\chi^2, \chi^2, 1-\chi^2, \chi^2)\,,\end{aligned} \tag{4.112}$$

$$\begin{aligned}&\mathrm{Res}_{\{\mathcal{G}_i\}} X^{**}_{1,1,2}(1,\ldots,1,3,0,0) = \\ &\qquad \frac{1}{16(1+\chi)\chi^3 s_{12}^5}(-1, 1+\chi^3, -\chi^3, -1, 1+\chi^3, -\chi^3, 1+\chi^3, -\chi^3, 1+\chi^3, -\chi^3)\,.\end{aligned} \tag{4.113}$$

Applying the projectors to eq. (4.112) yields

$$\begin{aligned}&X^{**}_{1,1,2}(2,1,\ldots,1,0,0) = \\ &\qquad + \frac{1}{\chi s_{12}} X^{**}_{1,1,2}(1,\ldots,1,0,0) - \frac{4}{\chi s_{12}^2} X^{**}_{1,1,2}(1,\ldots,1,-1,0) + \cdots\end{aligned} \tag{4.114}$$

and similarly for eq. (4.113),

$$X^{**}_{1,1,2}(1\ldots,1,3,0,0) = \\ + \frac{1}{\chi^2 s_{12}^2} X^{**}_{1,1,2}(1,\ldots,1,0,0) - \frac{4(1-\chi)}{\chi^2 s_{12}^3} X^{**}_{1,1,2}(1,\ldots,1,-1,0) + \cdots . \quad (4.115)$$

The validity of the predictions (4.114)-(4.115) has been verified against IBP identities obtained from `FIRE` [103]. Taking the $\epsilon = 0$ limit of the following relations,

$$X^{**}_{1,1,2}(2,1,\ldots,1,0,0) = \\ + \frac{(1+2\epsilon)(1+(3+2\chi)\epsilon)}{(1+\epsilon)\chi s_{12}} X^{**}_{1,1,2}(1,\ldots,1,0,0) \\ - \frac{4(1+2\epsilon)(1+4\epsilon)}{(1+\epsilon)\chi s_{12}^2} X^{**}_{1,1,2}(1,\ldots,1,-1,0) + \cdots \quad (4.116)$$

$$X^{**}_{1,1,2}(1,\ldots,1,3,0,0) = \\ + \frac{(1+2\epsilon)(2+(9(1+\epsilon)+2\chi(1+2\epsilon-2(1+\epsilon)\chi))\epsilon)}{(2+\epsilon)\chi^2 s_{12}^2} X^{**}_{1,1,2}(1,\ldots,1,0,0) \\ - \frac{4(1+2\epsilon)(1+4\epsilon)(2-2\chi(1+\epsilon)+3\epsilon)}{(2+\epsilon)\chi^2 s_{12}^3} X^{**}_{1,1,2}(1,\ldots,1,-1,0) + \cdots \quad (4.117)$$

shows that our results are consistent.

We have also calculated hepta-cuts of all other massless four-point nonplanar double-box integrals with single doubled propagator. The results are similar to those in eq. (4.107) and can be found in ref. [61].

Elliptic Functions and Maximal Unitarity 5

Es ist wahr, ein Mathematiker, der nicht etwas Poet ist,
wird nimmer ein vollkommener Mathematiker sein.
— Karl Weierstrass (1815–1897)

Cutting seven propagators on-shell at two loops leads to a one-dimensional complex manifold. For example, the maximal cuts of the purely massless planar and nonplanar double-box topologies define degenerate algebraic curves that are topologically equivalent to multiply pinched Riemann surfaces of genus $g = 1$ and $g = 3$ respectively. In fact, the irreducible components are just Riemann spheres.

The origin of the degeneracy may be traced back to the presence of massless external (and internal) lines, as alluded in the previous chapters. Given a diagram, we may first consider the prime case with the maximal number of massive external (and internal) particles. Typically, the maximal cut then defines a high-genus irreducible curve. Next we examine all distinct degenerate cases with fewer external legs or several massless particles. In this case, the maximal cut typically yields a reducible curve. For genus-0 irreducible components there always exists a rational parametrization. However, if the genus is larger than zero, it is not possible to describe the solution space by rational parameters in any coordinates. Moreover, curves of nonzero genus give rise to additional nontrivial topological cycles.

Here we take the first steps to develop a generalized unitarity method for the case of higher-genus Riemann surfaces, using as a phenomenologically relevant example the two-loop double box with internal masses. In this case the maximal cut defines a non-degenerate elliptic curve associated with a genuine torus. Our method is based on the theory of Weierstrass elliptic functions and meromorphic differential forms. The principal result is a highly nontrivial addition to the large body of evidence of the uniqueness conjecture for two-loop master contours. This chapter is a moderately augmented version of paper I.

5.1 Elliptic Curves from Maximal Cuts

In this section we present two distinct, yet intimately related, examples of elliptic curves generated by maximal cuts of two-loop diagrams with external massive legs or massive particles propagating in the loops. The following examples are very brief and we do not pretend to give a comprehensive treatment.

5.1.1 10-Gluon Double Box

Our first example of an elliptic curve from maximal cuts involves the most general two-loop planar double-box integral with neither massive internal lines nor doubled propagators. The integral is given by

$$P_{2,2}(K_1,\ldots,K_6)[\Phi(\ell_1,\ell_2)] = \int \frac{d^D\ell_1}{(2\pi)^D}\int \frac{d^D\ell_2}{(2\pi)^D}\frac{\Phi(\ell_1,\ell_2)}{\ell_1^2(\ell_1-K_1)^2(\ell_1-K_{12})^2\ell_2^2(\ell_2-K_5)^2(\ell_2-K_{45})^2(\ell_1+\ell_2+K_6)^2}\,, \tag{5.1}$$

where we denoted the numerator polynomial by $\Phi(\ell_1,\ell_2)$. The momentum flow conventions are shown in fig. 5.1. For technical reasons, we continue to evaluate unitarity cuts in $D = 4$ dimensions.

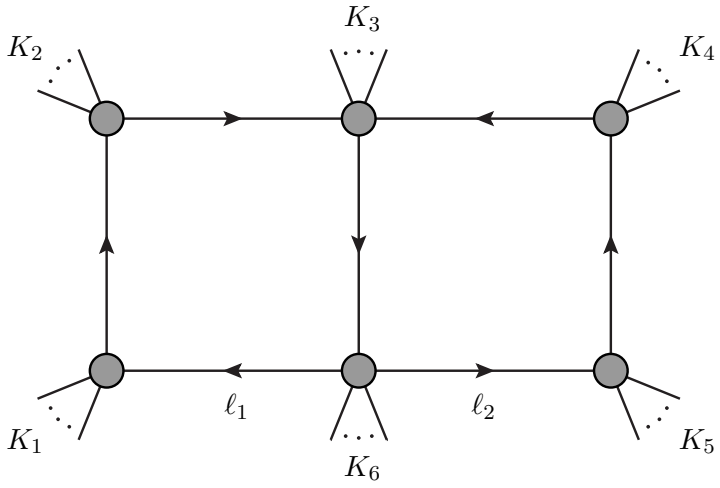

Figure 5.1: The planar double-box diagram with an arbitrary number of external outgoing momenta.

In order to simplify and linearize as many as possible of the hepta-cut equations,

$$\ell_1^2 = (\ell_1-K_1)^2 = (\ell_1-K_{12})^2 = 0\,, \tag{5.2}$$
$$\ell_2^2 = (\ell_2-K_5)^2 = (\ell_2-K_{45})^2 = 0\,, \tag{5.3}$$
$$(\ell_1+\ell_2+K_6)^2 = 0\,, \tag{5.4}$$

the loop momenta may be expanded in a momentum basis constructed from flat projections of some of the external momenta, say $(K_1^\flat, K_2^\flat)$ and $(K_4^\flat, K_5^\flat)$, along the lines of sec. 3.2.5. More specifically,

$$\ell_1^\mu = \alpha_1 K_1^{\mu,\flat} + \alpha_2 K_2^{\mu,\flat} + \alpha_3\langle K_1^\flat|\gamma^\mu|K_2^\flat] + \alpha_4\langle K_2^\flat|\gamma^\mu|K_1^\flat]\,, \tag{5.5}$$
$$\ell_2^\mu = \beta_1 K_4^{\mu,\flat} + \beta_2 K_5^{\mu,\flat} + \beta_3\langle K_4^\flat|\gamma^\mu|K_5^\flat] + \beta_4\langle K_5^\flat|\gamma^\mu|K_4^\flat]\,, \tag{5.6}$$

where the massless momenta are defined as follows,

$$K_1^{\mu,\flat} = \frac{K_1^\mu - (S_1/\gamma_1)K_2^\mu}{1-S_1S_2/\gamma_1^2}\,, \quad K_2^{\mu,\flat} = \frac{K_2^\mu - (S_2/\gamma_1)K_1^\mu}{1-S_1S_2/\gamma_1^2}\,, \tag{5.7}$$

and similarly for $(K_4^\flat, K_5^\flat)$. In the equations above,

$$\gamma_{1,\pm} = (K_1 \cdot K_2) \pm \sqrt{\Delta_1}\ , \quad \Delta_1 = (K_1 \cdot K_2)^2 - K_1^2 K_2^2\ , \quad S_i \equiv K_i^2\ . \tag{5.8}$$

For simplicity, we start by solving the on-shell constraints (5.2)-(5.3) associated with the six outer-edge propagators, which depend only on either ℓ_1 or ℓ_2. It is straightforward to obtain the desired solution [56],

$$\begin{aligned}
&\alpha_1 = \frac{\gamma_1(S_2+\gamma_1)}{\gamma_1^2 - S_1 S_2}\ , \qquad \alpha_2 = \frac{S_1 S_2 (S_1+\gamma_1)}{\gamma_1(S_1 S_2 - \gamma_1^2)}\ , \quad \alpha_3\alpha_4 = -\frac{S_1 S_2 (S_1+\gamma_1)(S_2+\gamma_1)}{4(\gamma_1^2 - S_1 S_2)^2}\ , \\
&\beta_1 = \frac{S_4 S_5 (S_5+\gamma_2)}{\gamma_2(S_4 S_5 - \gamma_2^2)}\ , \quad \beta_2 = \frac{\gamma_2(S_4+\gamma_2)}{\gamma_2^2 - S_4 S_5}\ , \qquad \beta_3\beta_4 = -\frac{S_4 S_5 (S_4+\gamma_2)(S_5+\gamma_2)}{4(\gamma_2^2 - S_4 S_5)^2}\ .
\end{aligned} \tag{5.9}$$

The on-shell equation (5.4) for the middle-rung propagator $1/(\ell_1+\ell_2+K_6)^2$ now involves a quartic polynomial that is quadratic in two variables, for instance, α_4 and β_4. The naive solution of β_4 as a function of α_4 takes the form,

$$\beta_4 = \frac{A(\alpha_4) + \sqrt{\Delta(\alpha_4)}}{B(\alpha_4)}\ , \tag{5.10}$$

where A, B, and Δ are rational functions of α_4.

The hepta-cut double-box integral is easily evaluated by means of nondegenerate multivariate residues. Including the Jacobians associated with the change of variables from the loop momenta to the parametrization (5.6), we arrive at the result [56, 67],

$$\begin{aligned}
&P_{2,2}(K_1,\ldots,K_6)[\Phi(\ell_1,\ell_2)]\big|_{7-\text{cut}} = \\
&\qquad \frac{\gamma_1\gamma_2}{32(\gamma_1^2 - S_1 S_2)(\gamma_2^2 - S_4 S_5)} \oint d\alpha_4 \frac{\Phi(\alpha_4)}{\sqrt{\Delta(\alpha_4)}}\ ,
\end{aligned} \tag{5.11}$$

where $\Delta = \alpha_4^2(B_0(\alpha_4)^2 - 4B_1(\alpha_4)B_{-1}(\alpha_4))$ for rational functions B_1, B_0 and B_{-1} defined as follows,

$$\begin{aligned}
B_1(\alpha_4) &= \langle K_4^\flat | \gamma^\mu | K_5^\flat] \Big(\alpha_1 K_{1,\mu}^\flat + \alpha_2 K_{2,\mu}^\flat + K_{6,\mu} \\
&\qquad + \alpha_3 \langle K_1^\flat | \gamma_\mu | K_2^\flat] + \alpha_4 \langle K_2^\flat | \gamma_\mu | K_1^\flat] \Big)\ ,
\end{aligned} \tag{5.12}$$

$$\begin{aligned}
B_0(\alpha_4) &= \Big(\beta_1 K_4^{\mu,\flat} + \beta_2 K_5^{\mu,\flat} + K_6^\mu \Big) \\
&\qquad \times \Big(\alpha_1 K_{1,\mu}^\flat + \alpha_2 K_{2,\mu}^\flat + \alpha_3 \langle K_1^\flat | \gamma_\mu | K_2^\flat] \\
&\qquad + \alpha_4 \langle K_2^\flat | \gamma_\mu | K_1^\flat] + K_{6,\mu} \Big) - \frac{1}{2} S_6\ ,
\end{aligned} \tag{5.13}$$

$$\begin{aligned}
B_{-1}(\alpha_4) &= -\frac{S_4 S_5 (S_4+\gamma_2)(S_5+\gamma_2) \langle K_5^\flat | \gamma^\mu | K_4^\flat])}{4(\gamma_2^2 - S_4 S_5)^2} \\
&\qquad \times \Big(\alpha_1 K_{1,\mu}^\flat + \alpha_2 K_{2,\mu}^\flat + \alpha_3 \langle K_1^\flat | \gamma_\mu | K_2^\flat] + \alpha_4 \langle K_2^\flat | \gamma_\mu | K_1^\flat] \Big)\ .
\end{aligned} \tag{5.14}$$

We remind the reader that in eqs. (5.12)-(5.14) it is understood that expressions for $\alpha_1, \alpha_2, \alpha_3$ and $\beta_1, \beta_2, \beta_3$ are those obtained by solving the bowtie hexa-cut equations, see eq. (5.9).

The structure of the four roots $(e_1, \ldots, e_4)$ of the radicand Δ is rather complicated, but fortunately it is not necessary to solve for them analytically. Indeed, for our purposes it suffices to verify numerically that the roots are in fact distinct for generic external kinematics. Consequently, $\eta^2 = \Delta$ defines a *nondegenerate* elliptic curve.

5.1.2 Internal Masses

We claim that the maximal cuts of the planar double-box integral with (i) internal masses throughout the diagram and only four massless external legs and (ii) 10 external massless particles are equivalent from a mathematical point of view; both of them define a nondegenerate elliptic curve.

Without loss of main features[1] of the calculation, we may assume that the six outer-edge propagators have mass m_1, while the mass of the particle propagating in the middle-rung is m_2. The external kinematics thus depends on just four invariants, namely s, t, m_1, m_2.

In order to prove the above assertion, let us examine the hepta-cut equations with internal masses,

$$\ell_1^2 - m_1^2 = (\ell_1 - k_1)^2 - m_1^2 = (\ell_1 - K_{12})^2 - m_1^2 = 0 \,, \tag{5.15}$$

$$\ell_2^2 - m_1^2 = (\ell_2 - k_4)^2 - m_1^2 = (\ell_2 - K_{34})^2 - m_1^2 = 0 \,, \tag{5.16}$$

$$(\ell_1 + \ell_2)^2 - m_2^2 = 0 \,, \tag{5.17}$$

using the loop-momentum parametrization,

$$\ell_1^\mu = \alpha_1 k_1^\mu + \alpha_2 k_2^\mu + \alpha_3 \frac{s}{2} \frac{\langle 1|\gamma^\mu|2]}{\langle 14\rangle[42]} + \alpha_4 \frac{s}{2} \frac{\langle 2|\gamma^\mu|1]}{\langle 24\rangle[41]} \,, \tag{5.18}$$

$$\ell_2^\mu = \beta_1 k_3^\mu + \beta_2 k_4^\mu + \beta_3 \frac{s}{2} \frac{\langle 3|\gamma^\mu|4]}{\langle 31\rangle[14]} + \beta_4 \frac{s}{2} \frac{\langle 4|\gamma^\mu|3]}{\langle 41\rangle[13]} \,. \tag{5.19}$$

Following the strategy outlined above, we start by solving the equations for the bowtie-shaped hexa-cut. In analogy with eq. (5.9) this quickly leads to the solution,

$$\begin{aligned} &\alpha_1 = 1 \,, && \alpha_2 = 0 \,, && \alpha_3\alpha_4 = \frac{m_1^2 t(s+t)}{s^3} \,, \\ &\beta_1 = 0 \,, && \beta_2 = 1 \,, && \beta_3\beta_4 = \frac{m_1^2 t(s+t)}{s^3} \,. \end{aligned} \tag{5.20}$$

The middle-rung propagator is again a quartic polynomial which is quadratic in, say, α_4 and β_4; solving the on-shell constraint exactly yields a result of the form (5.10), with the functions A and B given by

$$A(\alpha_4) = -s^2 t \left(a_4 s^2 \left(2m_1^2 - m_2^2 + t \right) + a_4^2 s^3 + m_1^2 t(s+t) \right) \,, \tag{5.21}$$

$$B(\alpha_4) = 2s^3 \left(a_4^2 s^3 + a_4 s^2 t + m_1^2 t^2 \right) \,. \tag{5.22}$$

Put differently, the maximal cut gives rise to an elliptic curve.

5.2 Weierstrass' Elliptic Functions

The principal mathematical prerequisite for this chapter is the theory of elliptic curves and elliptic functions. Standard references are for instance text books by Silverman [116] and Whittaker [117]. For the benefit of readers who are unfamiliar with this material, a brief review of Weierstrass' elliptic functions is provided in this section.

In complex analysis, an elliptic function is defined as a meromorphic function which is doubly-periodic.[2] Let us recall that for a nonconstant meromorphic function f of a single complex variable z, periodicity is expressed as

$$\forall z \in \mathbb{C} : f(z + 2\omega) = f(z) \,, \tag{5.23}$$

[1] In fact, a uniform internal mass is sufficient.

[2] A doubly-periodic holomorphic function is constant.

and $\omega \in \mathbb{C}$ is called the half-period of f. The set of all periods of f forms a lattice structure Λ, that can be either

- trivial, $\Lambda = \{0\}$,
- simple, $\Lambda = \{2n\omega \,|\, n \in \mathbb{Z}\}$,
- double, $\Lambda = \{2n_1\omega_1 + 2n_2\omega_2 \,|\, n_1, n_2 \in \mathbb{Z}\}$.

The simplest example of a singly-periodic function is perhaps the complex exponential function, $\exp z$, whose half-period is $\omega = \pi i$. In the remainder of this chapter, we will frequently encounter the doubly-periodic meromorphic Weierstrass $\wp$-function, which has the series representation,

$$\wp(z) = \frac{1}{z^2} + \sum_{n_1,n_2=-\infty}^{\infty} \left(\frac{1}{(z - 2n_1\omega_2 - 2n_2\omega)^2} - \frac{1}{(2n_1\omega_1 + 2n_2\omega_2)^2} \right) , \tag{5.24}$$

The periodic lattice is

$$\Lambda = \{2n_1\omega_1 + 2n_2\omega_2 \,|\, n_1, n_2 \in \mathbb{Z}\} , \tag{5.25}$$

with half-periods ω_1, ω_2 such that $\omega_1/\omega_2 \notin \mathbb{R}$.

5.2.1 Periods and Inverse Functions

Inverse functions of periodic functions are in general multivalued functions. For example, the inverse function of the exponential function, $w = \exp z$, is the natural logarithm, $z = \ln w$. Similarly, for the Weierstrass $\wp$-function, $w = \wp(z)$, the inverse function is an *elliptic integral*,

$$z = \int_w^{\infty} \frac{dx}{\sqrt{4x^3 - g_2x - g_3}} , \quad g_2 = 60 \sum_{\omega\in\Lambda\setminus\{0\}} \frac{1}{\omega^4} , \quad g_3 = 140 \sum_{\omega\in\Lambda\setminus\{0\}} \frac{1}{\omega^6} . \tag{5.26}$$

In these equations, the constants g_2 and g_3 are the Weierstrass invariants and the equation,

$$y^2 = 4x^3 - g_2x - g_3 , \tag{5.27}$$

defines an elliptic curve in the Weierstrass normal form. The elliptic curve is nondegenerate if and only if the modular discriminant is nonzero,

$$\Delta_{\text{mod}} = g_2^3 - 27g_3^2 \neq 0 . \tag{5.28}$$

Periods of elliptic functions can, analogously to the exponential function, be expressed as integrals involving only algebraic functions. The period of the exponential function is

$$\pi i = i \int_{-1}^{1} \frac{dx}{\sqrt{1 - x^2}} \tag{5.29}$$

which is trivially verified by direct integration. We assume that $\Delta_{\text{mod}} > 0$ so that the roots $e_1 > e_2 > e_3$ obtained by solving the cubic equation

$$4t^3 - g_2t - g_3 = 0 \tag{5.30}$$

are purely real. The half-periods ω_1 and ω_2 of the Weierstrass $\wp$-function can then be calculated as

$$\omega_1 = \int_{e_1}^{e_2} \frac{dx}{\sqrt{4x^3 - g_2x - g_3}} , \quad \omega_2 = \int_{e_3}^{e_2} \frac{dx}{\sqrt{4x^3 - g_2x - g_3}} . \tag{5.31}$$

5.2.2 Identities and Differential Equations

We are primarily interested in nondegenerate elliptic curves over the field of complex numbers, governed by the Weierstrass equation,

$$y^2 = 4x^3 - g_2 x - g_3 \ , \quad g_2^3 - 27 g_3^2 \neq 0 \ , \tag{5.32}$$

where g_2, g_3 are called the modular invariants. This elliptic curve is topologically equivalent to a genus-1 Riemann surface that is naturally parametrized by the Weierstrass $\wp$-function along with its first derivative. Indeed, the ordinary differential equation

$$\wp'(z; g_2, g_3)^2 = 4\wp(z; g_2, g_3)^3 - g_2 \wp(z; g_2, g_3) - g_3 \tag{5.33}$$

is precisely of the form (5.27). This fact will prove very advantageous in what follows.

Recall that Weierstrass' $\wp$-function is uniquely fixed once either g_2, g_3 or the half-periods ω_1, ω_2 are specified. For compactness we will therefore just write $\wp(z)$ from now on.

An essential property of Weierstrass' $\wp$-function is that it obeys the so-called addition law, which can be stated as follows,

$$\wp(z) + \wp(w) + \wp(z+w) = \frac{1}{4}\left(\frac{\wp'(z) - \wp'(w)}{\wp(z) - \wp(w)}\right)^2 \ , \tag{5.34}$$

where $z, w \in \mathbb{C}$ are chosen arbitrarily. The quantity in the parenthesis on the right hand side of eq. (5.34) appears frequently in the calculations below, hence we define the function

$$\varphi(z, w) \equiv \frac{1}{2}\frac{\wp'(z) - \wp'(w)}{\wp(z) - \wp(w)} \ . \tag{5.35}$$

It is important to note that this function can be expressed as a linear combination of Weierstrass ζ-functions,

$$\varphi(z, w) = \zeta(z+w) - \zeta(z) - \zeta(w) \ , \tag{5.36}$$

with $\zeta'(z) = -\wp(z)$. Now, differentiating both sides of eq. (5.36) with respect to z immediately gives the relation

$$\frac{d}{dz}\varphi(z, w) = \wp(z) - \wp(z+w) \ . \tag{5.37}$$

Finally, we also need to introduce Weierstrass' σ-function. We can define it for example through a logarithmic derivative,

$$\frac{d}{dz}\log\sigma(z) = \zeta(z) \ . \tag{5.38}$$

The Weierstrass σ-function obeys the periodicity relation,

$$\sigma(z + 2\omega_k) = -e^{2\eta_k(z+\omega_k)}\sigma(z) \ , \quad \eta_k \equiv \zeta(\omega_k) \ , \tag{5.39}$$

which we will not prove here.

5.3 The Weierstrass Parametrization

The quartic radicand Δ that arises in the integrand of the maximally-cut double-box integral is conveniently reexpressed as

$$\Delta = q_0(\alpha_4 - q)^4 + 6q_2(\alpha_4 - q)^2 + 4q_3(\alpha_4 - q) + q_4 \tag{5.40}$$

where the constant q has been introduced in order to remove the cubic term from the polynomial. Explicitly,

$$q = -\frac{1}{2}\left(\frac{t}{s} - \frac{m_2^2}{s - 4m_1^2}\right) . \tag{5.41}$$

We can now set $\eta^2 = \Delta$ and apply a suitably chosen birational transformation to the elliptic curve in eq. (5.40) to gain more insight into the structure of the maximal cut of the double-box integral with internal masses. More specifically, the transformation

$$x = \frac{q_0(\alpha_4 - q)^2 + \eta\sqrt{q_0} + q_2}{2q_0} , \tag{5.42}$$

$$y = \frac{(\alpha_4 - q)\left(q_0(\alpha_4 - q)^2 + \eta\sqrt{q_0} + 3q_2\right) + q_3}{q_0} \tag{5.43}$$

brings the elliptic curve in question into the Weierstrass standard form (5.27) with the modular invariants

$$g_2 = \frac{3q_2^2 + q_0q_4}{q_0^2} , \quad g_3 = -\frac{q_2^3 - q_0q_2q_4 + q_0q_3^2}{q_0^3} . \tag{5.44}$$

This can be verified by direct calculation and we encourage the interested reader to do so. In particular, the inverse of the transformation in eq. (5.43) is

$$\alpha_4 = \frac{1}{2}\frac{y - q_3/q_0}{x + q_2/q_0} + q , \quad \eta = \sqrt{q_0}\left(2x - \frac{q_2}{q_0} - \frac{1}{4}\left(\frac{y - q_3/q_0}{x + q_2/q_0}\right)^2\right) . \tag{5.45}$$

The crucial step is now to introduce a complex variable z for the torus associated with the Weierstrass elliptic curve,

$$x = \wp(z) , \quad y = \wp'(z) , \tag{5.46}$$

which readily leads to

$$\alpha_4(z) = \frac{1}{2}\frac{\wp'(z) - q_3/q_0}{\wp(z) + q_2/q_0} + q , \tag{5.47}$$

$$\eta(z) = \sqrt{q_0}\left(2\wp(z) - \frac{q_2}{q_0} - \frac{1}{4}\left(\frac{\wp'(z) - q_3/q_0}{\wp(z) + q_2/q_0}\right)^2\right) . \tag{5.48}$$

The Weierstrass parametrization may be further simplified by defining a constant u with the properties

$$\wp(u) = -q_2/q_0 , \quad \wp'(u) = q_3/q_0 . \tag{5.49}$$

Note that u is uniquely determined from the fact that $(x, y) = (-q_2/q_0, q_3/q_0)$ is indeed a point on the elliptic curve. Invoking the addition law (5.34) leaves us with the very compact result,

$$\eta(z) = \sqrt{q_0}(\wp(z) - \wp(z + u)) , \quad \alpha_4(z) = \varphi(z, u) + q , \tag{5.50}$$

where φ is defined in eq. (5.35).

Let us now investigate the implications of the Weierstrass parametrization for the maximally-cut scalar double-box integral. Thanks to eq. (5.37) it is immediately clear that

$$\frac{d}{dz}\alpha_4(z) = \frac{1}{\sqrt{q_0}}\eta(z) \tag{5.51}$$

which remarkably trivializes the integrand of the cut double box,

$$I[1]\big|_{7-\text{cut}} \propto \oint \frac{d\alpha_4}{\sqrt{\Delta}} = \frac{1}{\sqrt{q_0}} \oint dz \ . \tag{5.52}$$

5.3.1 Chiral Insertions and Global Poles

Evaluated on the hepta-cut, a generic double-box numerator function is a polynomial in $\alpha_3(z)$, $\alpha_4(z)$, $\beta_3(z)$ and $\beta_4(z)$. The two ISPs (see sec. 3.1.2) are conventionally chosen to be $\ell_1 \cdot k_4$ and $\ell_2 \cdot k_1$. A short exercise shows that

$$\ell_1 \cdot k_4 = \frac{1}{2}(\alpha_3 s + \alpha_4 + s + t) \ , \quad \ell_2 \cdot k_1 = \frac{1}{2}(\beta_3 s + \beta_4 + s + t) \ . \tag{5.53}$$

Accordingly before we can shed light on the question of uniqueness of master integral projectors, it is necessary to work out the Weierstrass parametrization of the remaining three chiral[3] insertions, α_3, β_3 and β_4. Recall from eq. (5.45) that

$$\frac{1}{\alpha_4} = \frac{1}{\frac{1}{2}\frac{y-q_3/q_0}{x+q_2/q_0} + q} \ . \tag{5.54}$$

By partial fractioning,

$$\alpha_3 = \frac{m_1^2 t(s+t)}{s_3 \alpha_4} = \frac{1}{2}\bigg(- \frac{y-y_3}{x-x_3} + \frac{y-y_4}{x-x_4}\bigg) \ , \tag{5.55}$$

where

$$x_3 = \frac{s^2(m_2^2-t)^2 + 16m_1^4 t(s+t) - 4m_1^2 s(m_2^2 s + t(s+2t))}{12s^3(s-4m_1^2)} \ , \tag{5.56}$$

$$x_4 = \frac{s^2(m_2^2-t)^2 - 32m_1^4 t(s+t) + 4m_1^2 s(t(2s+t) - m_2^2 s)}{12s^3(s-4m_1^2)} \ , \tag{5.57}$$

and

$$y_3 = 0 \ , \quad y_4 = -\frac{m_1^2 t(s+t)(m_2^2 s + 4m_1^2 t - st)}{s^4(4m_1^2 - s)} \ . \tag{5.58}$$

The points (x_3, y_3) and (x_4, y_4) lie on the elliptic curve and therefore we define constants z_3 and z_4 such that

$$\wp(z_3) = x_3 \ , \quad \wp'(z_3) = -y_3 \ , \quad \wp(z_4) = x_4 \ , \quad \wp'(z_4) = -y_4 \ . \tag{5.59}$$

This means that $z = z_3$ and $z = z_4$ are the two poles of $\alpha_3(z)$, and equivalently the two zeros of $\alpha_4(z)$. It turns out that z_3 and z_4 are related to the poles of $\alpha_4(z)$ by half-period shifts,

$$z_3 = \omega_1 + \omega_2 = z_1 + \omega_1 + \omega_2 \ , \tag{5.60}$$

$$z_4 = z_2 + \omega_1 + \omega_2 \ . \tag{5.61}$$

[3]Chiral here refers to the fact that e.g. $\alpha_4 \propto \langle 1|\ell_1^\mu|2]$ and $\beta_4 \propto \langle 3|\ell_2^\mu|4]$.

An explicit Laurent expansion order-by-order surprisingly shows that

$$\alpha_3(z) = \alpha_4(z - z_3) = \alpha_4(z - \omega_1 - \omega_2) \,, \tag{5.62}$$

so in words, $\alpha_3(z)$ is also simply a shift of $\alpha_4(z)$.

This pattern remarkably extends also to $\beta_3(z)$ and $\beta_4(z)$. We find that

$$\beta_4 = \frac{A(\alpha_4) + \sqrt{\Delta(\alpha_4)}}{B(\alpha_4)} = \frac{1}{2}\left(\sqrt{\frac{(s-4m_1^2)t^2}{s^3}} - \frac{t}{s} - \frac{y-y_5}{x-x_5} + \frac{y-y_6}{x-x_6}\right) . \tag{5.63}$$

where (x_5, y_5) and (x_6, y_6) are again points on the elliptic curve. Explicitly,

$$x_5 = \frac{s^2\left(t-m_2^2\right)^2 + 16m_1^4 t(t-2s) + 4m_1^2 s\left(2t(s-t) - m_2^2(s-3t)\right)}{12s^3\left(s-4m_1^2\right)} \,, \tag{5.64}$$

$$y_5 = \frac{m_1^2\left(-4m_1^2 + m_2^2 + s\right)\sqrt{s^9t^2\left(s-4m_1^2\right)}\left(s\left(t-m_2^2\right) - 4m_1^2 t\right)}{s^8\left(s-4m_1^2\right)^2} \,, \tag{5.65}$$

and likewise for the other pair. If we now set $\wp(z_5) = x_5$, $\wp'(z_5) = -y_5$, $\wp(z_6) = x_6$ and $\wp'(z_6) = -y_6$, the poles of $\beta_4(z)$ are z_5 and z_6. We have verified that $z_6 = z_5 + z_2$ and

$$\beta_4(z) = \alpha_4(z - z_5) \,. \tag{5.66}$$

Furthermore, if z_7 and z_8 are the two poles of $\beta_3(z)$,

$$z_7 = z_5 + \omega_1 + \omega_2 \,, \tag{5.67}$$

$$z_8 = z_6 + \omega_1 + \omega_2 = z_5 + z_2 + \omega_1 + \omega_2 \,. \tag{5.68}$$

Finally, by comparing the Laurent expansions order by order,

$$\beta_3(z) = \alpha_4(z - z_7) \,. \tag{5.69}$$

This remarkable structure of the locus of poles is demonstrated in fig. 5.2.

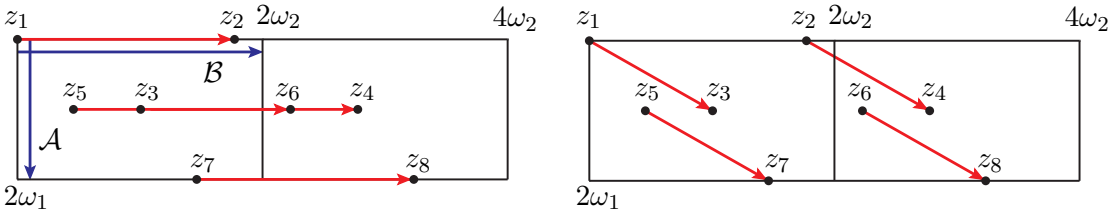

Figure 5.2: The eight poles $(z_1, \ldots, z_8)$ of the numerator factors are here depicted in the underlying of the elliptic functions. The poles are related by shifts, $z_{2i} = z_{2i-1} + z_2$ for $i = 1, 2, 3, 4$ and $z_{i+2} = z_i + \omega_1 + \omega_2$ for $i = 1, 2, 5, 6$.

5.3.2 Periods and Residues

The half-periods of the torus associated with our elliptic curve are ω_1 and ω_2. For the sake of simplicity it is assumed that the internal and external invariants, i.e. the masses m_1 and m_2 of the propagators and the Mandelstam invariants s_{12}, s_{14}, are purely real quantities. In those these circumstances we may choose ω_1 to be purely imaginary and negative and ω_2 to be real and positive.

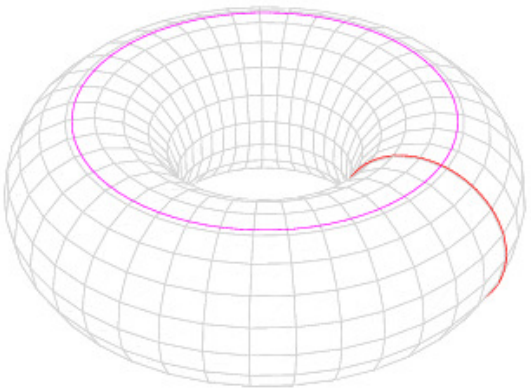

Figure 5.3: An alternative view of the fundamental cycles on the torus.

In order to specify the discussion, the first fundamental cycle $\mathcal{A}$ is defined to be the line from ϵ to $\epsilon + 2\omega_1$, while the second fundamental cycle $\mathcal{B}$ is the line from $-i\epsilon$ to $-i\epsilon + 2\omega_2$. Here, ϵ is a small positive constant. Refer to figs. 5.2-5.3 for illustrations of the fundamental cycles.

Let us consider the completion of the contour for the maximally-cut scalar double-box integral. The integrand is trivial in this case and contains no singularities so there are no residue cycles to examine. By construction, integrating over the fundamental cycles merely produces the two periods,

$$\oint_{\mathcal{A}} dz = 2\omega_1 \ , \quad \oint_{\mathcal{B}} dz = 2\omega_2 \ . \tag{5.70}$$

However, in the generic case with a nontrivial numerator insertion, the fundamental cycle integrations give rise to more complicated expressions involving Weierstrass functions evaluated at certain values. For example, with a $\alpha_4(z)$ insertion,

$$\oint_{\mathcal{A}} dz\alpha_4(z) = 2q\omega_1 + \oint_{\mathcal{A}} dz \frac{1}{2}\frac{\wp'(z) - \wp'(u)}{\wp(z) - \wp(u)} = 2q\omega_1 + 2(u\eta_1 - \omega_1\zeta(u)) \ , \tag{5.71}$$

$$\oint_{\mathcal{B}} dz\alpha_4(z) = 2q\omega_2 + \oint_{\mathcal{B}} dz \frac{1}{2}\frac{\wp'(z) - \wp'(u)}{\wp(z) - \wp(u)} = 2q\omega_2 + 2(u\eta_2 - \omega_2\zeta(u)) \ . \tag{5.72}$$

These results are rather easy to derive. For the sake of definiteness, let us work out the details that lead to eq. (5.71). Using the alternative addition law (5.36) allows us to write

$$\oint_{\mathcal{A}} dz\left(q + \frac{1}{2}\frac{\wp'(z) - \wp'(w)}{\wp(z) - \wp(w)}\right) = \oint_{\mathcal{A}} dz\big(q + \zeta(z+u) - \zeta(z) - \zeta(u)\big) \ . \tag{5.73}$$

The integral over the Weierstrass ζ-functions on the right hand side is now easily evaluated by means of eqs. (5.38)-(5.39). It follows that

$$\begin{aligned} \oint_{\mathcal{A}} dz\big(\zeta(z+u) - \zeta(z) - \zeta(u)\big) &= -2\omega_1\zeta(u) + \log\frac{\sigma(z+u)}{\sigma(z)}\bigg|_{\epsilon}^{\epsilon+2\omega_1} \\ &= -2\omega_1\zeta(u) + \log\frac{\sigma(u+\epsilon+2\omega_1)\sigma(\epsilon)}{\sigma(u+\epsilon)\sigma(\epsilon+2\omega_1)} \\ &= -2(\omega_1\zeta(u) - u\eta_1) \ , \end{aligned} \tag{5.74}$$

which suffices to complete the proof as the integral for the constant term in eq. (5.71) is trivial. This derivation seamlessly applies to the second fundamental cycle by replacing $\omega_1 \to \omega_2$ and $\eta_1 \to \eta_2$.

The $\alpha_4(z)$ insertion gives rise to two simple poles in the integrand as we discussed above. Accordingly, there are two residue cycles with nonvanishing integrations in addition to the two fundamental cycles. We call these cycles $\mathcal{C}_1$ and $\mathcal{C}_2$. The residues are computed by examining the Laurent expansions of $\varphi(z,u)$ around the poles at $z=0$ and $z=-u$. Near $z=0$ and $z=-u$ the function $\varphi(z,u)$ has the respective behaviors

$$\varphi(z,u) = -\frac{1}{z} + \frac{1}{2}\Big(\frac{m_2^2}{s-4m_1^2} - \frac{t}{s}\Big) + \wp(u)z + \mathcal{O}(z^2) \,, \tag{5.75}$$

$$\varphi(z,u) = +\frac{1}{z+u} + \frac{1}{2}\Big(\frac{m_2^2}{s-4m_1^2} - \frac{t}{s}\Big) - \wp(u)(z+u) + \mathcal{O}((z+u)^2) \,. \tag{5.76}$$

Accordingly, the residue cycle integrations yield

$$\oint_{\mathcal{C}_1} dz\alpha_4(z) = -2\pi i \,, \quad \oint_{\mathcal{C}_2} dz\alpha_4(z) = +2\pi i \,, \tag{5.77}$$

which concludes our treatment of the $\alpha_4(z)$ insertion.

The remaining three linear insertions produce no new results compared to the residues and fundamental cycle integrations obtained above. To understand this, recall that $\alpha_3(z)$, $\beta_3(z)$ and $\beta_4(z)$ are all obtained by shifting $\alpha_4(z)$. In particular, this shift clearly leaves the residues and periods invariant. More specifically,

$$\oint_{\mathcal{C}_3} dz\alpha_3(z) = -2\pi i \,, \quad \oint_{\mathcal{C}_4} dz\alpha_3(z) = +2\pi i \,, \tag{5.78}$$

where $\mathcal{C}_3$ and $\mathcal{C}_4$ encircle z_3 and z_4 respectively. Similarly, for $\beta_4(z)$,

$$\oint_{\mathcal{C}_5} dz\beta_4(z) = -2\pi i \,, \quad \oint_{\mathcal{C}_6} dz\beta_4(z) = +2\pi i \,, \tag{5.79}$$

and finally,

$$\oint_{\mathcal{C}_7} dz\beta_3(z) = -2\pi i \,, \quad \oint_{\mathcal{C}_8} dz\beta_3(z) = +2\pi i \,. \tag{5.80}$$

If we define the tensor integral

$$I_{a,b,c,d} \equiv I[\alpha_3^a \alpha_4^b \beta_3^c \beta_4^d] \,, \tag{5.81}$$

the partial results obtained until this point can be summarized as follows,

$$\begin{aligned}
I_{0,0,0,0} &\longrightarrow (2\omega_1, 2\omega_2, 0,0,0,0,0,0,0,0) \,, \\
I_{0,1,0,0} &\longrightarrow (\mathcal{A}_{0,1,0,0}, \mathcal{B}_{0,1,0,0}, -2\pi i, 2\pi i, 0,0,0,0,0,0) \,, \\
I_{1,0,0,0} &\longrightarrow (\mathcal{A}_{1,0,0,0}, \mathcal{B}_{1,0,0,0}, 0,0, -2\pi i, 2\pi i, 0,0,0,0) \,, \\
I_{0,0,0,1} &\longrightarrow (\mathcal{A}_{0,0,0,1}, \mathcal{B}_{0,0,0,1}, 0,0,0,0, -2\pi i, 2\pi i, 0,0) \,, \\
I_{0,0,1,0} &\longrightarrow (\mathcal{A}_{0,0,1,0}, \mathcal{B}_{0,0,1,0}, 0,0,0,0,0,0, -2\pi i, 2\pi i) \,,
\end{aligned} \tag{5.82}$$

where the periods are given by

$$\begin{aligned}
\mathcal{A}_{1,0,0,0} &= \cdots = \mathcal{A}_{0,0,0,1} = 2q\omega_1 + 2(u\eta_1 - \omega_1\zeta(u)) \,, \\
\mathcal{B}_{1,0,0,0} &= \cdots = \mathcal{B}_{0,0,0,1} = 2q\omega_2 + 2(u\eta_2 - \omega_2\zeta(u)) \,.
\end{aligned} \tag{5.83}$$

Note that ω_1 and ω_2 are related by

$$\eta_1\omega_2 - \eta_2\omega_1 = \frac{i\pi}{2} \,. \tag{5.84}$$

5.4 Uniqueness of Projectors

The remaining arbitrary one-dimensional integration contour may be expressed in a overcomplete basis of the first homology group of the z torus with the eight poles excluded. In order to maintain a compact notation, the weights of the two fundamental cycles and the eight residue cycles will be written

$$\mathbf{\Omega} = (\Omega_{\mathcal{A}}, \Omega_{\mathcal{B}}, \Omega_1, \ldots, \Omega_8)^T \,. \tag{5.85}$$

Then for an arbitrary numerator insertion $\Phi(z)$ we define the operation of applying the hepta-cut to the double-box integral and subsequently completing the contour by replacing

$$I[\Phi] \longrightarrow \Omega_{\mathcal{A}} \oint_{\mathcal{A}} dz \Phi(z) + \Omega_{\mathcal{B}} \oint_{\mathcal{B}} dz \Phi(z) + 2\pi i \sum_{j=1}^{8} \Omega_j \operatorname*{Res}_{z=z_j} \Phi(z) \,, \tag{5.86}$$

for weights that are a priori undetermined. According to the Global Residue Theorem discussed in sec. 4.2, only seven of the residues are independent. The extraneous weight is simply set to zero at a later stage when we reduce to a linearly independent basis.

We have used the Mathematica package `FIRE` [103] to generate IBP relations to verify the number of master integrals for the double-box topology with internal masses m_1 and m_2. There are four masters and as we have seen in the previous examples, these are normally chosen to be of the form

$$I_{m,n} \equiv I[(\ell_1 \cdot k_4)^m (\ell_2 \cdot k_1)^n] \,. \tag{5.87}$$

But from a calculational point of view it is much more advantageous to work with master integrals which have chiral numerator insertions instead. A suitable set of linearly independent integrals is for example

$$(I_1, \ldots, I_4) = (I_{0,0,0,0}, I_{0,1,0,0}, I_{0,2,0,0}, I_{0,1,1,0}) \,. \tag{5.88}$$

Evidently, imposing the orthonormality constraints on the master contours leaves five weights to be fixed by other means. Remarkably, it turns out that there are exactly five linearly independent constraints, whose origin are Levi-Civita insertions that integrate to zero on the real slice or left-right symmetry of the double-box diagram in the presence of only four massless external particles. All constraints from IBP reduction are satisfied automatically.

The constraints take the form of a matrix equation

$$M\mathbf{\Omega} = 0 \tag{5.89}$$

and the 10×5 coefficient matrix M is surprisingly simple as it has only has integer entries,

$$M = \begin{pmatrix} 1 & -1 & 0 & 0 & 0 & 0 & 0 & 2 & 0 & -2 \\ 0 & 0 & 1 & 0 & 0 & -1 & 0 & 1 & -1 & 0 \\ 0 & 0 & 0 & 1 & 0 & -1 & 0 & 1 & 0 & -1 \\ 0 & 0 & 0 & 0 & 1 & -1 & 0 & 0 & -1 & 1 \\ 0 & 0 & 0 & 0 & 0 & 0 & 1 & -1 & -1 & 1 \end{pmatrix} . \tag{5.90}$$

Furthermore, we implement the constraint from the Global Residue Theorem by requiring that

$$G\boldsymbol{\Omega} = 0 \,, \quad G = (0,0,0,0,0,0,0,0,0,1) \,. \tag{5.91}$$

Let $\mathcal{M}_i$ denote the ith master contour which extracts I_i and normalizes its cut expression to unity, while respecting the constraints. A clean way of presenting the projectors is via solutions to inhomogeneous matrix equations. To that end we construct the 10×10 matrix F,

$$F = \Big(\begin{array}{cccccc} M & G & I_1 & I_2 & I_3 & I_4 \end{array} \Big)^T \Big|_{\text{aug}} \,. \tag{5.92}$$

Here, the aug subscript implies that the master integrals are evaluated on the hepta-cut with the remaining contour being expanded as in eq. (5.86). Also note that transposition is understood with respect to the six blocks. It is not hard to verify that F has full rank, so all four projectors are uniquely determined. Defining the four 10-tuples $\delta_1, \ldots, \delta_4$ by

$$\Big(\begin{array}{cccc} \delta_1 & \delta_2 & \delta_3 & \delta_4 \end{array} \Big) = \begin{pmatrix} 0 & 0 & 0 & 0 \\ \vdots & \vdots & \vdots & \vdots \\ 0 & 0 & 0 & 0 \\ 1 & 0 & 0 & 0 \\ 0 & 1 & 0 & 0 \\ 0 & 0 & 1 & 0 \\ 0 & 0 & 0 & 1 \end{pmatrix} \,, \tag{5.93}$$

we thus have $\mathcal{M}_i = F^{-1}\delta_i$. Therefore our final formula for the double-box master integral coefficients reads

$$\boxed{c_i = \Omega^{(i)}_{\mathcal{A}} \oint_{\mathcal{A}} dz \prod_{k=1}^{6} A^{\text{tree}}_{(k)}(z) + \Omega^{(i)}_{\mathcal{B}} \oint_{\mathcal{B}} dz \prod_{k=1}^{6} A^{\text{tree}}_{(k)}(z) + 2\pi i \sum_{j=1}^{8} \Omega^{(i)}_{j} \operatorname*{Res}_{z=z_j} \prod_{k=1}^{6} A^{\text{tree}}_{(k)}(z)} \tag{5.94}$$

for $\mathcal{M}_i = (\Omega^{(i)}_{\mathcal{A}}, \Omega^{(i)}_{\mathcal{B}}, \Omega^{(i)}_{1}, \ldots, \Omega^{(i)}_{8})$. This result represents the natural generalization of, say, eq. (3.26) to the case where topological cycles must be taken into account. We remind the reader that the products of tree-level amplitudes in eq. (5.94) are implicitly summed over all internal on-shell states in the theory.

5.5 Exact Meromorphic Differential Forms

Following the resolution on the question of uniqueness of the master integral projectors we present an amazing property, namely the relation between exact meromorphic differential forms and the leading-topology part of planar double-box IBP identities.

Suppose that F is some meromorphic elliptic function and assume regularity of F on $\mathbf{T} \setminus \mathcal{S}$. Recall that $\mathcal{S} = \{z_1, \ldots, z_8\}$ where $z_1, \ldots, z_8$ are the eight poles on the z-torus associated with the maximal cut. Now we can immediately construct an exact differential form on $\mathbf{T}^2 \setminus \mathcal{S}$,

$$dF = f dz \,. \tag{5.95}$$

Stokes' Theorem implies that the one-form in question has vanishing integrations on all cycles on the torus. In particular, dF integrates to zero on both topological cycles,

$$\oint_{\mathcal{A}} dF = \oint_{\mathcal{B}} dF = 0 \tag{5.96}$$

and on all residue cycles,

$$\oint_{\mathcal{C}_i} dF = 0 \,, \quad i = 1, \ldots, 8 \,. \tag{5.97}$$

According to eq. (5.86), the equation

$$I[f] = \cdots \,, \tag{5.98}$$

where the trailing dots hide other integrals with fewer than seven propagators, is an on-shell IBP identity. This is precisely the part of the IBP relation that is typically used to derive the consistency equations for the master contours. Invoking various properties of the Weierstrass functions, we can for example derive the following exact differential forms,

$$d(f_1(\alpha_4)\eta) = \frac{f_1'(\alpha_4)\Delta + \frac{1}{2}f_1(\alpha_4)\Delta'(\alpha_4)}{\sqrt{q_0}} dz \,, \tag{5.99}$$

$$d(f_2(\alpha_4)) = \frac{f_2'(\alpha_4)(B(\alpha_4)\beta_4 - A(\alpha_4))}{\sqrt{q_0}} dz \,, \tag{5.100}$$

where f_1 and f_2 are arbitrary polynomials in α_4. These expressions immediately yield two additional highly nontrivial on-shell IBP equations, namely

$$I[f_1'(\alpha_4)\Delta + \tfrac{1}{2}f_1(\alpha_4)\Delta'(\alpha_4)] = \cdots \,, \tag{5.101}$$

$$I[f_2'(\alpha_4)(B(\alpha_4)\beta_4 - A(\alpha_4))] = \cdots \,. \tag{5.102}$$

In order to demonstrate the strength of relation between exact meromorphic differential forms and IBP identities, take for example the function $f_2(\alpha_4) = \alpha_4$. We almost effortlessly obtain

$$\begin{aligned} &m_1^2 t^2 (s+t) I_{0,0,0,0} + 2s^4 I_{0,2,0,1} + s^3 t I_{0,2,0,0} + 2s^3 t I_{0,1,0,1} \\ &\qquad + s^2 t (2m_1^2 - m_2^2 + t) I_{0,1,0,0} + 2m_1^2 s t^2 I_{0,0,0,1} = \cdots \end{aligned} \tag{5.103}$$

which is a actually rather nontrivial IBP identity to derive by other means, in particular analytically using public computer codes such as `FIRE` [103]. More evidence for the efficiency of the method is easily provided. Since Δ is a quartic polynomial in α_4, the integral $I_{0,3,0,0}$ is clearly reducible in terms of $I_{0,2,0,0}$, $I_{0,1,0,0}$ and $I_{0,0,0,0}$. To be accurate,

$$\begin{aligned} &\left[m_1^2 t(s+t)\left(s\left(t-m_2^2\right) - 4m_1^2 t\right)\right] I_{0,0,0,0} \\ &\quad + \left[s\left(s^2\left(t-m_2^2\right)^2 - 8m_1^4 t(s+t) + 2m_1^2 s\left(t(s-t) - 2m_2^2 s\right)\right)\right] I_{0,1,0,0} \\ &\quad + \left[3s^3\left(s\left(t-m_2^2\right) - 4m_1^2 t\right)\right] I_{0,2,0,0} + 2s^4\left(s - 4m_1^2\right) I_{0,3,0,0} = \cdots \,. \end{aligned} \tag{5.104}$$

Also, $I_{3,0,0,0}$ can be expressed as a linear combination of $I_{2,0,0,0}$, $I_{1,0,0,0}$ and $I_{0,0,0,0}$,

$$\begin{aligned} &\left[m_1^2 t(s+t)\left(s\left(t-m_2^2\right) - 4m_1^2 t\right)\right] I_{0,0,0,0} \\ &\quad + \left[s\left(s^2\left(t-m_2^2\right)^2 - 8m_1^4 t(s+t) + 2m_1^2 s\left(t(s-t) - 2m_2^2 s\right)\right)\right] I_{1,0,0,0} \\ &\quad + \left[3s^3\left(s\left(t-m_2^2\right) - 4m_1^2 t\right)\right] I_{2,0,0,0} + 2s^4\left(s - 4m_1^2\right) I_{3,0,0,0} = \cdots \,, \end{aligned} \tag{5.105}$$

with the same coefficients as in eq. (5.104). Consequently, the leading-topology part of the IBP relation for $I[(\ell_1 \cdot k_4)^3]$ in terms of $I[1]$, $I[(\ell_1 \cdot k_4)]$ and $I[(\ell_1 \cdot k_4)^2]$ is now readily available by combining eqs. (5.104)-(5.105).

The fact that eqs. (5.101)-(5.102) generate the full set of IBP identities without doubled propagators for the planar double-box topology with internal masses on the hepta-cut, suggests that this relation between meromorphic exact forms and IBPs would hold for other two-loop diagrams as well. This could have very important consequences for calculations in practice. In particular, this has potential to lead to an extremely efficient algorithm for generating IBPs analytically.

Conclusion and Outlook 6

The present thesis has reviewed recent advances in the field of two- and three-loop scattering amplitudes reported in a sequence of papers I-V. The philosophy of the developments is completely general and all statements and results obtained here are expected to hold in all gauge theories, in particular QCD. The work comprises several important extensions of the maximal unitarity formalism of refs. [55, 56] along with techniques and mathematical theory from computational algebra which together pave the way for further progress. The conclusion of the thesis is divided into in three headlines.

Nonplanar Integrals and Maximal Unitarity. The first steps towards extending the maximal unitarity method at two loops [55, 56] to integrals with nonplanar topologies were taken by the author in paper I. Although the intermediate calculations are slightly more involved compared to the planar case, we find that all salient features carry over directly to the nonplanar sector. In particular, the master integral projectors were found to be unique, and very compact results were derived. Paper IV extended the analysis to all nonplanar double-box integrals with up to four massive external legs and confirmed an unexpected simplicity [57, 58] that now is believed to be much more general. In summary, papers I and IV has shown that instead of being disconnected calculations, the inequivalent kinematic configurations of the nonplanar double-box integrals are related through an underlying structure that apparently is controlled by the global structure derived from the maximal unitarity cut.

Multivariate Residues and Maximal Unitarity. Paper II presented the first steps towards developing an extended framework that works for multiloop amplitude contributions, whose maximal cuts define multidimensional algebraic varieties. The technique is seemlingly valid to higher orders in perturbation theory, but was here explicitly demonstrated at three loops in gauge theories with an arbitrary number of adjoint fermions and scalars. We formulated the problem in terms of degenerate and nondegenerate multivariate residues and showed how to solve the problem via computational algebraic geometry. The principal results are unique projectors for all master integral coefficients for the triple-box topology with four massless external legs. The ideas and techniques described in paper II were applied also to two-loop integrals in paper III. In particular, an extended notion of generalized unitarity cuts that accommodate multiloop integrals with higher powers of propagators was given. Previously, such integrals appeared to be incompatible with generalized unitarity.

Elliptic Functions and Maximal Unitarity. Paper V presented the to this date most nontrivial addition to the body of evidence of the uniqueness conjecture of

projectors for two-loop master integrals. Zhang and the present author gave a practical exhibition on how to use Weierstrass' elliptic functions to parametrize maximal cuts that are associated with irreducible elliptic curves. As a phenomenologically relevant example a unique and compact prescription for the two-loop planar double-box contribution with internal massive lines was derived. Paper V also explained how to extract the leading-topology part of otherwise infeasible IBP relations analytically from exact meromorphic differential forms. The calculations presented in paper V revealed an intimate connection between algebraic geometry and multivariate complex analysis and the structure of maximal cuts; this interplay may lead to important implications for practical calculations in the future.

6.1 Future Directions

The intriguing developments and results achieved in this thesis spawn a host of new exciting directions in the area of generalized unitarity to explore over the next couple of years.

The most important extension that remains is to formalize maximal cuts of planar and nonplanar two-loop integrals in D dimensions. We expect that multivariate residues can be generalized to arbitrary dimensions by analytic continuation. Alternatively it could be useful to work with a basis with coefficients that are independent of the dimensional regulator [66]. More specifically, a consistent and efficient framework that works in D dimensions will allow us to compute complete results for scattering amplitudes at two loops, to gradually meet the acute demand for precise theoretical predictions from the LHC at CERN.

Calculating full amplitudes requires that we are able to capture the contributions from all integrals in a two-loop basis. In addition to planar and nonplanar double boxes, this basis will contain integrals with fewer than seven propagators at four points, such as bowtie, butterfly and slashed-box integrals. In general, the basis will also contain integrals with eight propagators. At two loops, integrals with more than eight propagators, or more than four propagators involving only one of the loop momenta, can be expressed in terms of simpler integrals [53]. A complete survey of octa-cuts and higher-point integrals and hexa-cuts, penta-cuts etc. of lower-point integrals will hopefully lead to compact expressions for all integral coefficients, expressed solely as a function of tree-level input. The appearance of numerous basis integrals poses an immediate complication. However, we hope that the freedom in completing the cut integral can be exploited to in a sense derive contours that are orthogonal to each other and thus only pick up a single basis integral. The theory of degenerate multivariate residues is likely to find application in solving these problems. It may be advantageous to calculate the multivariate residues by means of the Bezoutian matrix method. Indeed, for typical planar and nonplanar examples at two loops with and without doubled propagators, the Bezoutian matrix method is considerably faster than the transformation law [62].

Another very important next step is to work out the projectors for the basis integrals contributing to scattering of five massless particles. Some of the integrals are pentaboxes, turtle boxes, one-mass double boxes and related nonplanar diagrams. Results for $2 \to 3$ gluon scattering are highly important for phenomenological reasons. We also believe that a generalization beyond four external particles will offer new insight in the uniqueness of projectors [65]. It is our impression that multivariate residues and the appearance of nonhomologous integration contours will be decisive [64].

The global structure of maximal cuts appears to hide surprisingly rich information

about the arrangement of and relations between global poles and the associated multivariate residues. It is of course desirable to gain an understanding of the nature of the constraints imposed on the projectors by IBP relations in vast detail. On the other hand, the parity-odd constraints are very intuitive. Is it possible to fully determine the constraints from the underlying algebraic geometry and algebraic topology without reference to integral reduction identities? The unexpected systematics of the IBP constraints observed in the planar [55, 57, 58] and nonplanar sectors [59, 62] leave us with a well-founded hope. In fact, recent progress shows that discrete symmetries derived from the global structure to some extent determine the IBP constraints for the planar double-box diagram. However, these symmetries seem to be less constraining for more complicated problems. It will be fascinating to see if future investigations will allow us to trivialize the projectors by an appropriate representation of the planar and nonplanar two-loop integrals, for example with chiral numerator insertions that by construction vanish on most of the global poles and thus produce only a few nonzero residues [56].

It would be very interesting to understand the structure of maximal cuts which define not only nondegenerate elliptic curves, but also genuine hyperelliptic curves, for example from the nonplanar double-box diagram. More generally, we are enthusiastic about applying principles of algebraic geometry to examine the global structure of topologically nontrivial surfaces generated by more complicated generalized unitarity cuts of two- and three-loop integrals. The techniques reported in refs. [79, 80] may become increasingly valuable over the next years. Given that the Weierstrass parametrization is so powerful for the genus-1 problem, we are curious to understand how these ideas can be applied more generally. Abelian functions which are generalizations of elliptic functions (also called hyperelliptic functions) will ostensibly play a role of significance.

As previously alluded, the planar double-box contributions to (1) massless 10-particle scattering and (2) four-gluon scattering with internal massive particles are mathematically equivalent. Our method based on Weierstrass' elliptic functions and meromorphic differential forms demonstrated explicitly for (2) presumably carries over directly to (1), with minor adjustments along the way. We expect that the relation between meromorphic exact forms and IBP relations would find application for other two-loop diagrams than the planar double box. It may lead to a highly efficient analytic IBP algorithm and this could have a major impact on our ability for derive master integral projectors without relying on input from memory consuming computer codes such as `FIRE` [103] and `Reduze` [104, 105]. A closely related problem that naturally comes to mind is to investigate and precisely quantify the relation between maximal cuts and evaluation of master integrals. For example, the maximal cut of the two-loop double-box integral which contains no chiral vertices is associated with an elliptic curve. The presence of an elliptic curve presumably reflects that this integral cannot be expressed in terms of polylogarithms solely.

We feel that it may be possible to examine the UV properties of supergravity theories by applying the ideas presented in this thesis. The conjectured color/kinematics duality of gauge theory and double-copy structure of gravity theories [93–95] could maybe be rephrased in terms of multivariate residues and thus allow us to shortcut certain loop-level calculations.

The problems suggested above provide avenues for discovering further pathbreaking relations between areas of modern mathematics and quantum field theory scattering amplitudes at the multiloop level.

Acknowledgements

It has been an immense pleasure to work with and study theoretical physics at the Niels Bohr Institute and Niels Bohr International Academy throughout the last more than eight years. Accordingly I would like to thank everyone here for contributing to a highly stimulating academic environment and a great social atmosphere.

I am indebted to my academic advisors at the Niels Bohr International Academy, Poul Henrik Damgaard and Emil Bjerrum-Bohr, who have provided me with absolutely outstanding possibilities both scientifically and financially. Thank you for your guidance, encouragement, patience and numerous invaluable stimulating discussions reaching all the way back to my undergraduate studies. I find myself extraordinaly privileged for the chances I have been given.

I feel delighted to thank my outstanding collaborators Rijun Huang, Henrik Johansson, David Kosower, Kasper Larsen and foremost Yang Zhang, whom I owe much gratitude for acting as a mentor for me.

A special thank to goes to Zvi Bern for advice and encouraging remarks during my visit at UCLA, February through April 2013, and to the Theoretical Elementary Particle Physics group there, in particular Scott Davies and Josh Nohle for hospitality and a warm welcome. I am happy to have learned the duality between color and kinematics under your supervision and for the invitation to carry out research along these lines.

It is a pleasure to thank David Kosower for collaboration and for inviting me to participate in several research projects while I was visiting Institut de Physique Theorique, CEA Saclay, January through April 2014, and again in June 2014. I am grateful to you for sharing your enourmous knowledge and deep insights in scattering amplitudes through many discussions. Moreover, I thank Samuel Abreu, Ruth Britto, Rijun Huang, Alexander Ochirov and Pierre Vanhove at IPhT for delightful conversations and hospitality.

I owe gratitude to Lance Dixon. Thank you for hospitality during my visit at SLAC National Accelerator Laboratory, Stanford University, in September 2014 and not least for introducing me to cutting edge calculations of scattering amplitudes in maximally supersymmetric Yang-Mills theory. It is an honour to have been given the opportunity to work on an ambitious project in this direction.

I have benefitted from a strong profile in amplitude physics at the Niels Bohr International Academy and accordingly I send thanks to former and current members Simon Badger, Simon Caron-Huot, Tristan Dennen, Hjalte Frellesvig, Rijun Huang, Ricardo Monteiro, Donal O'Connell, Thomas Søndergaard and Yang Zhang. Moreover, I acknowledge the group of PhD students in the theoretical high energy group at the Niels Bohr Institute and in particular my former office mate, Hjalte Frellesvig.

I have enjoyed the teaching tasks given to me at the Niels Bohr Institute while

enrolled as a PhD student and I acknowledge Jørgen Beck Hansen, Mogens Dam, Poul Henrik Damgaard, Joachim Mathiesen and Kim Splittorf for pleasant collaboration. In particular, I would like to thank Joachim Mathiesen for giving me the opportunity to present a series of lectures on complex analysis.

I am grateful for invitations to present parts of the work described in this thesis at ETH Zürich, Freiburg University and twice at UCLA. Furthermore, it has been instructive to give talks at various PhD schools. Also, the Amplitude Journal at the Niels Bohr International Academy and the High Energy Theory Journal Club and the Niels Bohr Institute have provided appreciated venues for several talks related to the subject of this thesis.

During my PhD studies I have participated in a broad range of schools, conferences and workshops including the Cargese Summer School in June 2012, Physics and Geometry of Scattering Amplitudes at Stony Brook University in December 2013, Amplitudes at IPhT, CEA Saclay, in June 2014 just to mention a few. I would like to thank the organizers and participants for many pleasant and stimulating moments.

Helle Kiilerich, administrative coordinator at the Niels Bohr International Academy, deserves a warm thank for taking care of a widespread of practical things and for her always fantastic nature.

I acknowledge the Niels Bohr Institute, the Niels Bohr International Academy, the Discovery Center and the Lundbeck Foundation for funding my PhD studies.

A special thanks goes to Rasmus Larsen for friendship, enlightening discussions and brilliant collaborations throughout our education at the Niels Bohr Institute.

Thank you, Karen and Mette.

March, 2015
Mads Søgaard

Bibliography

[1] R. Britto, F. Cachazo and B. Feng, Nucl. Phys. B **715**, 499 (2005) [hep-th/0412308].

[2] R. Britto, F. Cachazo, B. Feng and E. Witten, Phys. Rev. Lett. **94**, 181602 (2005) [hep-th/0501052].

[3] Z. Bern, L. J. Dixon, D. C. Dunbar and D. A. Kosower, Nucl. Phys. B **435**, 59 (1995) [hep-ph/9409265].

[4] Z. Bern, L. J. Dixon, D. C. Dunbar and D. A. Kosower, Nucl. Phys. B **425**, 217 (1994) [hep-ph/9403226].

[5] Z. Bern and A. G. Morgan, Nucl. Phys. B **467**, 479 (1996) [hep-ph/9511336].

[6] Z. Bern, L. J. Dixon and D. A. Kosower, Nucl. Phys. B **513**, 3 (1998) [hep-ph/9708239].

[7] R. Britto, F. Cachazo and B. Feng, Nucl. Phys. B **725**, 275 (2005) [hep-th/0412103].

[8] R. Britto, F. Cachazo and B. Feng, Phys. Rev. D **71**, 025012 (2005) [hep-th/0410179].

[9] Z. Bern, N. E. J. Bjerrum-Bohr, D. C. Dunbar and H. Ita, JHEP **0511**, 027 (2005) [hep-ph/0507019].

[10] S. J. Bidder, N. E. J. Bjerrum-Bohr, D. C. Dunbar and W. B. Perkins, Phys. Lett. B **612**, 75 (2005) [hep-th/0502028].

[11] R. Britto, E. Buchbinder, F. Cachazo and B. Feng, Phys. Rev. D **72**, 065012 (2005) [hep-ph/0503132].

[12] R. Britto, B. Feng and P. Mastrolia, Phys. Rev. D **73**, 105004 (2006) [hep-ph/0602178].

[13] P. Mastrolia, Phys. Lett. B **644**, 272 (2007) [hep-th/0611091].

[14] A. Brandhuber, S. McNamara, B. J. Spence and G. Travaglini, JHEP **0510**, 011 (2005) [hep-th/0506068].

[15] G. Ossola, C. G. Papadopoulos and R. Pittau, Nucl. Phys. B **763**, 147 (2007) [hep-ph/0609007].

[16] C. Anastasiou, R. Britto, B. Feng, Z. Kunszt and P. Mastrolia, JHEP **0703**, 111 (2007) [hep-ph/0612277].

[17] Z. Bern, L. J. Dixon and D. A. Kosower, Annals Phys. **322**, 1587 (2007) [arXiv:0704.2798 [hep-ph]].

[18] D. Forde, Phys. Rev. D **75**, 125019 (2007) [arXiv:0704.1835 [hep-ph]].

[19] S. D. Badger, JHEP **0901**, 049 (2009) [arXiv:0806.4600 [hep-ph]].

[20] W. T. Giele, Z. Kunszt and K. Melnikov, JHEP **0804**, 049 (2008) [arXiv:0801.2237 [hep-ph]].

[21] R. Britto and B. Feng, Phys. Rev. D **75**, 105006 (2007) [hep-ph/0612089].

[22] R. Britto and B. Feng, JHEP **0802**, 095 (2008) [arXiv:0711.4284 [hep-ph]].

[23] Z. Bern, J. J. Carrasco, T. Dennen, Y. -t. Huang and H. Ita, Phys. Rev. D **83**, 085022 (2011) [arXiv:1010.0494 [hep-th]].

[24] C. Anastasiou, R. Britto, B. Feng, Z. Kunszt and P. Mastrolia, Phys. Lett. B **645**, 213 (2007) [hep-ph/0609191].

[25] P. Mastrolia, Phys. Lett. B **678**, 246 (2009) [arXiv:0905.2909 [hep-ph]].

[26] R. K. Ellis, W. T. Giele and Z. Kunszt, JHEP **0803**, 003 (2008) [arXiv:0708.2398 [hep-ph]].

[27] C. F. Berger, Z. Bern, L. J. Dixon, F. Febres Cordero, D. Forde, H. Ita, D. A. Kosower and D. Maitre, Phys. Rev. D **78**, 036003 (2008) [arXiv:0803.4180 [hep-ph]].

[28] G. Ossola, C. G. Papadopoulos and R. Pittau, JHEP **0803**, 042 (2008) [arXiv:0711.3596 [hep-ph]].

[29] P. Mastrolia, G. Ossola, C. G. Papadopoulos and R. Pittau, JHEP **0806**, 030 (2008) [arXiv:0803.3964 [hep-ph]].

[30] W. T. Giele and G. Zanderighi, JHEP **0806**, 038 (2008) [arXiv:0805.2152 [hep-ph]].

[31] C. F. Berger, Z. Bern, L. J. Dixon, F. Febres Cordero, D. Forde, T. Gleisberg, H. Ita and D. A. Kosower *et al.*, Phys. Rev. Lett. **102**, 222001 (2009) [arXiv:0902.2760 [hep-ph]].

[32] S. Badger, B. Biedermann and P. Uwer, Comput. Phys. Commun. **182**, 1674 (2011) [arXiv:1011.2900 [hep-ph]].

[33] C. F. Berger, Z. Bern, L. J. Dixon, F. Febres Cordero, D. Forde, T. Gleisberg, H. Ita and D. A. Kosower *et al.*, Phys. Rev. Lett. **106**, 092001 (2011) [arXiv:1009.2338 [hep-ph]].

[34] V. Hirschi, R. Frederix, S. Frixione, M. V. Garzelli, F. Maltoni and R. Pittau, JHEP **1105**, 044 (2011) [arXiv:1103.0621 [hep-ph]].

[35] Z. Bern, J. S. Rozowsky and B. Yan, Phys. Lett. B **401**, 273 (1997) [hep-ph/9702424].

[36] Z. Bern, L. J. Dixon and D. A. Kosower, JHEP **0001**, 027 (2000) [hep-ph/0001001].

[37] E. W. N. Glover, C. Oleari and M. E. Tejeda-Yeomans, Nucl. Phys. B **605**, 467 (2001) [hep-ph/0102201].

[38] Z. Bern, A. De Freitas and L. J. Dixon, JHEP **0203**, 018 (2002) [hep-ph/0201161].

[39] C. Anastasiou, E. W. N. Glover, C. Oleari and M. E. Tejeda-Yeomans, Nucl. Phys. B **601**, 318 (2001) [hep-ph/0010212].

[40] C. Anastasiou, E. W. N. Glover, C. Oleari and M. E. Tejeda-Yeomans, Nucl. Phys. B **601**, 341 (2001) [hep-ph/0011094].

[41] C. Anastasiou, E. W. N. Glover, C. Oleari and M. E. Tejeda-Yeomans, Nucl. Phys. B **605**, 486 (2001) [hep-ph/0101304].

[42] F. Cachazo, P. Svrcek and E. Witten, JHEP **0409**, 006 (2004) [hep-th/0403047].

[43] K. Risager, JHEP **0512**, 003 (2005) [hep-th/0508206].

[44] E. I. Buchbinder and F. Cachazo, JHEP **0511**, 036 (2005) [hep-th/0506126].

[45] F. Cachazo, arXiv:0803.1988 [hep-th].

[46] F. Cachazo, M. Spradlin and A. Volovich, Phys. Rev. D **78**, 105022 (2008) [arXiv:0805.4832 [hep-th]].

[47] Z. Bern, J. J. M. Carrasco, L. J. Dixon, H. Johansson and R. Roiban, Phys. Rev. D **82**, 125040 (2010) [1008.3327 [hep-th]].

[48] J. J. M. Carrasco and H. Johansson, J. Phys. A **44**, 454004 (2011) [1103.3298 [hep-th]].

[49] J. J. M. Carrasco and H. Johansson, Phys. Rev. D **85**, 025006 (2012) [1106.4711 [hep-th]].

[50] Z. Bern, J. J. M. Carrasco, H. Johansson and R. Roiban, Phys. Rev. Lett. 109:241602 (2012) [1207.6666 [hep-th]].

[51] Z. Bern, J. J. M. Carrasco, H. Johansson and D. A. Kosower, Phys. Rev. D **76**, 125020 (2007) [0705.1864 [hep-th]].

[52] Z. Bern, J. J. M. Carrasco, L. J. Dixon, H. Johansson and R. Roiban, Phys. Rev. D **78**, 105019 (2008) [0808.4112 [hep-th]].

[53] J. Gluza, K. Kajda and D. A. Kosower, Phys. Rev. D **83**, 045012 (2011) [arXiv:1009.0472 [hep-th]].

[54] R. M. Schabinger, JHEP **1201**, 077 (2012) [arXiv:1111.4220 [hep-ph]].

[55] D. A. Kosower and K. J. Larsen, Phys. Rev. D **85**, 045017 (2012) [arXiv:1108.1180 [hep-th]].

[56] S. Caron-Huot and K. J. Larsen, JHEP **1210**, 026 (2012) [arXiv:1205.0801 [hep-ph]].

[57] H. Johansson, D. A. Kosower and K. J. Larsen, Phys. Rev. D **87**, 025030 (2013) [arXiv:1208.1754 [hep-th]].

[58] H. Johansson, D. A. Kosower and K. J. Larsen, arXiv:1308.4632 [hep-th].

[59] M. Sogaard, JHEP **1309**, 116 (2013) [arXiv:1306.1496 [hep-th]].

[60] M. Sogaard and Y. Zhang, JHEP **1312**, 008 (2013) [arXiv:1310.6006 [hep-th]].

[61] M. Sogaard and Y. Zhang, JHEP **1407**, 112 (2014) [arXiv:1403.2463 [hep-th]].

[62] M. Sogaard and Y. Zhang, JHEP **1412**, 006 (2014) [arXiv:1406.5044 [hep-th]].

[63] M. Sogaard and Y. Zhang, arXiv:1412.5577 [hep-th].

[64] H. Johansson, D. A. Kosower, K. J. Larsen and M. Sogaard, to appear.

[65] H. Johansson, D. A. Kosower, K. J. Larsen and M. Sogaard, to appear.

[66] R. Huang, D. A. Kosower, M. Sogaard and Y. Zhang, to appear.

[67] K. J. Larsen, Phys. Rev. D **86**, 085032 (2012) [arXiv:1205.0297 [hep-th]].

[68] S. Badger, H. Frellesvig and Y. Zhang, JHEP **1204**, 055 (2012) [arXiv:1202.2019 [hep-ph]].

[69] P. Mastrolia and G. Ossola, JHEP **1111**, 014 (2011) [arXiv:1107.6041 [hep-ph]].

[70] S. Badger, H. Frellesvig and Y. Zhang, JHEP **1208**, 065 (2012) [arXiv:1207.2976 [hep-ph]].

[71] Y. Zhang, JHEP **1209**, 042 (2012) [arXiv:1205.5707 [hep-ph]].

[72] S. Badger, H. Frellesvig and Y. Zhang, arXiv:1310.1051 [hep-ph].

[73] B. Feng and R. Huang, JHEP **1302**, 117 (2013) [arXiv:1209.3747 [hep-ph]].

[74] P. Mastrolia, E. Mirabella, G. Ossola and T. Peraro, Phys. Lett. B **718**, 173 (2012) [arXiv:1205.7087 [hep-ph]].

[75] P. Mastrolia, E. Mirabella, G. Ossola and T. Peraro, arXiv:1209.4319 [hep-ph].

[76] P. Mastrolia, E. Mirabella, G. Ossola, T. Peraro and H. van Deurzen, PoS LL **2012** (2012) 028 [arXiv:1209.5678 [hep-ph]].

[77] R. H. P. Kleiss, I. Malamos, C. G. Papadopoulos and R. Verheyen, JHEP **1212**, 038 (2012) [arXiv:1206.4180 [hep-ph]].

[78] P. Mastrolia, E. Mirabella, G. Ossola and T. Peraro, arXiv:1307.5832 [hep-ph].

[79] R. Huang and Y. Zhang, JHEP **1304**, 080 (2013) arXiv:1302.1023 [hep-ph].

[80] J. D. Hauenstein, R. Huang, D. Mehta and Y. Zhang, JHEP **1502**, 136 (2015) [arXiv:1408.3355 [hep-th]].

[81] B. Feng, J. Zhen, R. Huang and K. Zhou, arXiv:1401.6766 [hep-th].

[82] N. Arkani-Hamed, F. Cachazo, C. Cheung and J. Kaplan, JHEP **1003**, 020 (2010) [arXiv:0907.5418 [hep-th]].

[83] N. Arkani-Hamed, F. Cachazo and C. Cheung, JHEP **1003**, 036 (2010) [arXiv:0909.0483 [hep-th]].

[84] N. Arkani-Hamed, J. Bourjaily, F. Cachazo and J. Trnka, JHEP **1101**, 108 (2011) [arXiv:0912.3249 [hep-th]].

[85] N. Arkani-Hamed, J. Bourjaily, F. Cachazo and J. Trnka, JHEP **1101**, 049 (2011) [arXiv:0912.4912 [hep-th]].

[86] J. L. Bourjaily, S. Caron-Huot and J. Trnka, JHEP **1501**, 001 (2015) [arXiv:1303.4734 [hep-th]].

[87] N. Arkani-Hamed, J. L. Bourjaily, F. Cachazo, S. Caron-Huot and J. Trnka, JHEP **1101**, 041 (2011) [arXiv:1008.2958 [hep-th]].

[88] N. Arkani-Hamed, J. L. Bourjaily, F. Cachazo and J. Trnka, JHEP **1206**, 125 (2012) [arXiv:1012.6032 [hep-th]].

[89] Z. Bern, L. J. Dixon and V. A. Smirnov, Phys. Rev. D **72**, 085001 (2005) [hep-th/0505205].

[90] C. Anastasiou, Z. Bern, L. J. Dixon and D. A. Kosower, Phys. Rev. Lett. **91**, 251602 (2003) [hep-th/0309040].

[91] F. Cachazo, M. Spradlin and A. Volovich, Phys. Rev. D **74**, 045020 (2006) [hep-th/0602228].

[92] Z. Bern, M. Czakon, D. A. Kosower, R. Roiban and V. A. Smirnov, Phys. Rev. Lett. **97**, 181601 (2006) [hep-th/0604074].

[93] Z. Bern, J. J. M. Carrasco and H. Johansson, Phys. Rev. D **78**, 0850

[94] Z. Bern, T. Dennen, Y. t. Huang and M. Kiermaier, Phys. Rev. D **82**, 065003 (2010) [arXiv:1004.0693 [hep-th]].

[95] Z. Bern, J. J. M. Carrasco and H. Johansson, Phys. Rev. Lett. **105**, 061602 (2010) [arXiv:1004.0476 [hep-th]].

[96] N. E. J. Bjerrum-Bohr, P. H. Damgaard and P. Vanhove, Phys. Rev. Lett. **103**, 161602 (2009) [arXiv:0907.1425 [hep-th]].

[97] Z. Bern, J. J. M. Carrasco, H. Ita, H. Johansson and R. Roiban, Phys. Rev. D **80**, 065029 (2009) [arXiv:0903.5348 [hep-th]].

[98] M. Sogaard, Phys. Rev. D **84**, 065011 (2011) [arXiv:1106.3785 [hep-th]].

[99] H. Elvang, Y. t. Huang and C. Peng, JHEP **1109**, 031 (2011) [arXiv:1102.4843 [hep-th]].

[100] J. M. Henn, Phys. Rev. Lett. **110**, no. 25, 251601 (2013) [arXiv:1304.1806 [hep-th]].

[101] F. Caola, J. M. Henn, K. Melnikov and V. A. Smirnov, arXiv:1404.5590 [hep-ph].

[102] V. A. Smirnov, Phys. Lett. B **567**, 193 (2003) [hep-ph/0305142].

[103] A. V. Smirnov and V. A. Smirnov, arXiv:1302.5885 [hep-ph].

[104] C. Studerus, Comput. Phys. Commun. **181**, 1293 (2010) [arXiv:0912.2546 [physics.comp-ph]].

[105] A. von Manteuffel and C. Studerus, arXiv:1201.4330 [hep-ph].

[106] L. J. Dixon, In *Boulder 1995, QCD and beyond* 539-582 [hep-ph/9601359].

[107] H. Elvang and Y. t. Huang, arXiv:1308.1697 [hep-th].

[108] L. J. Dixon, arXiv:1310.5353 [hep-ph].

[109] G. Aad *et al.* [ATLAS Collaboration], Phys. Lett. B **716**, 1 (2012) [arXiv:1207.7214 [hep-ex]].

[110] S. Chatrchyan *et al.* [CMS Collaboration], Phys. Lett. B **716**, 30 (2012) [arXiv:1207.7235 [hep-ex]].

[111] P. Griffiths, J. Harris, Wiley-Interscience [John Wiley & Sons], New York, 1978.

[112] D. R. Grayson and M. E. Stillman, `http://www.math.uiuc.edu/Macaulay2/`.

[113] R. Hartshorne, 1977. Graduate Texts in Mathematics, No. 52.

[114] E. Cattani and A. Dickenstein. Springer Berlin Heidelberg, 2005.

[115] D. A.Cox. and J. Little, and Donal . O'Shea, Springer, New York, 2005

[116] J. H. Silverman, Springer, 2010.

[117] E. T. Whittaker and G. N. Watson, Cambridge University Press, 1996.

[118] K. J. Larsen, PhD Thesis, Uppsala Universitet, 2012.

[119] M. Srednicki, Cambridge, UK, Univ. Pr. (2007)

[120] M. E. Peskin and D. V. Schroeder, Reading, USA, Addison-Wesley (1995)